Catalogue of floods recorded at tide-gauge station Bakar in the northeastern Adriatic Sea (Mediterranean)

Iva Međugorac[1, 2, 3], Karla Jambrošić[4], Domagoj Dolički[5], Josipa Kuzmić[5], Jadranka Šepić[6], Iva Vrkić Seidl[3], Goran Gašparac[7]

[1]University of Nova Gorica, Vipavska 13, SI-5000 Nova Gorica, Slovenia

[2]Slovenian Environment Agency, Vojkova 1b, 1000 Ljubljana, Slovenia

[3]Department of Geophysics, Faculty of Science, University of Zagreb, Horvatovac 95, 10000, Zagreb, Croatia

[4]Croatia Control Ltd., Ul. Rudolfa Fizira 2, 10410 Velika Gorica, Croatia

[5]Croatian Meteorological and Hydrological Service, Ravnice 48, 10000 Zagreb, Croatia

[6]Faculty of Science, University of Split, R. Boškovića 33, 21000 Split, Croatia

[7]Amego Ltd., Vinogorska 59a, Zagreb, Croatia

Correspondence to: Iva Međugorac (iva.medugorac@gfz.hr)

Abstract

Flooding in the northern Adriatic Sea occasionally occurs in late fall and winter as a result of storm surges that combine with other sea-level processes at different spatial and temporal scales. This paper presents (empirical) analysis of the 27 most intense floods recorded at the Croatian tide-gauge station Bakar on the northeastern coast of the Adriatic Sea in the period 1929–2022. Floods were defined as events in which the hourly sea level rose by at least 89 cm (99.99th percentile threshold) above the long-term average. The study examines: (i) the evolution of sea level, analysed through five components: *local processes*, *tide*, *synoptic component* (storm surge and basin-wide seiche), *long-period sea-level variability* and *mean sea-level changes*, (ii) the meteorological conditions, based on reanalysis series and fields (mean sea-level pressure, 10-m wind, 500-hPa surface geopotential heights), (iii) the impact of flooding on natural and built environments along the Croatian coastline, and (iv) the relevant scientific literature on these flood episodes. The study is complemented by the online catalogue, which contains supplementary information and is continuously updated with the latest flooding episodes (https://projekti.pmfst.unist.hr/floods/storm-surges/).

1 Introduction

The Adriatic Sea is a sub-basin of the Mediterranean Sea, surrounded by mountain ranges, everywhere but at the narrow Otranto gate. It is ~850 km long and ~250 km wide, with depths ranging from 50 m in the northern shelf to 1250 m in the southern Adriatic Pit (Fig. 1). In late fall and winter, the Adriatic is exposed to frequent passages of Mediterranean cyclones (we use "cyclones" to refer to "extratropical cyclones"), which cause pronounced mean sea level pressure gradients and

30 consequently a southeast wind Sirocco over the Adriatic (e.g., Trigo and Davies, 2002; Lionello et al., 2021). Under these conditions, the water accumulates in the basin and forms a storm surge which floods the coast. During these events, the northern Adriatic Sea does not behave coherently, i.e. the induced storm surge has a spatial structure that depends on the bathymetry of the basin and the distribution of atmospheric forcing fields (Međugorac et al., 2018). This ultimately determines whether the sea level (SL) response is stronger along the western or the eastern coastline. Although storm surge

35 is a dominant contributor to inundation in the northern Adriatic, other SL processes can have an influence on the formation of extreme SLs on temporal scales of minutes to decades and on some occasions their role can be decisive (Ferrarin et al., 2021; Lionello et al., 2021; Šepić et al., 2022; Ruić et al., 2023). Here we give an overview of all processes contributing to the northeastern Adriatic flooding episodes according to their period, from shorter to longer ones: *local processes*, *tide*, *synoptic component*, *long-period sea-level component* and *mean sea-level changes*.

40 The total SL measured at tide-gauge station Bakar (TG Bakar) includes several *local processes (*also referred to as *local component*), i.e., processes that occur on temporal scales of up to 9 h. TG Bakar is situated in Bakar Bay (Fig. 1), which is part of the wider Kvarner Bay region (Kvarner Bay is an area bounded on the outside by a line connecting Cape Kamenjak and Cape Skala, as indicated by the dashed black line in Fig. 1; Goldberg and Kempni, 1938), with both of these bays known for strong seiches. If hourly data is considered, *local component*, usually defined as part of the spectrum up to 10 h (Ferrarin

45 et al., 2021; Šepić et al., 2022), is controlled by oscillations induced by mesoscale perturbations and short period seiches (Goldberg and Kempni, 1938; Šepić et al., 2022), with the latter defined by topography and bathymetry of the area.

The Adriatic *tide* is one of the main contributors to positive and negative SL extremes along the entire eastern coast (Šepić et al., 2022). It is of mixed type and usually modelled as a sum of seven main components — four semidiurnal (K2, S2, M2, N2) and three diurnal (K1, O1, P1). Semidiurnal spring tides occur near the full moon and new moon, while diurnal neap

50 tides occur near the first and last quarter moons. Its amplitude increases towards the closed northern end of the Adriatic: an average daily range in Bakar Bay is ~60 cm, while in Trieste Bay it reaches its maximum at ~120 cm (Medvedev et al., 2020).

Synoptic component, driven by atmospheric synoptic disturbances, includes both forced and free oscillations – storm surges (described at the beginning of the Introduction) and basin-wide seiches, and plays a significant role in contributing to floods

55 in the northern Adriatic (e.g., Pasarić and Orlić, 2001; Međugorac et al., 2018; Ferrarin et al., 2021; Lionello et al., 2021; Šepić et al., 2022). When basin-wide seiches are already present in the basin, they can amplify or attenuate an incoming storm surge. The fundamental Adriatic mode has a period of ~21.2 h (e.g., 21.9 h in Schwab and Rao, 1983; 21.2 h in Cerovečki et al., 1997; 21.2 h in Raicich et al. 1999). It is a longitudinal oscillation of the entire basin with a nodal line at the

Strait of Otranto (Fig. 1). Once triggered, usually after a storm surge peak when Sirocco suddenly stops or turns to Bora
60 (northeastern wind, c.f., Grisogono and Belušić, 2009), the seiche decays slowly, with an e-folding time of 3.2±0.5 d
(Cerovečki et al., 1997). Its initial amplitude can be several tens of centimetres and, due to its long duration, it can amplify or
attenuate an upcoming storm surge depending on its phase with regard to other involved processes (Šepić et al., 2022).
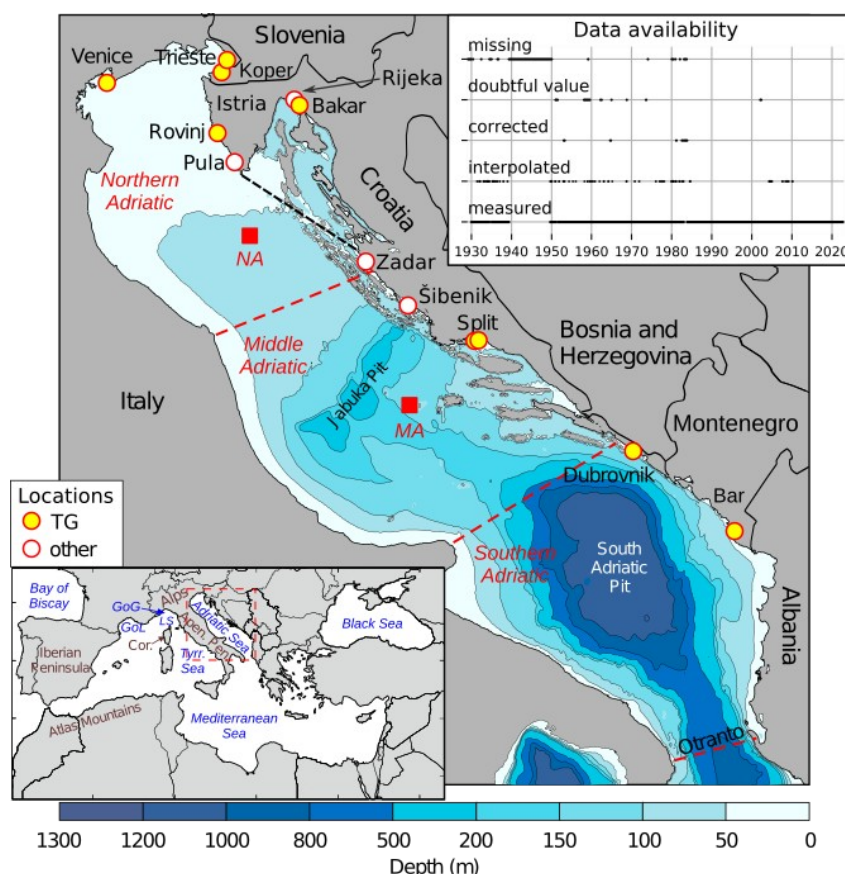
Figure 1: Bathymetry of the Adriatic Sea. Locations of tide gauges (TG) with records of at least 60 y (Pérez Gómez et al., 2022) are
65 marked with red-yellow circles. Other major towns along the Croatian Adriatic coast are marked with red-white circles. The subdivision of
the Adriatic into sub-basins is marked with red dashed lines and the area of the Kvarner Bay is to the northeast of the black dashed line.
The red rectangles mark grid points for which the atmospheric series were analysed. The position of the Adriatic in relation to the
Mediterranean is shown in the small inset in the lower left corner, and the data availability of TG Bakar time series is shown in the upper
right corner. On the Mediterranean map, frequently referenced regions are labelled: Gulf of Genoa (GoG), Gulf of Lion (GoL), Ligurian
70 Sea (LS), Tyrrhenian Sea (Tyrr. Sea), Apennine Peninsula (Apen. Pen.), Corsica (Cor.).

It should be mentioned that wave setup, defined in Toomey et al. (2022) as the "temporal rise above the mean sea level due
to dissipation and breaking of waves in shallow waters close to the shore" contributes to total SL, particularly during extreme
events characterised by high wind waves. This phenomenon occurs over temporal scales ranging from hours to days,

encompassing both *local processes* and *synoptic component*. Its impact on SL extremes is pronounced in several
75   Mediterranean locations, including the eastern Adriatic coastline. In front of Bakar Bay, the 99th percentile of wave setup
during extremes is evaluated to be between 10 and 20 cm (Toomey et al., 2022; their Fig. 9).

Another important factor contributing to coastal flooding in the Adriatic is the *long-period sea-level variability* (here also
referred to as *long-period sea-level component* and, sometimes in scientific literature, *planetary-scale variability*; Međugorac
et al., 2021; Šepić et al., 2022), which prevails in periods of 10–100 d, and is predominantly controlled by atmospheric
80   planetary waves (Rossby waves) through the effects of surface atmospheric pressure and wind (Pasarić, 2000; Pasarić et al.,
2000; Pasarić and Orlić, 2001). Prolonged intervals of raised SL, i.e. positive phases of *long-period sea-level variability*, are
particularly threatening as their amplitudes in Bakar can exceed 30 cm (Pasarić, 2000; Šepić et al., 2022), therefore even not-
so-intense cyclones can cause high total SLs during these periods (Međugorac et al., 2021).

Mean sea-level changes (here also referred to as *mean sea-level component*) occurring over time scales longer than 100 d,
85   encompass seasonal cycle, interannual variations, (multi)decadal fluctuations, and secular change (here also referred to as
linear rate of change or linear trend). These changes are influenced by atmospheric and oceanic drivers across a broad region,
including the Atlantic Ocean (detailed in Appendix A). Although their contribution to Adriatic flooding is secondary
compared to *synoptic component*, it has become increasingly important in recent years (Međugorac and Pasarić, 2024).

It is assumed that these five processes are independent of each other, as they have sufficiently small amplitudes compared to
90   the depth of the basin so that nonlinear interactions are negligible. This has been confirmed for the interactions between the
strongest components, tides and storm surges as well as tides and seiches by empirical analyses (e.g., Cerovečki et al., 1997;
Marcos et al., 2009) and by numerical experiments (e.g., Lionello et al., 2005; 2006). Therefore, we assume that floods in the
Adriatic Sea form as a positive linear superposition of all active processes, and that by studying these processes separately,
we can also distinguish between various sources of these processes, and that the intensity and timing of floods depend on the
95   phases and the amplitudes of all processes involved.

Floods that occurred in Venice between 787 and 1867 are documented in the study by Enzi and Camuffo (1995). Several
flooding events in the northern Adriatic have been analysed by performing numerical or empirical analyses and by
investigating various aspects of floods (e.g., predictability, synoptic/hydrological background, contribution of different
processes to their generation, and their impact). Some of these episodes were studied in great deal, mainly because they were
100 intense in Venice (e.g., 4 November 1966 and 13 November 2019), while episodes that were more pronounced on the east
coast were less studied (e.g., flood of 1 November 2012).

The aim of this paper is to provide: (i) a list of the most intense floods recorded at TG Bakar in the period 1929–2022, (ii)
process-oriented analysis of these floods, (iii) a summary of the impacts of the floods on people's lives and on the
environment along the Croatian Adriatic coast, and (iv) a list of previous studies dealing with these episodes.
105 The paper is organised as follows. Following the introductory section Sect. 1, Sect. 2 provides details of the sea-level,
meteorological, and archival data used. The methodology and spectral analysis is described in Sect. 3. Section 4 provides a

detailed analysis of the most intense floods observed in the northern Adriatic. Section 5 summarises and concludes the paper.

2 Sea-level, meteorological and archival data and lists of previous studies

2.1 Sea-level and meteorological data

110 The analysis of SL is based on hourly data measured at TG Bakar in the period December 1929–December 2022. TG Bakar (Međugorac et al., 2022; 2023) was established on 5 December 1929, it was in operation until the beginning of the Second World War (May 1939), it was put back into operation in August 1949 and has been in operation with minor interruptions ever since (Fig. 1). Further information about the station can be found on the station's website (Tide-gauge station Bakar). All SL are given as values above mean SL calculated over the 18.6 y period around 1971.5 (1962–1980; HVRS71 National

115 Geodetic System; Rožić, 2009).

The atmospheric background of floods, on synoptic and planetary scale, were analysed using following atmospheric fields from the ERA5 Global Reanalysis Dataset (C3S; Hersbach et al., 2020; Hersbach et al., 2023a; 2023b): mean sea-level pressure (MSLP), 10-m wind (u10, v10 - referred to as **W10** in our paper), geopotential heights of the 500 hPa level (Z500). For floods that occurred before 1 January 1940 (one episode), atmospheric background analyses were performed using the

120 NOAA-CIRES-DOE Twentieth Century Reanalysis Project version 3 dataset (Slivinski et al., 2019). For the analyses, we also used reanalysis series of MSLP and Z500 taken at the sea grid point closest to the Bakar station (lon = 14.540, lat = 45.305) and **W10** (u10, v10) series taken at the sea grid points in the northern and the middle Adriatic (shown in Fig. 1) closest to the points (lon = 14, lat = 44.3) and (lon = 15.7, lat = 43). The atmospheric reanalysis was complemented by measurements provided by the Croatian Meteorological and Hydrological Service (DHMZ): 24 h accumulated precipitation

125 recorded at 06:00 UTC on specified days, and hourly wind speeds (along with wind gusts, if recorded), both measured at coastal stations in Croatia. Also used were synoptic maps from Deutscher Wetterdienst (DWD).

2.2 Archival data

To examine the impacts of flooding, daily newspapers in print or microfilmed form in the National and University Library were reviewed (Table 1). Articles related to floods were found for 20 events. No records were found in daily newspapers for

130 the events of 17 and 18 December 1958, 2 October 1993, 26 November 1996, 23 December 2009, 8 December 2020 and 22 November 2022. For more recent episodes (starting with the flood of 1 December 2008), we also checked available online sources (listed under *Flood Impacts* for each event).

Table 1: Title of a serial publication, form (microfilm or print) of a newspaper, ID number of a document (in the National and University Library), interval for which a newspaper was printed, and IDs of flood episodes (from Table 2) described in the newspapers.

Newspapers	Form	Signature	Time interval	Floods ID
Hrvatski dnevnik	microfilm	85.562	1936–1941	
Jutarnji list	microfilm	86.013	1912–1941	
	printed	213.804	2000–	16, 21, 22, 23
Narodne novine	microfilm	85.110	1861–1945	
Novi list	printed	89.732	1954–	5, 6, 7, 8, 9, 10, 11, 12, 13, 16, 17, 20, 21, 22, 26
Obzor (Zagreb, 1920)	microfilm	85.135	1920–1941	1
Primorske novine	microfilm	85.123	1935–1941	1
Slobodna Dalmacija	printed	89.653	1943–1984	4, 8, 10
		213.405	1984–	9, 11, 12, 13, 16, 19, 20, 21, 22, 24
Večernji list	printed	213.327	1959–	6, 7, 8, 9, 10, 13, 16, 21
Vjesnik	printed	210.69	1962–2012	6, 13, 16, 19

135 2.3 Previous studies

We conducted a literature search using sources such as the Web of Science and Google Scholar to compile a list of papers studying extracted flooding episodes. Only studies focusing on the meteo-oceanographic aspects of the floods are included. Papers that merely mention the floods or address unrelated topics are excluded. For example, the storm Vaia (October 2018, A catastrophic event: the Vaia Storm, 2024), which caused severe flooding in the Adriatic (Table 2, ID = 21), has been 140 widely analysed in studies focusing on topics such as forest damage, heavy precipitation, hydro-geomorphological responses in mountainous areas, etc. These topics fall outside the scope of our research.

3 Methodology

3.1 Definition of flooding episodes

Floods were defined as occasions in which the measured SL exceeded the 99.99th percentile threshold (89 cm for 1929– 145 2022) of SL series. The inundation of most sea promenades in the northern Adriatic (built in the second half of the 20th century to be 50–75 cm above the mean SL at that time) occurs before 89 cm is reached in Bakar, but here only the most intense episodes were studied. Consecutive values exceeding the given threshold were combined into one event, represented

by the maximum SL reached during that event. Furthermore, consecutive events, separated by SL lower than 89 cm, but

150   associated with a single atmospheric disturbance (e.g., a cyclone) were merged into a single episode. Only one such episode
(consisting of two events) was identified: 4 November 1966. Therefore, an episode may consist of several events (i.e.,
several sea-level peaks within the episode), which are e.g., due to the tidal peaks occurring on top of SL elevated due to other
processes (as in the 4 November 1966 flood; Međugorac et al., 2015). We assigned a rank to each flood based on the
maximum total sea level reached during an episode (Table 2).

3.2 Decomposition of sea-level and meteorological series

155   Figure 2 shows the spectrum of the SL in Bakar with indicated cut-off frequencies used to filter the SL time series into five
components: (i) *local processes* (2 < T < 9 h), (ii) *tide* (semidiurnal and diurnal constituents), (iii) *synoptic component* (9 h <
T < 10 d), (iv) *long-period sea-level component* (10 < T < 100 d) and (v) *mean sea-level changes* (100 d < T). The
components were defined considering sea-level drivers, spectral properties and established methodologies (e.g., Šepić et al.,
2022). First, *tide* was calculated using harmonic analysis and synthesis (MATLAB T_tide software; Pawlowicz et al., 2002)

160   based on year by year data. Here we considered seven main constituents (K1, O1, P1, K2, S2, M2, N2) which dominantly
shape the tidal signal in the Adriatic (Janeković and Kuzmić, 2005). Tidal constituents are visible in Fig. 2 as sharp peaks,
which are strongest at periods of ~12 and ~24 h, but also visible at shorter (~4.1 h, ~4.9 h, ~6.1 h, and ~8.2 h) and longer
(~13.6 d) periods. To ensure repeatability of the analysis, seven major tidal harmonics were taken each year to estimate *tide*,
as other harmonics, although obvious in Fig. 2, have a minor impact on the tidal signal. Šepić et al. (2022) found that the

165   mean absolute difference between tides estimated using all significant harmonics (43 components) and those using only the
seven dominant harmonics was 2.48 cm in Bakar (estimated for period 1956–2020). Then, de-tided SL was split into four
further components by applying digital low-pass filters from longer to shorter time scales. Kaiser windows with half-power
points at 9 h, 10 d and 100 d were used for filtering. Although the SL spectrum is monotonic at lower frequencies, splitting
of SL is justified due to differences in atmospheric forcing and the varying dynamics of atmosphere-sea interactions across

170   different spatio-temporal scales (e.g., Pugh and Thompson, 1986; Pasarić and Orlić, 2001). Residual sea-level components
defined in this way are: *local component, synoptic component, long-period sea-level component* and *mean sea-level changes*.
Local component consists of *local processes* i.e., long ocean waves, oscillations induced by mesoscale perturbations, the
Kvarner Bay seiche (broad peak at ~6 h) and the second higher harmonic of the Adriatic-wide seiche (broad peak at ~7.3 h).
To our knowledge, the origin of the increased energy at a period of ~3.2 h is unclear; the peak was reported but not explained

175   by (Šepić et al., 2022). It should be noted that tidal oscillations at periods of ~8.2 h and shorter are also contained in this
component.

Synoptic component mainly consists of forced and free oscillations i.e. storm surges and seiches, caused by synoptic
atmospheric disturbances. The fundamental mode of the Adriatic seiche is visible as a broad peak at ~21.2 h and the first

higher harmonic as a peak at ~10.8 h. For each flood, we estimated the presence of pre-existing fundamental basin-wide
180 seiches contributing to *synoptic component* by visual inspection of residual SL series. If seiche, manifested as obvious
oscillations with a period of 21.2 h, was present in the basin, up to three days before an event, it was assumed that this
process was also active during the flood. The method is semi-empirical and has been used in previous studies (Međugorac et
al., 2015; Šepić et al., 2022). Here we use it only to determine the presence of the basin-wide seiche, but not to evaluate its
contribution.

185
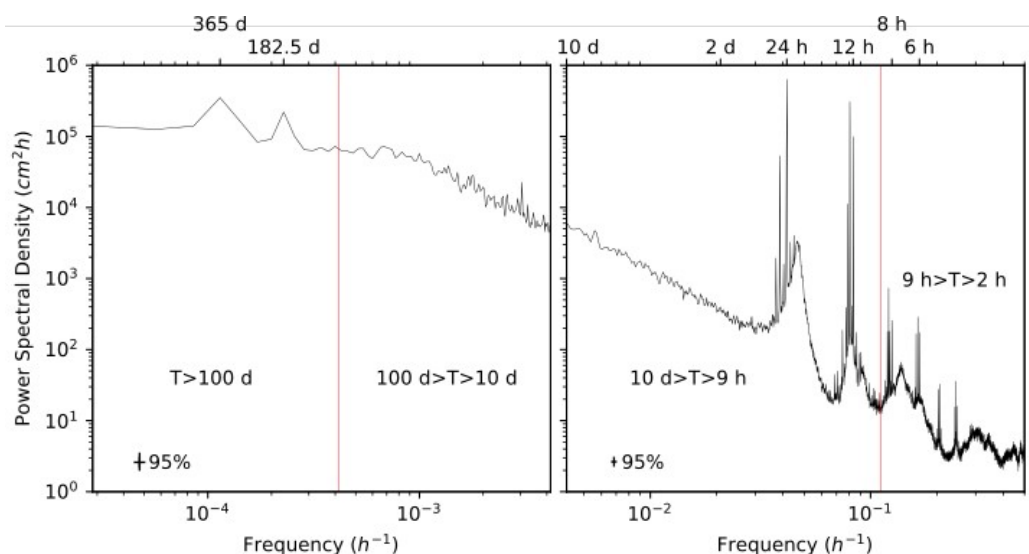
Figure 2: Power spectral densities of total SL measured at TG Bakar (1950–2022) for periods longer than 10 d (left) and periods shorter
than 10 d (right). Corresponding 95% confidence intervals are indicated. Spectra were calculated using 4 y (left) and 1 y (right) long
Hamming 50%-overlapping windows. Red vertical lines indicate a period of 100 d (left) and 9 h (right). Boundaries between sea-level
processes are indicated with vertical lines (red lines and edges of subfigures).

190 The *long-period sea-level component* is primarily a response of SL to atmospheric Rossby waves (pronounced in the middle
troposphere, ~500 hPa, and most energetic in the cold part of a year).

Mean sea-level changes include seasonal cycle (visible peaks at periods of 182.5 and 365 d), interannual variability,
(multi)decadal variability and secular change. In ~~the main body of the article~~, *mean sea-level changes* are considered to be a
single component. However, in Appendix A (Figs. A1, A2 and A3) we discuss in more detail contribution of following
195 individual processes to *mean sea-level changes*: (i) seasonal cycle and interannual variability (100 d < T < 5 y); (ii)
(multi)decadal changes (SL series at 5 y < T reduced by secular change); (iii) and secular change (linear trend calculated for
the entire time series).

Given the high concentration of flood episodes at the end of the studied period (seven episodes since 2018), we note that for
these episodes additional attention should be given to reliability of *mean sea-level component*, especially in relation to

200 multi(decadal) variability (5 y < T). Filtering can heavily affect the edges of time series. To check whether this is an issue for our problem, we compared multi(decadal) variability (5 y < T) calculated first for a full interval (1929–2022; black line in Fig. A2a) and then for a shorter interval (1957–1992; red line in Fig. A2a), and paid special attention to differences between these two series at the edges of the shorter series (1957–1962; 1987–1992). In this way we get an idea about the length of the unreliable marginal period. From Fig. A2a it is evident that (multi)decadal variability (5 y < T) is significantly affected by

205 boundary values, especially in situations when sea level is anomalously high or low, as was the case in 1992 (anomalously low).

To analyse atmospheric forcing on a planetary scale and the corresponding SL response (*long-period sea-level component*), we compared low-pass series of MSLP, Z500 and **W10** (filtered with a 10-d cut-off frequency) with joint *long-period* and *mean sea-level* components. While planetary atmospheric forcing acts over periods 10 < T < 100 d and thus presumably

210 affects only *long-period sea-level component* (10 < T < 100 d) we use the low-pass filtered series (and not the band-pass ones) because at periods longer than 100 d both atmospheric and SL series show minimal variations over the time frames presented in figures (approximately one month), i.e., series at periods longer than 100 d effectively act as mean values. We focus on these four time series because, during the colder part of the year (over periods 10 < T < 100 d), the atmosphere exhibits quasi-barotropic behavior. This allows disturbances in the mid-troposphere (500 hPa) to be reflected at the surface

215 (MSLP and accompanying **W10**), making Z500 a reliable indicator of long-term surface meteorological conditions. In this paper, both in the text and figures, these low-pass series are labelled as MSLP (lp), Z500 (lp), and for sea level, as long + mean.

4 Descriptions of the floods

Flooding episodes are listed from the most recent to the earliest (Table 2) to highlight the stronger and more relevant recent

220 events, making them easier to find within the paper. We describe the meteorological background of the floods, the processes in the sea that contribute to the total SL, and effects of the floods on people's lives, coastal infrastructure and environment, from different sources (Table 1).

Table 2: List of floods recorded at TG Bakar in the period 1929–2022. From left- to right-hand columns: ID of the episode, rank of a flood (floods are ranked based on maximum SL reached during a flood), date, time (UTC) at which maximum SL was recorded, maximum SL

225 reached during a flood, pre-existing basin-wide seiches, and a list of scientific publications that studied a flood.

Episode (ID)	Rank	Date	Time (UTC)	Max SL (cm)	Pre-existing seiche	Literature
27	4	22 November 2022	06:00	101		Mel et al. (2023)

26	7	8 December 2021	23:00	97		
25	12	8 December 2020	13:00	92	yes	
24	10	23 December 2019	05:00	94	yes	Bajo et al. (2023)
23	12	15 November 2019	09:00	92		Bajo et al. (2023) Ferrarin et al. (2021) Lionello et al. (2021) Rus et al. (2023) Rus et al. (2024) Žust et al. (2021)
22	5	13 November 2019	06:00	99		Bajo et al. (2023) Cavaleri et al. (2020) Ferrarin et al. (2021) Lionello et al. (2021) Orlić and Pasarić (2024) Rus et al. (2023) Rus et al. (2024) Žust et al. (2021)
21	7	29 October 2018	20:00	97		Biolchi et al. (2019) Cavaleri et al. (2019) Ferrarin et al. (2020; 2022) Korbar et al. (2022) Ličer et al. (2020) Lionello et al. (2021) Morucci et al. (2020) Pervan and Šepić (2023)
20	1	1 November 2012	06:00	113		Međugorac et al. (2016)
19	13	3 December 2010	05:00	91	yes	
18	3	25 December 2009	01:00	103	yes	Bajo et al. (2019)
17	6	23 December 2009	02:00	98	yes	

16	2	1 December 2008	07:00	105	yes	Bajo et al. (2019)
						Bertotti et al. (2011)
						Lionello et al. (2021)
						Međugorac et al. (2015; 2016)
						Zampato et al. (2016)
15	14	26 November 1996	06:00	90	yes	
14	14	2 October 1993	20:00	90		Canestrelli et al. (2001)
13	13	10 December 1990	02:00	91		Canestrelli et al. (2001)
12	14	24 November 1987	22:00	90		Pasarić (2000)
11	9	1 February 1986	00:00	95		Canestrelli et al. (2001)
						Lionello et al. (2021)
10	9	25 October 1980	10:00	95		
9	7	22 December 1979	09:00	97		Bertotti et al. (2011)
						Canestrelli et al. (2001)
						Cavaleri et al. (2010)
						Lionello et al. (2021)
8	8	25 November 1969	23:00	96		Canestrelli et al. (2001)
7	14	3 November 1968	06:00	90		Canestrelli et al. (2001)
6	10	4 November 1966	12:00 20:00	94		Accerboni and Manca (1973)
						Bertotti et al. (2011)
						Canestrelli et al. (2001)
						Cavaleri et al. (2010)
						De Zolt et al. (2006)
						Finizio et al. (1972)
						Lionello et al. (2021)
						Malguzzi et al. (2006)
						Međugorac et al. (2015)
						Mosetti (1985)
						Roland et al. (2009)
						Stravisi and Marussi (1973)
						Trincardi et al. (2016)
5	10	23 January 1966	05:00	94	yes	
4	11	24 December 1958	05:00	93		

3	12	18 December 1958	02:00	92	yes
2	8	17 December 1958	02:00	96	yes
1	13	15 December 1937	05:00	91	

4.1 The flood of 22 November 2022 (ID 27; rank 4)

To our knowledge, this flood has only been studied in a paper by (Mel et al., 2023). They evaluated the effectiveness of the ISPRA sea state monitoring system by modelling a hypothetical scenario without the Mo.S.E. (Modulo Sperimentale Elettromeccanico) flood defense system and demonstrated that, without regulation, the sea level at Chioggia would have

230 exceeded 200 cm above the reference datum – an unprecedented level in the monitoring history of the Venice Lagoon.

4.1.1 Meteorological background

In the weeks leading up to the flood, two pronounced low-pressure systems moved over the Adriatic Sea, the first one on 4 November, and second on 18 November (Fig. 3a).

235
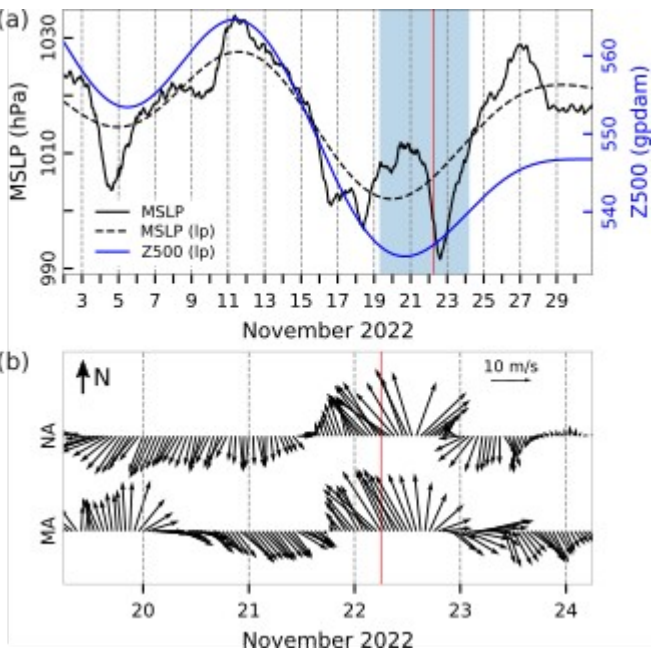
Figure 3: Series of ERA5 reanalysis data related to the flood of 22 November 2022. (a) MSLP (hourly) and MSLP (lp) (low-pass filtered with a cut-off frequency of 10 d) and Z500 (lp) (low-pass filtered with a cut-off frequency of 10 d) at a grid point near TG Bakar. (b) Hourly **W10** during the period marked in blue in the upper plot for the middle (MA) and northern (NA) Adriatic (all locations marked in Fig. 1). The red line indicates onset of SL maximum.

240

245

250 On the night of 21/22 November, a rapid cyclogenesis was underway in the Ligurian Sea (Fig. 4a). The cyclone, accompanied by its frontal system, moved slowly across the Apennine Peninsula towards the Adriatic Sea on 22 November, with MSLP dropping to less than 990 hPa at its centre (Fig. 4b). As a result, a strong and gale southeasterly and southerly wind (according to Beaufort scale, strong wind: 10.8–13.8 m/s; gale wind: 17.2–20.70 m/s) blew over the Adriatic for hours

before sea level peaked in Bakar (Figs. 3b and 4b), and when the cyclone left the area (during the night of 22/23 November),

255 a gale northeast and east wind prevailed in the northern part (Fig. 3b). In addition, large amounts of precipitation were measured along the Croatian coast: often more than 30 mm at stations in the middle Adriatic, but the largest amounts were recorded in the northern Adriatic (e.g. the Cres station in the northern Adriatic recorded 132.5 mm on 23 November).
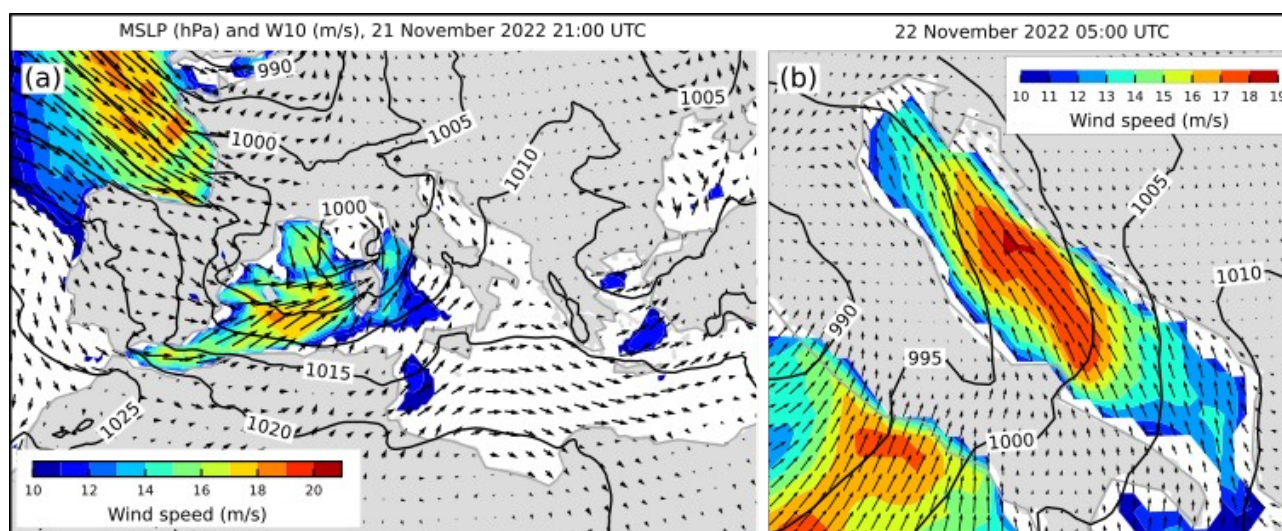
Figure 4: MSLP (black lines) and **W10** (arrows and colours) fields from the ERA5 reanalysis. Conditions (a) over the Mediterranean

260 depicting a cyclone over the Ligurian Sea that preceded the situation (b) over the Adriatic Sea an hour before maximum SL in Bakar. Only wind speeds exceeding 10 m/s are coloured.

4.1.2 Sea-level evolution

In the morning hours of 22 November 2022 (06:00 UTC), the SL in Bakar rose to 101 cm above the long-term average (Table 2, Fig. 5).

265 The total SL maximum occurred during the tidal peak (Fig. 5). At this time, the moon was in a phase between the last quarter and the new moon, resulting in a semidiurnal spring tide. *Tide* added substantial 30 cm to the flood.

Figure 5 shows that *local processes* during this episode were generally not pronounced, but the total SL maximum formed during their peak, which is why the contribution of *local processes* amounted to 12 cm.

Before the cyclone crossed the Adriatic on 22 November, another atmospheric disturbance passed over the basin on 18

270 November, but it was not as pronounced as the decisive one (Fig. 4a) and did not trigger strong basin-wide oscillations (Fig. 5b). Therefore, there were no pre-existing seiches (T~21.2 h) and *synoptic component* consisted mainly of the forced part, i.e., of storm surge. Although the induced storm surge reached a significant maximum of 56 cm, the total SL peak occurred before its peak (Fig. 4a), when *synoptic component* was 20 cm. This was because the other components were strong before the storm surge peaked and, above all, because *tide* (which had a large amplitude) was in its negative phase at the time of

275 *synoptic component* maximum.
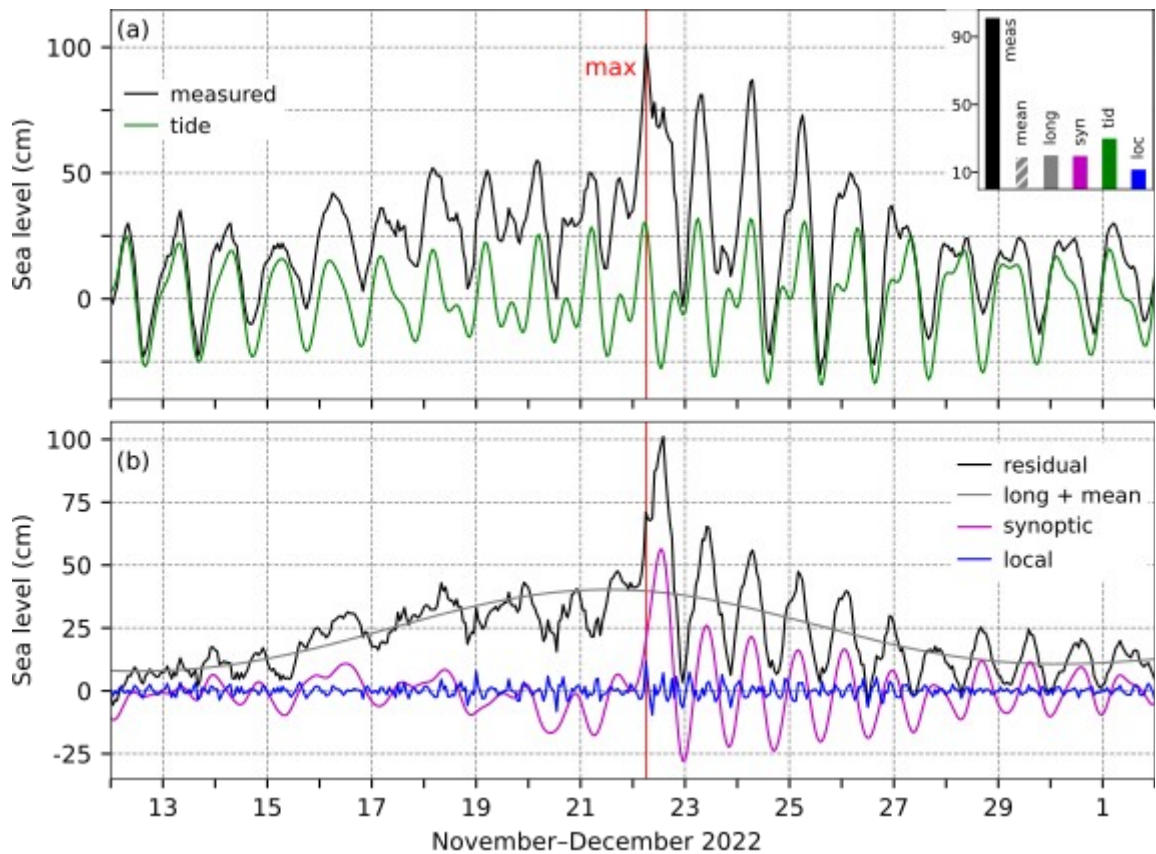
Figure 5: SL series for the flood of 22 November 2022. (a) Measured sea level (black) and *tide* (green). The inset figure shows the contributions (cm) of the five sea-level components to the maximum measured sea level ("meas"; 06:00 UTC): "loc" refers to *local component* (9 h < T), "syn" to *synoptic component* (9 h < T < 10 d), "tid" to *tide*, "long" to *long-period sea-level component* (10 < T < 100

280 d), "mean" to *mean sea-level changes* (100 d < T). (b) Residual sea level (black), the combined series of *long-period sea-level component* and *mean sea-level changes* (grey; long + mean), *synoptic component* (purple), and *local component* (blue). The red line indicates the time of occurrence of the total SL maximum.

Preconditioning (estimated by assessing *long-period sea-level component*) began ten days before the episode under the influence of a drop in MSLP (lp) that began on 12 November (Fig. 4a), when the SL started to rise (long + mean, Fig. 5b).

285 Comparison of Z500 (lp), MSLP (lp) and long + mean shows that all three series varied coherently which, as Pasarić (2000), Pasarić et al. (2000) and Pasarić and Orlić (2001) showed, indicates that *long-period sea-level component* was dominantly controlled by a passage of planetary Rossby waves. This component contributed 20 cm to the flood, the same as *synoptic component*.

Mean sea-level changes (100 d < T) contributed 19 cm to this episode, which was comparable to the contributions from

290 *synoptic* and *long-period sea-level components* (Fig. 5a, histogram). This high contribution was mainly due to the seasonal cycle and interannual variability (13 cm), as the episode occurred during the annual maximum (Figs. A1 and A2), as well as the influence of secular change (6 cm, Fig. A3a). The (multi)decadal fluctuations during this period were negligible (0 cm, Fig. A3b). However, since the 2022 episode is at the end of the analysed time series, the contribution from *mean sea-level changes* (occurring at periods longer than 100 d) may not have been accurately calculated due to edge effects (as discussed
295 in Sect. 3.2 and shown in Fig. A2a).

This flood was the result of a constructive superposition of all contributing processes. *Tide* had the greatest impact, while *synoptic, long-period*, and *mean sea-level changes* had similar effects, and *local processes* had the smallest influence (Fig. 5).

4.1.3 Flood impacts

300 On this day, DHMZ issued the highest, red wind warnings (corresponding to a very dangerous weather with likely major damages and accidents; METEOALARM) for the entire coastal region of the Adriatic. Wind gusts of up to 29 m/s and 35 m/s were registered in the middle and southern Adriatic, respectively. Online sources from 22 November 2022 (Novi list; Index.hr; Poslovni dnevnik; Jurarnji list; Portal Istra Terra Magica; Dubrovački vjesnik; Šibenski portal Moć komunikacije) revealed the following impacts of the event. Along the entire eastern Adriatic (Croatian) coast, there was widespread
305 flooding of basements, residential and commercial premises including restaurants, cáfes, shops, and farmer's markets; road closures; suspension of ferry and catamaran lines; fallen trees and rockslides. In the northern Adriatic, there were localised power outages, and for the middle Adriatic, journalists report collapse of dry-stone walls, river overflowing and flooding of a coastal town.

4.2 The flood of 8 December 2021 (ID 26; rank 7)

310 This event has not yet been addressed in the scientific literature.

4.2.1 Meteorological background

A series of cyclones crossed the Adriatic from 26 November to 12 December (Fig. 6a). The cyclones were related to upper level trough which persisted over the area. During 6 and 7 December, a deep cyclone, the so-called Barra, formed over the Atlantic, in the centre of which the air pressure dropped to 960 hPa on 7 December (Storm Barra | Copernicus, 2024).
315 The frontal system associated with this cyclone approached the European mainland on 7 December and then moved further east. As a result of the movement of this system, leeward cyclogenesis occurred in the Gulf of Lion during the night of 7 December. Over the course of the next day (8 December), the newly formed cyclone first moved into the Gulf of Genoa (Fig.

7a), intensified there and then moved on towards the Adriatic Sea in the evening of 8 December (Fig. 7b). Under these synoptic conditions — simultaneous presence of the centre of the cyclone over the Adriatic and the centre of another deep cyclone over the North Sea (Barra) — strong to gale southeasterly winds developed over most of the Adriatic (Figs. 6b and 7b), accompanied by precipitation exceeding 30 mm along the Croatian coastline, with measurements on 8 December showing 52 mm in Rijeka, 59 mm in Bakar, and 53 mm in Makarska (near Split).
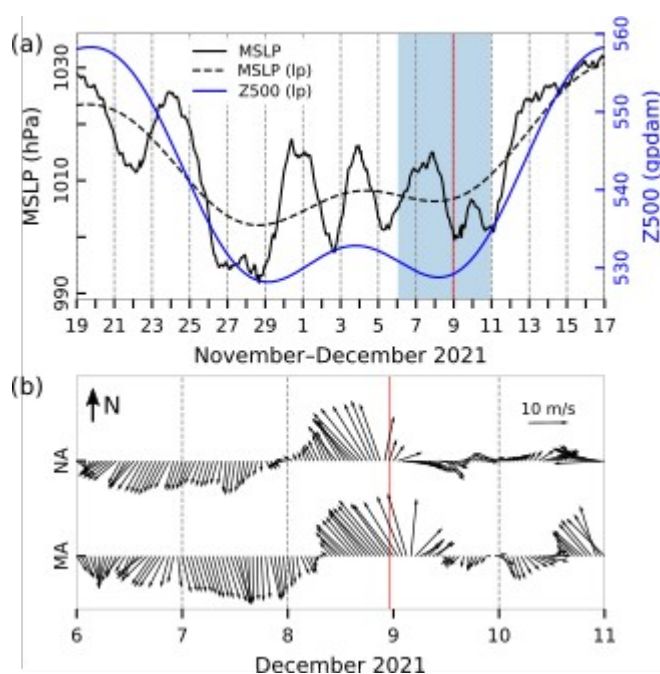
Figure 6: Series of ERA5 reanalysis data related to the flood of 8 December 2021. (a) MSLP (hourly) and MSLP (lp) (low-pass filtered with a cut-off frequency of 10 d) and Z500 (lp) (low-pass filtered with a cut-off frequency of 10 d) at a grid point near TG Bakar. (b) Hourly **W10** during the period marked in blue in the upper plot for the middle (MA) and northern (NA) Adriatic (all locations marked in Fig. 1). The red line indicates onset of SL maximum.
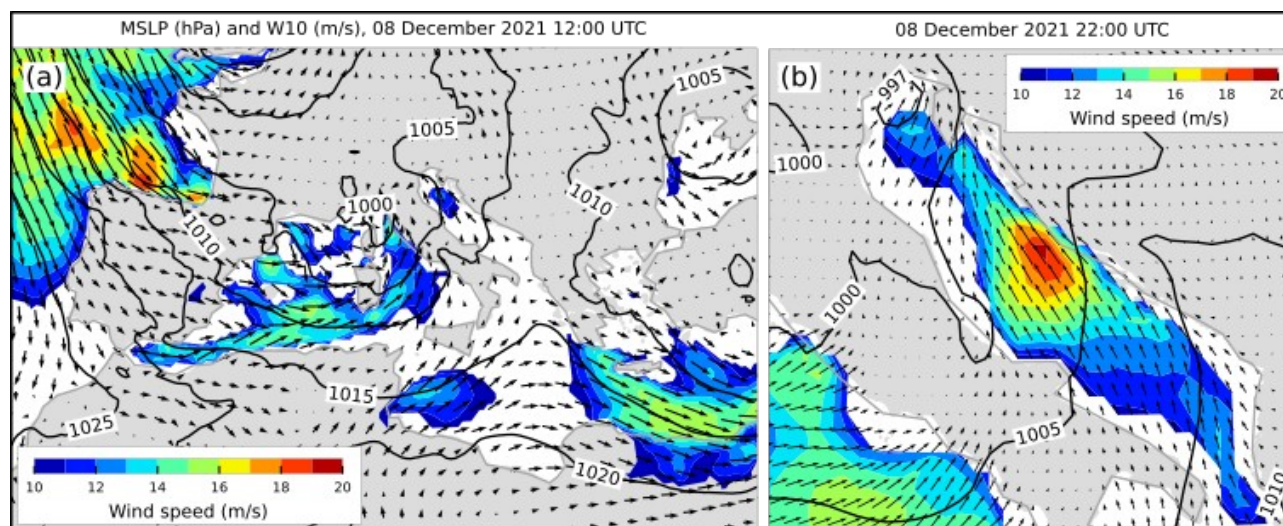
Figure 7: MSLP (black lines) and **W10** (arrows and colours) fields from the ERA5 reanalysis. Conditions (a) over the Mediterranean depicting a cyclone over the Gulf of Genoa that preceded the situation (b) over the Adriatic Sea (an hour before maximum SL in Bakar).
340 Only wind speeds exceeding 10 m/s are coloured.

4.2.2 Sea-level evolution

By 23:00 UTC of 8 December 2021, the sea level in Bakar rose to 97 cm above the long-term average (Table 2, Figure 8). The total SL reached its maximum near the daily peak of *tide*. The lunar phase was close to the first quarter, hence *tide* had a diurnal neap-tide character and contributed 10 cm to the maximum.
345 Figure 8b shows that the small-amplitude Kvarner Bay seiche (T~6h) was generated on 8 December and that the overall maximum formed at its peak (*local processes* contributed 7 cm).
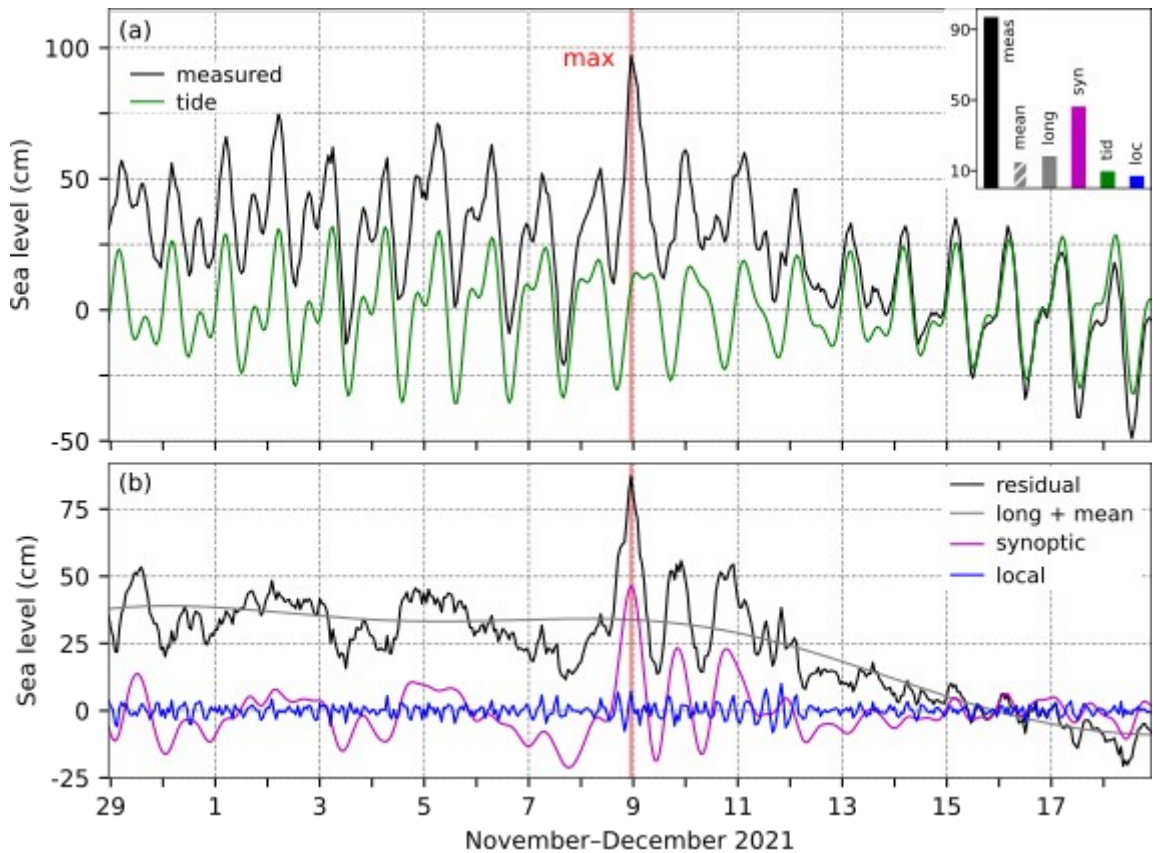
Figure 8: SL series for the flood of 8 December 2021. (a) Measured sea level (black) and *tide* (green). The inset figure shows the contributions (cm) of the five sea-level components to the maximum measured sea level ("meas"; 23:00 UTC): "loc" refers to *local*
350 *component* (9 h < T), "syn" to *synoptic component* (9 h < T < 10 d), "tid" to *tide*, "long" to *long-period sea-level component* (10 < T < 100 d), "mean" to *mean sea-level changes* (100 d < T). (b) Residual sea level (black), the combined series of *long-period sea-level component*

and *mean sea-level changes* (grey; long + mean), *synoptic component* (purple), and *local component* (blue). The red line indicates the time of occurrence of the total SL maximum.

Synoptic component was induced by the MSLP distribution and winds related to a rapidly developing Mediterranean cyclone
355   and a Barra system centered over the Atlantic (Fig. 7). Although several atmospheric disturbances moved across the basin in the days before the flood (Fig. 6a), they did not trigger basin-wide oscillations (T~21.2 h) due to the weak pressure gradients and slight wind changes over the basin, so there were no active seiches before this maximum (Fig. 8b). Therefore, *synoptic component* consisted only of the storm surge, which amounted to 46 cm at its peak. The storm surge began to build slowly at the end of 7 December, but the largest build up occurred during a short interval (~12 h) on 8 December under the influence
360   of the pressure gradient and Sirocco wind.

The preconditions for the flood began two weeks earlier, when *long-period sea-level component* started to rise as a result of a slow atmospheric-pressure drop and southwest wind. Figure 6a shows that the MSLP (lp) began to decrease around 20 November, at about the same time that the winds at these frequencies (10–100 d) turned toward the eastern Adriatic coast at a maximum speed of 5 m/s (not shown). Since *long-period sea-level component* mirrored the changes in MSLP (lp) and the
365   MSLP (lp) varied concurrently with the Z500 (lp), we conclude that on this occasion the long-period variations in sea level were driven by the passage of Rossby waves, which are visible as waveforms in the Z500 (lp) series (Fig. 6a). *Long-period sea-level component* added 18 cm to this episode.

Mean sea-level changes (100 d < T) contributed 16 cm to this flood (Fig. 8a, histogram). The episode occurred in early December, coinciding with the annual SL maximum of 10 cm (Figs. A1 and A2). During this period, (multi)decadal changes
370   made no contribution (0 cm, Fig. A3b), while the linear sea-level trend provided 6 cm (Fig. A3a). It is worth noting that the 2021 episode occurs near the end of the analysed time series, which may have led to an underestimation of the contribution from (multi)decadal processes due to edge effects (as discussed in Sect. 3.2 and shown in Fig. A2a).

This flood resulted from the positive superposition of all processes involved, with *synoptic component* having the strongest effect (Fig. 8).

375   **4.2.3 Flood impacts**

On 8 December 2021, DHMZ issued an orange weather warning (METEOALARM) for the Adriatic coast due to severe Sirocco winds ranging from 18 to 31 m/s. Additionally, a significant amount of precipitation was registered during both that day and the following one. A review of the available daily newspapers (Novi list, 10 December 2021) and online sources from 9 December 2021 (MorskiHR; Dalmacija Danas; Radio Dalmacija; Hrvatska Danas) revealed the following effects of
380   the flood: (i) interruption of numerous ferry and catamaran lines, especially in the middle and southern Adriatic; (ii) flooding of buildings on the coast, and boats being washed ashore in the northern Adriatic; (iii) numerous fallen trees in the middle Adriatic.

4.3 The flood of 8 December 2020 (ID 25; rank 12)

This episode has not yet been examined in the scientific literature.

385 ### 4.3.1 Meteorological background
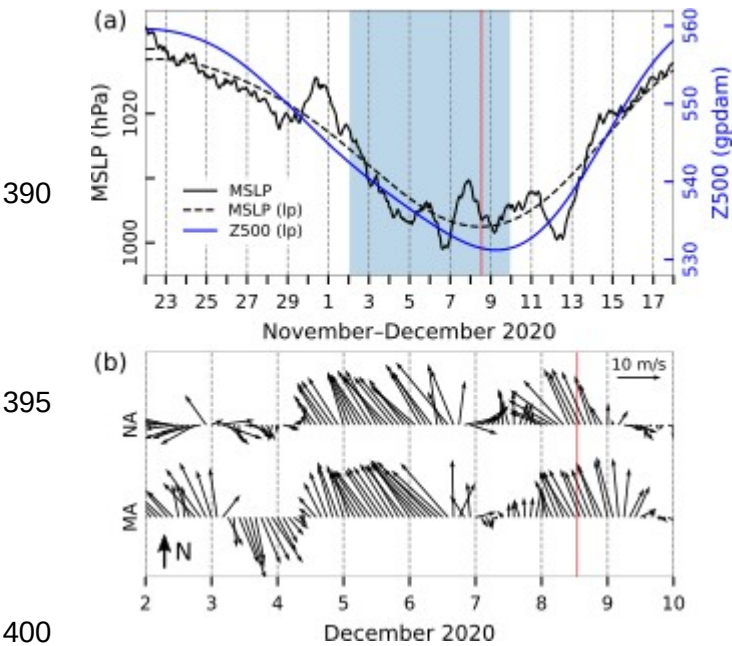
Figure 9: Series of ERA5 reanalysis data related to the flood of 8 December 2020. (a) MSLP (hourly) and MSLP (lp) (low-pass filtered with a cut-off frequency of 10 d) and Z500 (lp) (low-pass filtered with a cut-off frequency of 10 d) at a grid point near TG Bakar. (b) Hourly **W10** during the period marked in blue in the upper plot for the middle (MA) and northern (NA) Adriatic (all locations marked in Fig. 1). The red line indicates onset of SL maximum.

In the week prior to the occurrence of the extreme sea level in Bakar, several intense cyclones affected weather conditions over the Adriatic. According to the Z500 fields, the Adriatic was on the front of a significant trough that stretched from Greenland across western Europe and the Mediterranean to Africa. These conditions supported a pronounced southwesterly flow in the upper levels, bringing moist and relatively warm air. The main event was preceded by several episodes of strong and intense Sirocco (Fig. 9). On 6 December, an intense cyclone accompanied by a frontal system moved from the western Europe and Gulf of Genoa towards the northern Adriatic, causing strong southerly winds that gradually weakened towards the end of the day (Fig. 9). The cyclone also brought heavy precipitation along the Croatian coastline. On 7 December, coastal stations from the southern to northern Adriatic recorded over 30 mm of precipitation, including 65 mm in Pula, 44 mm in Rijeka, 39 mm in Zadar, 43 mm in Šibenik, 38 mm in Split-Marjan, and 39 mm at Dubrovnik airport.

By 00:00 UTC on 8 December, while a cyclone over western Europe remained active, another low-pressure centre formed over the Gulf of Lion and moved toward the Gulf of Genoa (Fig. 10a). This development triggered southeasterly winds, initially affecting the northern Adriatic and later spreading throughout the entire basin (Fig. 9b). Generally, the southeasterly

winds were more intense along the eastern than along the western Adriatic coast (Fig. 10b). The southeasterly winds reached

415 their maximum on the northern and middle Adriatic before the occlusion front moved across the basin, while a moderate

Bora prevailed in the Bay of Trieste.
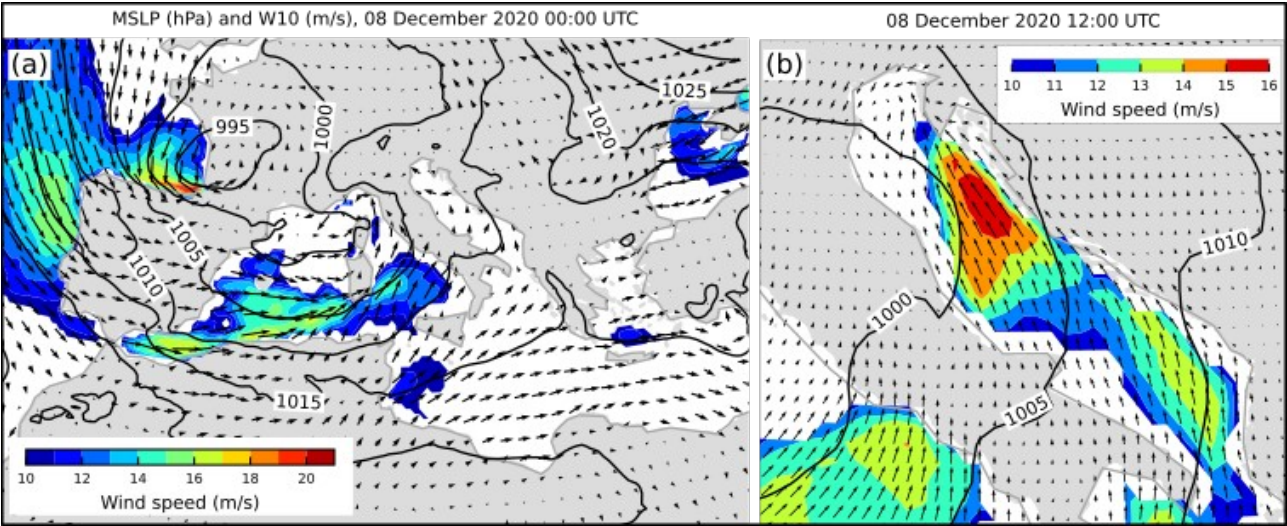
Figure 10: MSLP (black lines) and **W10** (arrows and colours) fields from the ERA5 reanalysis. Conditions (a) over the Mediterranean and western Europe that preceded the situation (b) over the Adriatic Sea (an hour before maximum SL in Bakar). Only wind speeds exceeding

420 10 m/s are coloured.

4.3.2 Sea-level evolution

On 8 December 2020 at 13:00 UTC, the sea level in Bakar rose to 92 cm above the long-term average (Table 2, Fig. 11).

On this day, the moon was in the last quarter, meaning that *tide* had a diurnal neap-tide character. The overall maximum

formed during the negative phase of *tide*, hence *tide* provided a negative contribution of 1 cm to this event (Fig. 11).

425 *Local processes* were also not pronounced — their contribution was negligible (1 cm).

The sequence of cyclones in the week before the main maximum led to the formation of basin-wide seiche (T~21.2 h). Based

on the residual and *synoptic component* (Fig. 11b), the first oscillations were triggered on 3 December and intensified on 6

December when the prolonged Sirocco shifted to a northwesterly wind (Fig. 9b) causing SL to rise to 88 cm. Thus, *synoptic

component* consisted of a storm surge and pre-existing Adriatic seiche, and at the time of the main maximum it amounted to

430 41 cm. The seiches amplified the flood because they were in a positive phase with the newly formed storm surge.

The preconditions began to develop around 29 November, marked by a rise in SL (Fig. 11b, long + mean), induced by a

decrease in atmospheric pressure (Fig. 9a, MSLP (lp)) and a persistent southeasterly wind at periods of 10–100 d. This wind

blew from southeast from 1 to 11 December, peaking at over 6 m/s on 6 December (not shown). The simultaneous variations

in Z500 (lp), MSLP (lp) (Fig. 9a), and SL (long + mean) suggest that atmospheric Rossby waves were responsible for *long-*

435 *period sea-level variability*. The amplitude of this component was substantial, comparable to *synoptic component*, reaching 33 cm at the time of the total maximum.
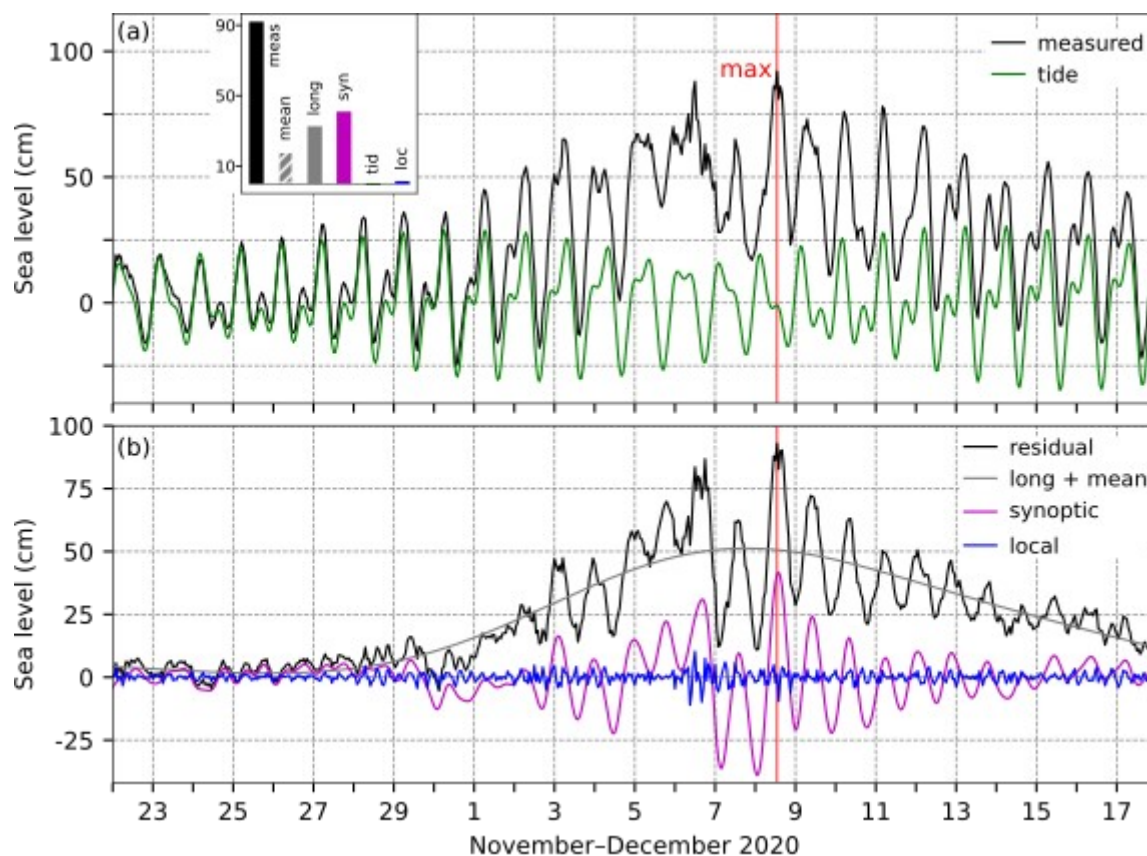
Figure 11: SL series for the flood of 8 December 2020. (a) Measured sea level (black) and *tide* (green). The inset figure shows the contributions (cm) of the five sea-level components to the maximum measured sea level ("meas"; 13:00 UTC): "loc" refers to *local*
440 *component* (9 h < T), "syn" to *synoptic component* (9 h < T < 10 d), "tid" to *tide*, "long" to *long-period sea-level component* (10 < T < 100 d), "mean" to *mean sea-level changes* (100 d < T). (b) Residual sea level (black), the combined series of *long-period sea-level component* and *mean sea-level changes* (grey; long + mean), *synoptic component* (purple), and *local component* (blue). The red line indicates the time of occurrence of the total SL maximum.

Mean sea-level changes (100 d < T) contributed 18 cm to this episode (Fig. 11a, histogram). The episode occurred in winter,
445 close to the annual SL peak (13 cm, Figs. A1 and A2). During this time, the contribution of (multi)decadal changes was negligible (0 cm, Fig. A3b), while secular changes added 5 cm (Fig. A3a). As noted for the later floods (2021 and 2022), estimating longer-period processes for episodes at the end of the analysed time series may be unreliable due to filtering effects.

To summarise, this episode resulted from the combined effects of large *synoptic* and *long-period sea-level components*,

450 superimposed on *mean sea-level changes*, with minimal or negative contributions from *local processes* and *tide* (Fig. 11).

4.3.3 Flood impacts

According to an online source (Jutarnji list, 8 December 2020), severe weather on 8 December 2020 impacted much of Croatia, particularly the Istria region (Fig. 1). Istramet reported strong Sirocco winds with gusts up to 36.4 m/s, heavy rain, and widespread flooding. Along the east coast of Istria, the sea overflowed waterfronts, flooding areas in Rovinj and Pula.

455 The high water levels caused road closures and significant traffic disruptions across Istria and Kvarner. Ferry services between Rijeka and the Kvarner islands, as well as Split and the central Dalmatian islands, were suspended. Dalmatian coastal towns, such as Zadar and Šibenik experienced street and property flooding, along with damage to boats, cars, shores, and piers. Traffic along the coast was heavily disrupted, with some areas rendered impassable, forcing residents to wade through ankle-deep water.

460 **4.4 The flood of 23 December 2019 (ID 24; rank 10)**

The November–December 2019 period was characterised by frequent cyclone activity over the Adriatic, leading to numerous storm surges and subsequent seiches. These conditions posed significant challenges for forecasting systems based on hydrodynamic models (Bajo et al., 2023) and machine learning approaches (Rus et al., 2023; 2024), making it an ideal case to evaluate their performance.

465 **4.4.1 Meteorological background**

On 18, 19, and 20 December, western and a large part of central and southern Europe was affected by a major upper-level trough associated with pronounced cyclonic activity at the low levels over the British Isles and along the coast of western Europe. At the same time, the influence of the upper-level ridge and surface-based anticyclone prevailed further east (air pressure over Turkey was 1030 hPa). In such a synoptic situation, a strong air pressure gradient was established over Europe,

470 between the northwest and southeast, and as a result, moderate to strong, locally gale southeast wind blew over the Adriatic (Fig. 12).

On 21 December, a cyclone formed over the Gulf of Genoa, and moved straight to the northern Adriatic during the day, intensified there to 990 hPa in its centre, and then continued further towards the northeast. The propagation of this cyclone supported the southerly flow over the Adriatic area. At the same time, a new cyclone was approaching the British Isles and

475 gradually intensifying (pressure up to 965 hPa in the centre), and it extended through the troposphere up to 500 hPa level. As its frontal system entered the European mainland, a secondary cyclone developed in the Gulf of Genoa in the first hours of 22 December. This cyclone further deepened (to less than 985 hPa; Fig. 13a) while rapidly propagating over the Adriatic

(Fig. 13b) and by the end of the day moved further to the east. In the upper levels, the trough, with the axis laid out in the NW-SE direction, propagated across the Adriatic. During the day (22 December), strong and gale southeasterly and

480   southwesterly wind blew over the Adriatic, accompanied by locally heavy precipitation (e.g., 46 mm in Bakar, 34 mm in Zadar). As the cyclone moved eastward, the wind shifted to the westerly and northwesterly over a greater part of the Adriatic (Fig. 12b).

485

490
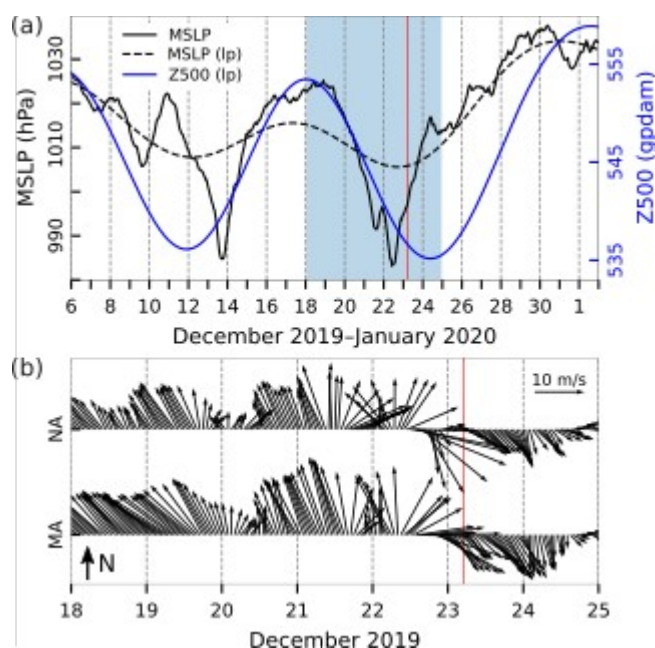
Figure 12: Series of ERA5 reanalysis data related to the flood of 23 December 2019. (a) MSLP (hourly) and MSLP (lp) (low-pass filtered with a cut-off frequency of 10 d) and Z500 (lp) (low-pass filtered with a cut-off frequency of 10 d) at a grid point near TG Bakar. (b) Hourly **W10** during the period marked in blue in the upper plot for the middle (MA) and northern (NA) Adriatic (all locations marked in Fig. 1). The red line indicates onset of SL maximum.
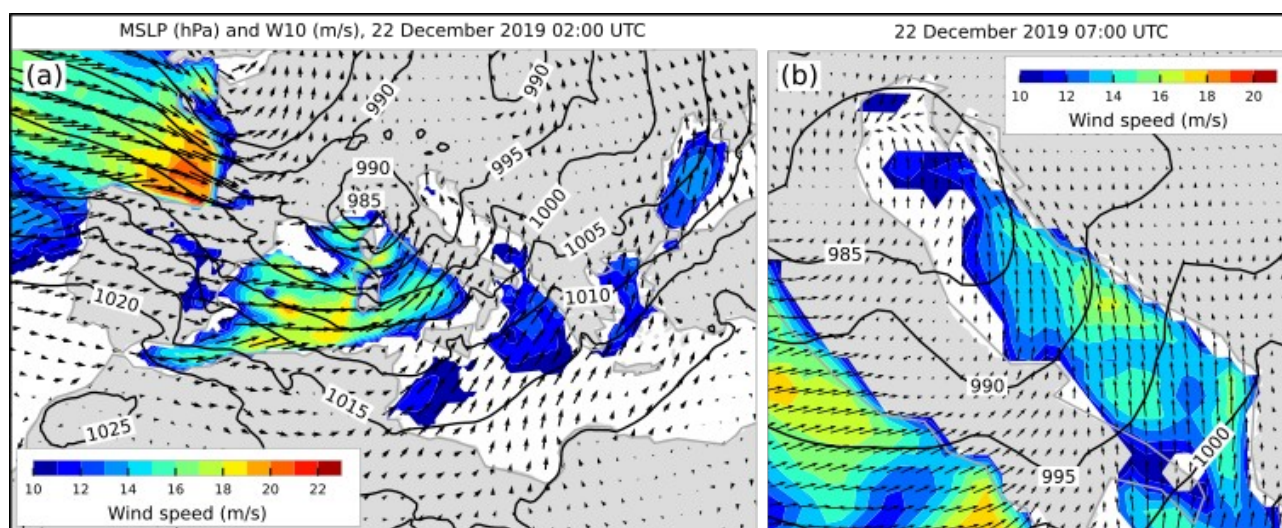
Figure 13: MSLP (black lines) and **W10** (arrows and colours) fields from the ERA5 reanalysis. Conditions (a) over the Mediterranean

495 depicting a cyclone over the Gulf of Genoa that preceded the situation (b) over the Adriatic Sea (22 h before the flood). Only wind speeds exceeding 10 m/s are coloured.

4.4.2 Sea-level evolution

In the morning hours of 23 December 2019 (05:00 UTC), the sea level in Bakar rose to 94 cm above the long-term average (Table 2, Fig. 14).

500 The moon phase was between the last quarter and the new moon, which gave *tide* a semidiurnal spring-tide character. The overall maximum formed during the daily maximum of *tide,* which amounted to a high 27 cm.

Local processes were not pronounced during this episode and contributed only 2 cm.
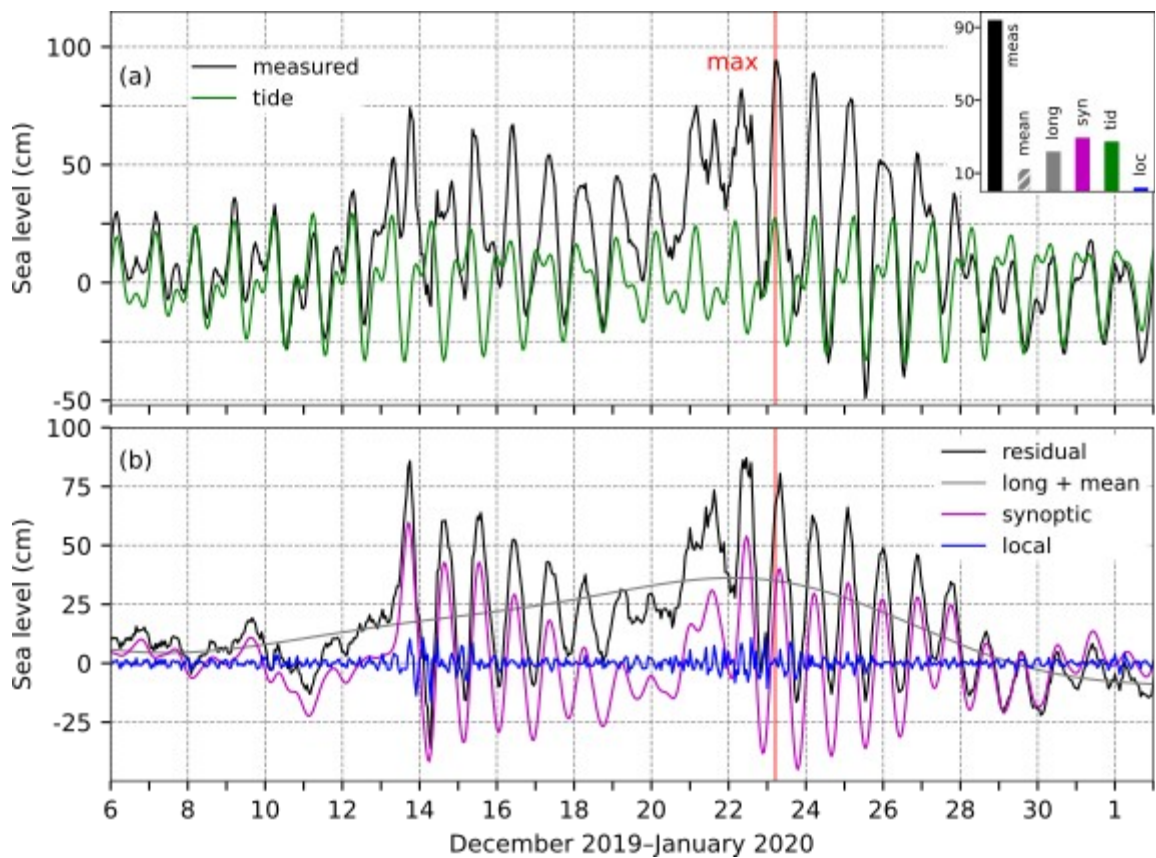
Figure 14: SL series for the flood of 23 December 2019. (a) Measured sea level (black) and *tide* (green). The inset figure shows the
505 contributions (cm) of the five sea-level components to the maximum measured sea level ("meas"; 05:00 UTC): "loc" refers to *local component* (9 h < T), "syn" to *synoptic component* (9 h < T < 10 d), "tid" to *tide,* "long" to *long-period sea-level component* (10 < T < 100 d), "mean" to *mean sea-level changes* (100 d < T). (b) Residual sea level (black), the combined series of *long-period sea-level component* and *mean sea-level changes* (grey; long + mean), *synoptic component* (purple), and *local component* (blue). The red line indicates the time

of occurrence of the total SL maximum.

510 Figure 12a shows that a cyclone passed over the Adriatic on 13 December, 10 days before the flooding event, causing a high storm surge and subsequent basin-wide oscillations (Fig. 14b). An exceptional SL was not recorded on 13 December, as the induced storm surge overlapped with the negative *tide* (the residual SL was 86 cm high). The seiche weakened until 21 December when another cyclone approached the Adriatic and triggered another series of seiches, which were further intensified by the decisive cyclone on 22 December (Fig. 13). The next day (23 December), as the wind field over the basin

515 weakened and turned to the westerly and northwesterly (Fig. 12b), the positive phase of the generated seiche overlapped with *tide*, resulting in a high total SL (Fig. 14). At the time of the highest water level, *synoptic component* consisted mainly of free oscillations generated the previous day and it amounted to 30 cm.

Long-period sea-level component contributed 22 cm to the overall SL maximum. Preconditioning began about two weeks before the flood, characterised by a steady SL increase (Fig. 14b, long + mean), which continued up to the flood, even

520 though MSLP (lp) did not show a consistent decrease (Fig. 12a). The primary driver of the long-period SL rise was the persistent, strong southerly wind (at periods 10–100 d), reaching speeds of 6 m/s on 19 December and lasting for over a week before the flood (not shown).

Mean sea-level changes (100 d < T) contributed 13 cm to this maximum (Fig. 14a, histogram). The episode occurred after the annual SL peak, which was particularly pronounced that year (Figs. A1, A2a, and A2c). Seasonal and interannual

525 variability contributed 7 cm. Similar to other recent episodes, the contribution from (multi)decadal changes was minimal (1 cm, Fig. A2b), while secular change contributed 5 cm (Fig. A3). It should also be noted that, since this episode is near the end of the analysed series, (multi)decadal variations may have been underestimated due to edge effects from filtering.

To summarise, the flood formed almost one day after the decisive cyclone crossed the Adriatic (Figs. 12b and 13b), mainly as a result of fine-tuning between a pre-existing seiche and *tide*, superimposed on an raised background SL. *Local processes*

530 had the weakest effect (Fig. 14).

4.4.3 Flood impacts

A review of available daily newspapers (Slobodna Dalmacija, 25 December 2019) and online sources from 23 December 2019 (Hrvatska vatrogasna zajednica; Zadarski.hr) and 24 December 2019 (Civilna zaštita; Otvoreno.hr; Šibenski.) revealed the following effects of the flood. The high sea level, strong winds and heavy rain led to traffic disruptions, fallen trees and

535 flooded roads along the entire coast. Numerous firefighters' operations were recorded, involving the removal of trees, pumping out water and recovering vehicles. The greatest damage was reported in the middle Adriatic, where: (i) one person drowned; (ii) a destructive waterspout, resulting in damage to roofs, electricity pylons, vehicles and trees, occurred; (iii) seafront promenades were damaged; (iv) several low-lying historic town centres were flooded.

4.5 The flood of 13 and 15 November 2019 (IDs 22 and 23; ranks 5 and 12)

540 As previously mentioned, the November–December 2019 period was characterised by frequent cyclonic activity, resulting in numerous storm surges and subsequent seiches in the Adriatic. These conditions provided an opportunity to evaluate the performance of forecasting systems based on hydrodynamic models (Bajo et al., 2023) and machine learning approaches (Žust et al., 2021; Rus et al., 2023; 2024). Also, the 12 November 2019 flood in Venice, the second worst ever recorded, has been analysed by several authors (Cavaleri et al., 2020; Ferrarin et al., 2021; 2023; Lionello et al., 2021; Orlić and Pasarić,

545 2024). The flood was underestimated by forecasting systems, including both hydrodynamic and machine-learning models, prompting an investigation into the contributing processes. Further motivation to study this event came from a small-scale atmospheric disturbance crossing the Venetian Lagoon, which triggered an unusually strong SL response at higher frequencies – a phenomenon rarely observed along the western Adriatic coast (Ferrarin et al., 2021; 2023).

4.5.1 Meteorological background

550 In the period from 10 to 15 November, the weather over the Adriatic was characterised by the passage of three cyclones (Fig. 15a), which resulted with variable-intensity winds over the Adriatic blowing for days, predominantly from the southeast (Fig. 15b). The generation and propagation of the mentioned cyclones was supported by upper-level conditions that included a wide upper-level trough in the western half of Europe, and a well-pronounced ridge in its eastern part.

On 10 November, in the western Mediterranean, a cyclone developed and gradually deepened during the next day. In the

555 upper-level, a closed circulation of low pressure developed within and near the base of the trough. At the leading side of this trough unstable air was transported towards the Adriatic Sea. As the cyclone slowly moved towards Sardinia, the southeast wind over the Adriatic gradually increased during 11 November (Fig. 15b). The next day, 12 November, the centre of the cyclone moved over the Tyrrhenian Sea (Fig. 16a), causing a further increase of southeast and south wind over the Adriatic. Over the south and middle Adriatic, the wind was strong to gale with hurricane gusts (e.g., 38 m/s in Split, 41 m/s in

560 Dubrovnik; according to Beaufort, hurricane winds are greater than 32.8 m/s), and locally heavy precipitation was measured (25–50 mm). The following day, 13 November, in the morning hours, the centre of the cyclone gradually moved over the Adriatic area (Fig. 16b). This led to strong and gale, and occasionally hurricane southeasterly wind over the Adriatic, accompanied by heavy precipitation. Amounts of precipitation ranged 30–50 mm along the Croatian coastline, with locally higher values, such as 71 mm in Lošinj (Kvarner), 61 mm in Zadar, and 101 mm in Supetar (near Split). The upper-level

565 flow was still southwesterly on the downstream side of a deep and well-pronounced trough that stretched from Iceland in the north to Egypt in the south. As the day progressed, the cyclone gradually filled over the Adriatic, leading to the air-pressure gradient weakening. Therefore, the southeasterly wind also gradually decreased, turning to southwesterly and southerly wind (Fig. 15b).

On 14 November, the above mentioned cyclone moved eastward, and air pressure over the Adriatic was around 1013 hPa
570 (Fig. 15a). In the upper-level, the flow was southwesterly on the downstream side of a vast trough that covered the entire
western half of Europe and whose axis stretched from the North Sea through France and the Mediterranean to the north of
Africa. This trough was accompanied by a surface low over the Bay of Biscay (with the air pressure in the centre of 990
hPa). As this cyclone approached the European mainland on 14 November, a new cyclone in the Gulf of Lion started to form
(Fig. 16c). This new cyclone moved towards the Gulf of Genoa and further towards the northeast. On 15 November, its
575 frontal system affected the Adriatic, remaining almost stationary there (Fig. 16d). At the same time, the upper-level ridge
accompanied by a surface high pressure remained in the east of the continent. As a result, there was a pronounced air
pressure gradient over the Adriatic which led to the strong and gale southeast wind (Fig. 15b).

580

585

590
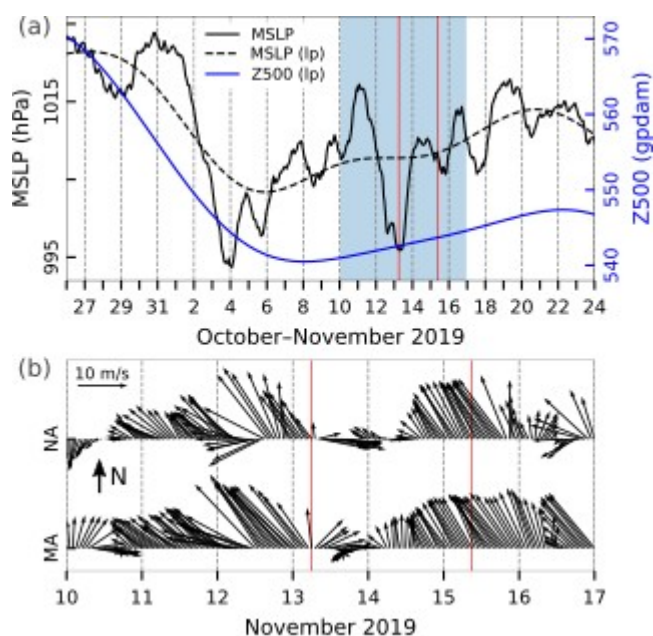
Fig. 15. Series of ERA5 reanalysis data related to the floods of 13
and 15 November 2019. (a) MSLP (hourly) and MSLP (lp) (low-
pass filtered with a cut-off frequency of 10 d) and Z500 (lp) (low-
pass filtered with a cut-off frequency of 10 d) at a grid point near TG
Bakar. (b) Hourly **W10** during the period marked in blue in the
upper plot for the middle (MA) and northern (NA) Adriatic (all
locations marked in Fig. 1). The red lines indicate onset of SL
maxima.
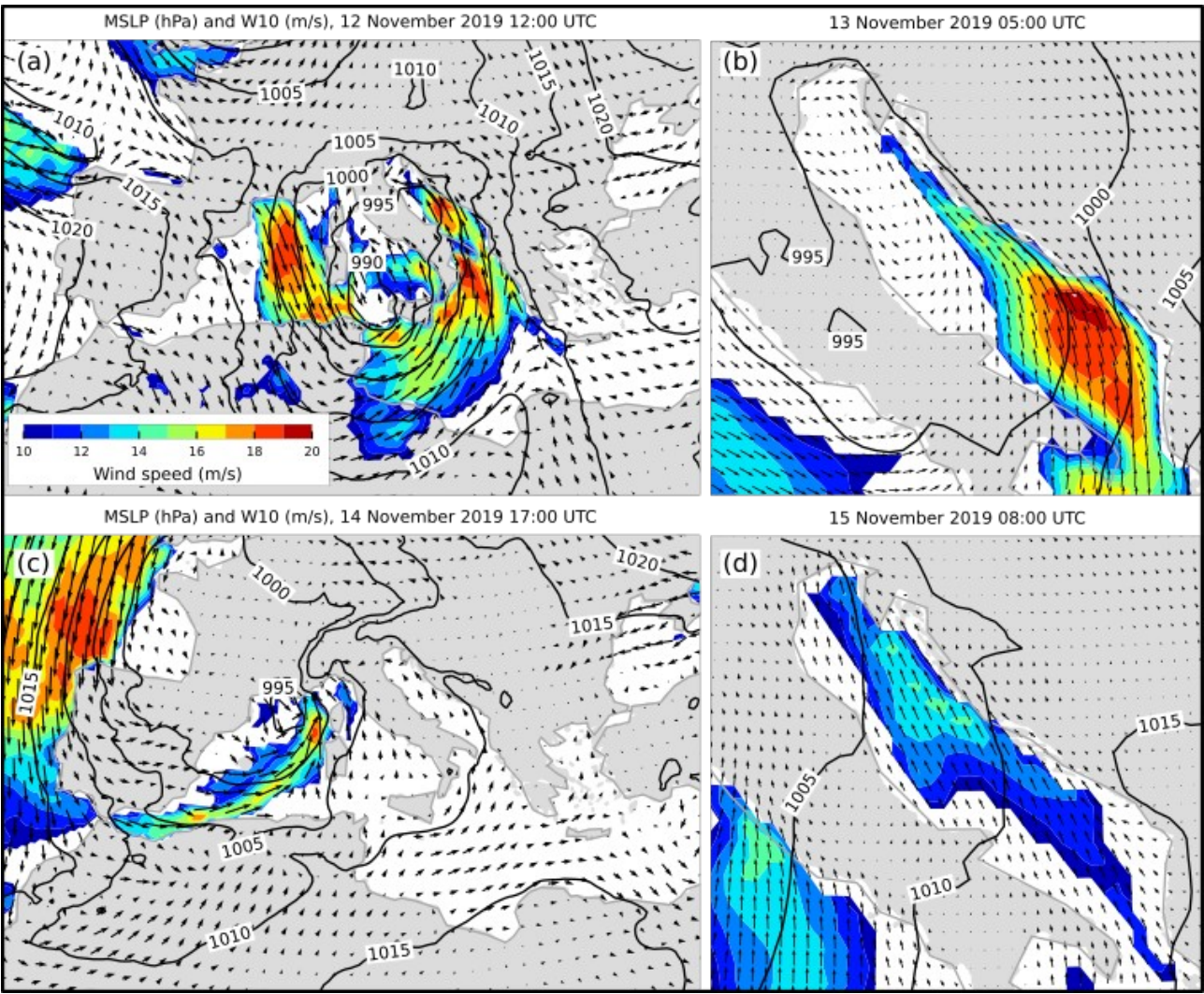
Fig. 16. MSLP (black lines) and **W10** (arrows and colours) fields from the ERA5 reanalysis. Conditions (a, c) over the Mediterranean
595   depicting cyclones in the western Mediterranean that preceded the situations (b, d) over the Adriatic Sea (an hour before SL maxima in
Bakar). Only wind speeds exceeding 10 m/s are coloured. One colormap for all cases.

4.5.2 Sea-level evolution

On 13 November 2019 at 06:00 UTC, the sea level in Bakar reached 99 cm, while on 15 November 2019 at 09:00 UTC, 92
cm was measured (Table 2, Fig. 17). The 13 November total SL maximum (99 cm) came after the peak of the residual sea
600   level, which occurred on 12 November and amounted to an exceptional 95 cm.

The moon was full on 12 November, so *tide* had a semidiurnal spring-tide character. The two SL maxima were reached

during the daily tidal peaks, which contributed 27 cm (to the flood of 13 November) and 22 cm (to the flood of 15 November) (Fig. 17a).
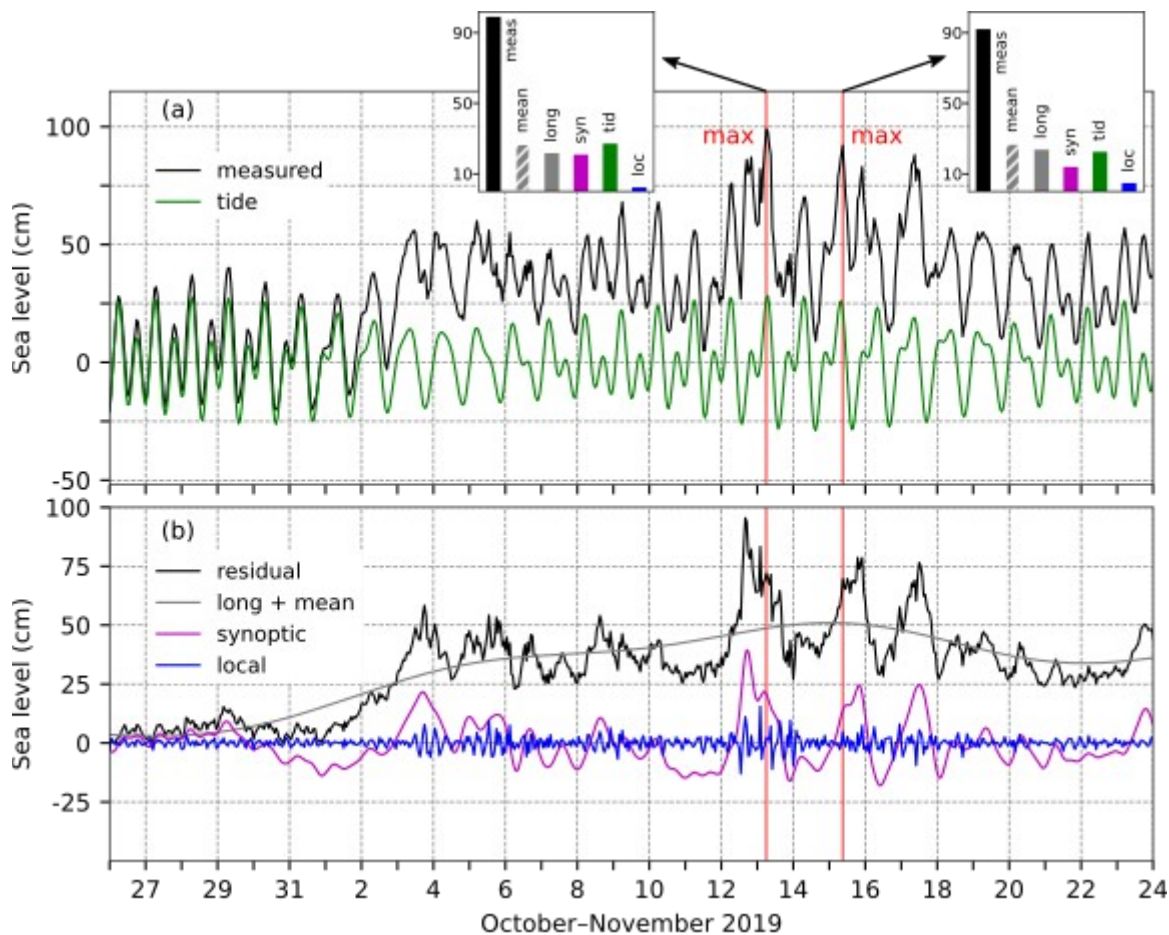
605 **Figure 17:** SL series for the floods 13 and 15 December 2019. (a) Measured sea level (black) and *tide* (green). The inset figures show the contributions (cm) of the five sea-level components to the maximum measured sea levels ("meas"; left: 13 December 2019 06:00 UTC, right: 15 December 2019 09:00 UTC): "loc" refers to *local component* (9 h < T), "syn" to *synoptic component* (9 h < T < 10 d), "tid" to *tide,* "long" to *long-period sea-level component* (10 < T < 100 d), "mean" to *mean sea-level changes* (100 d < T). (b) Residual sea level (black), the combined series of *long-period sea-level component* and *mean sea-level changes* (grey; long + mean), *synoptic component* (purple), and *local component* (blue). The red line indicates the time of occurrence of the total SL maximum.

Although *local processes* were active during these two episodes, and in particular during the 13 November flood (Fig. 17b) and had a considerable amplitude (compared to the amplitudes of *local processes* during other extracted floods; Table 2), their contribution to the overall maxima was 2 cm and 5 cm, respectively. It should be mentioned that during the first episode, a fast-moving small-scale atmospheric disturbance caused a strong local SL response in the Venice lagoon, which

615 significantly affected the overall sea level maximum there (Ferrarin et al., 2021; 2023).

The peak of *synoptic component* occured on 12 November (coinciding with the residual maximum) and was 39 cm high. As there were no apparent ~21.2 h oscillations in the basin prior to the two episodes, *synoptic component* was driven mainly by a storm surge, i.e., forced oscillations. By the SL peak on 13 November, the induced storm surge was already receding due to the weakening of the atmospheric forcing (Figs. 15b and 16b), reaching 21 cm (Fig. 17a), and by 15 November it was again

620 enhanced by the strong Sirocco (Figs. 15b and 16d), reaching 14 cm (Fig. 17a).

Long-period sea-level component was high during the floods, contributing 22 cm to the 13 November episode and 24 cm to the 15 November episode. Preconditioning began two weeks earlier, when sea levels began to rise gradually (Fig. 17b, long + mean). Comparing Fig. 15a and Fig. 17b shows that while Z500 (lp) and MSLP (lp) initially dropped and then slightly increased, SL (long + mean) continued to rise steadily throughout the period leading up to the floods. This indicates that

625 changes in MSLP (lp) did not support the SL rise during the entire period, however, a persistent southerly wind (at periods of 10–100 d), with a maximum speed of 4 m/s, blew from early to nearly late November, contributing to the rise in SL (Fig. 17b, long + mean).

Mean sea-level component (100 d < T) was exceptionally high during these episodes, contributing 27 cm to both events (Fig. 17a). This was mainly due to significant contribution from the seasonal cycle and interannual variability (21 cm, Figs. A1,

630 A2c), as well as an additional increase due to linear SL trend (5 cm, Fig. A3). Similar to other recent floods, the amplitude of (multi)decadal variations was minimal and contributed 1 cm to height of *mean sea-level component*. It is worth noting that, as this episode is near the end of the analysed series, (multi)decadal variations might have been underestimated due to edge effects from filtering.

In summary, these two floods resulted from a constructive superposition of all contributing processes, with all components,

635 except for *local processes*, playing similar roles (Fig. 17).

4.5.3 Flood impacts

A review of available daily newspapers (Jutarnji list, 14 and 17 November 2019) revealed the following effects of the floods. In the week before the floods, heavy precipitation was recorded in the northern Adriatic. This necessitated major interventions in which firefighters had to pump out the excess water. A day before the first flood on 12 November 2019, the

640 Croatian Hydrographic Institute (HHI) documented a record-breaking wave measuring 10.87 m in height near the island of St. Andrija (close to Dubrovnik; Fig. 1). For the following day, DHMZ, issued a warning for the northern Adriatic because of strong Sirocco and the possibility of flying debris carried by the wind. All along the Adriatic coast there were significant firefighters' interventions due to fallen trees, landslides and flooded streets, shops, restaurants, and business premises. Two days later, on 15 November 2019, another flood was recorded. Eyewitness reports describe a brief waterspout causing

645 significant material damage in the northern Adriatic. Ferry, boat, and catamaran services were widely disrupted along the

Adriatic coast, from Kvarner to Dubrovnik. Notably, in one incident in Dubrovnik, a tourist was pulled to the sea by large waves and unable to get back ashore on his own, but luckily local fishermen noticed and rescued him.

4.6 The flood of 29 October 2018 (ID 21; rank 7)

Several studies have analysed this flood, including: an empirical investigation of the event and its meteorological background in the middle Adriatic (Pervan and Šepić, 2023) and in Venice (Ferrarin et al., 2022); the use of an integrated web system for forecasting and managing coastal risks related to sea storms (Ferrarin et al., 2020); tracking the trajectory of a surfer lost at sea during the storm (Ličer et al., 2020); demonstration of the effectiveness of the ISPRA operational SL forecasting system (Morucci et al., 2020); quantification of a displacement of coastal boulders in the northern and middle Adriatic due to wave action (Biolchi et al., 2019; Korbar et al. 2022); the event's predictability, with an emphasis that its characteristics might not fit within historical patterns, hinting at a potential new class of storms (Cavaleri et al., 2019); or analysis of the episode as part of an overview study (Lionello et al., 2021).

4.6.1 Meteorological background

Three days before the flood, on 26 October, the surface-based anticyclone whose centre was over the eastern Mediterranean gradually weakened over the Adriatic, and an upper-level trough with significantly colder air began to descend from the north of the continent towards the Iberian Peninsula.

On 27 October, as the trough progressed further towards the south, a pronounced southwesterly flow in the upper levels was established over the Adriatic Sea, advecting relatively warm air towards the Adriatic region. The associated surface-based cyclone was located over the Baltic Sea, and its frontal system extended to the Alps leading to the formation of a secondary cyclone in the Ligurian Sea. In such synoptic conditions, a strong southeasterly wind blew over the Adriatic (Fig. 18).

The following day, on 28 October, the cold air within the trough over western Europe penetrated a little further to the south, causing a mid-tropospheric cutoff low over the south of France and the Iberian Peninsula, and consequently on the night of 29 October, there was a deepening of the surface cyclone over the Ligurian Sea. During the day (29 October), this cyclone, in the centre of which the air pressure dropped to less than 985 hPa (Fig. 19a), moved relatively quickly towards the north, with a cold front passing over the Adriatic. As a result, southeast wind which was strong and gale over the Adriatic on 28 October, increased to storm (e.g., 25–28 m/s at Palagruža island in the middle Adriatic) in the afternoon hours of 29 October (Fig. 18b). The wind slightly weakened by the time of the flood peak (Figs. 18b and 19b), due to the shift of the system (surface cyclone and upper level trough) to the north, and the fact that anticyclone from the east started to affect the weather (Fig. 18). On 29 October, next amounts of precipitation were measured along the Croatian coastline: 33 mm in Poreč (near Rovinj), 125 mm in Senj (near Bakar), and 19 mm at Dubrovnik airport. On 30 October, precipitation in the northern Adriatic reached up to 30 mm, while the southern Adriatic experienced much larger amounts, locally exceeding 50 mm (e.g.,

69 mm in Opuzen near Dubrovnik).
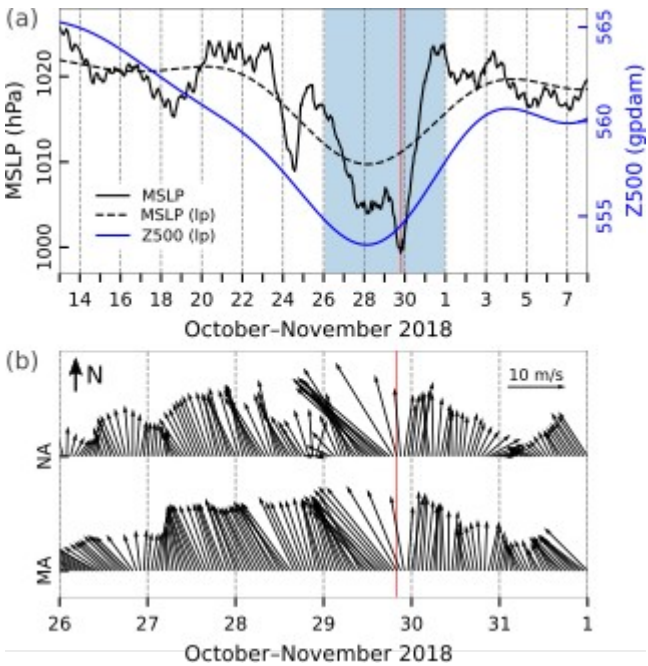
Figure 18: Series of ERA5 reanalysis data related to the flood of 29 October 2018. (a) MSLP (hourly) and MSLP (lp) (low-pass filtered with a cut-off frequency of 10 d) and Z500 (lp) (low-pass filtered with a cut-off frequency of 10 d) at a grid point near TG Bakar. (b) Hourly **W10** during the period marked in blue in the upper plot for the middle (MA) and northern (NA) Adriatic (all locations marked in Fig. 1). The red line indicates onset of SL maximum.

680

685

690
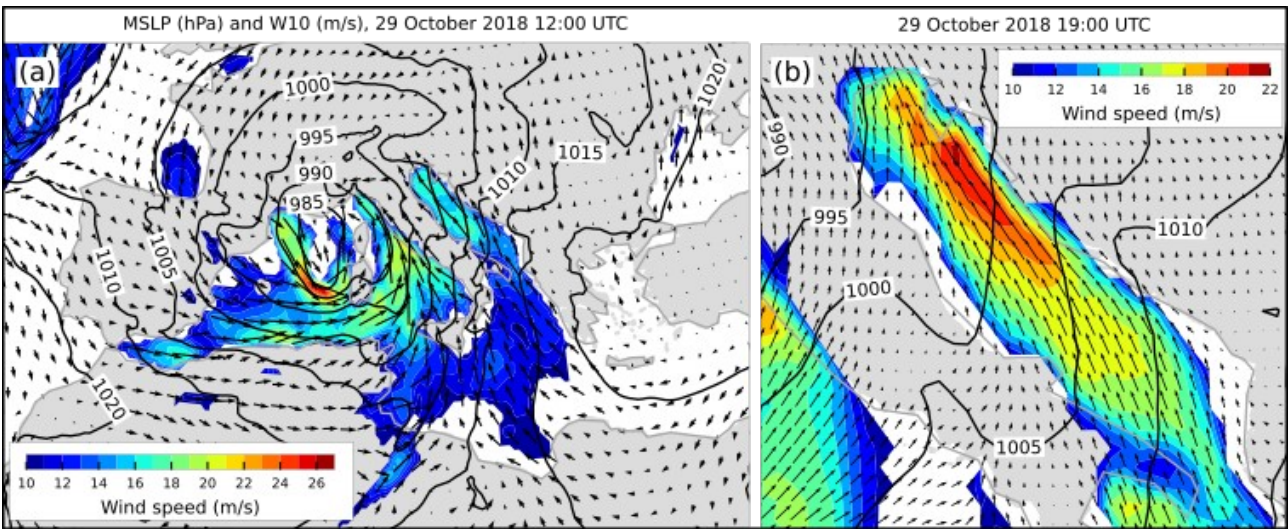
695 **Figure 19:** MSLP (black lines) and **W10** (arrows and colours) fields from the ERA5 reanalysis. Conditions (a) over the Mediterranean depicting a cyclone over the western Mediterranean that preceded the situation (b) over the Adriatic Sea (an hour before maximum SL in Bakar). Only wind speeds exceeding 10 m/s are coloured.

4.6.2 Sea-level evolution

In the evening hours of 29 October (20:00 UTC), the sea level in Bakar rose to 97 cm above the long-term average (Table 2,
700 Fig. 20).

The lunar phase was approaching the last quarter, which gave *tide* a diurnal neap-tide character. The overall SL maximum formed shortly after the daily tidal minimum, so *tide* contributed -12 cm to this episode.

Local processes were pronounced during this episode and contributed 12 cm.
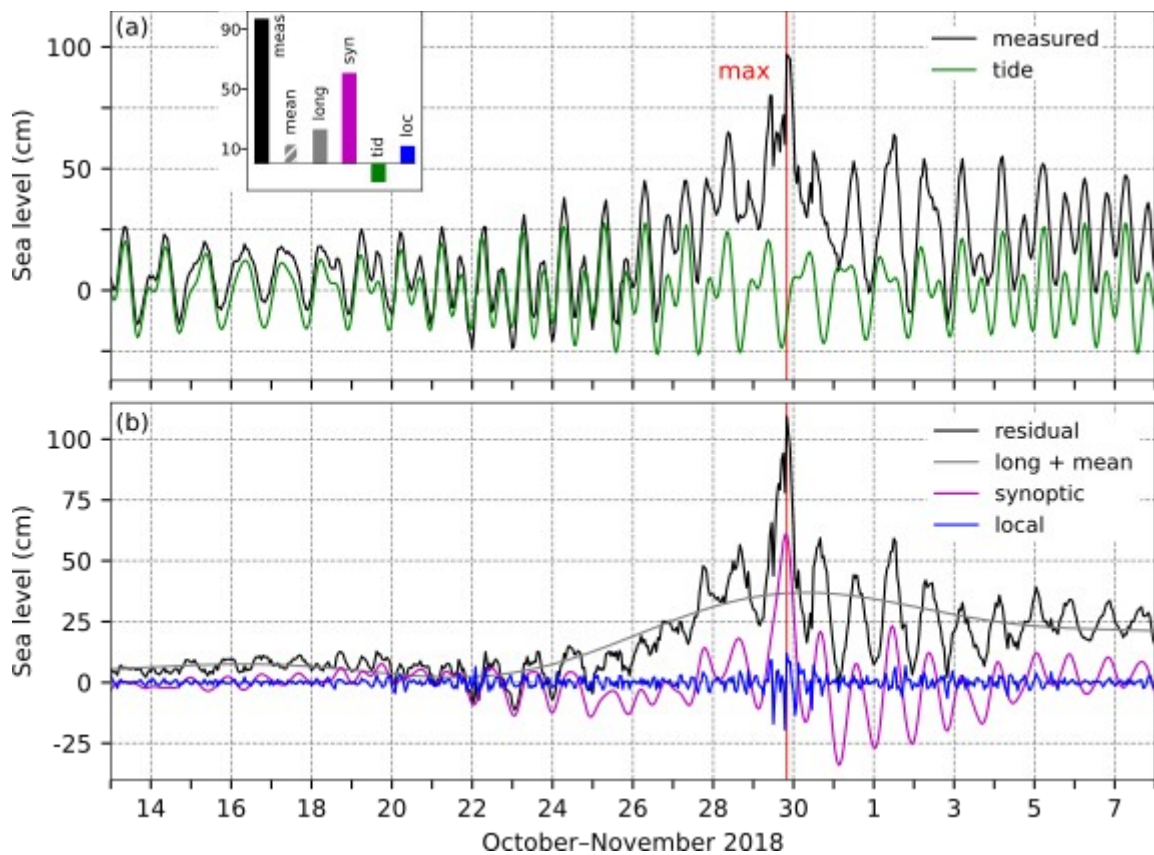
705 **Figure 20:** SL series for the flood of 29 October 2018. (a) Measured sea level (black) and *tide* (green). The inset figure shows the contributions (cm) of the five sea-level components to the maximum measured sea level ("meas"; 20:00 UTC): "loc" refers to *local component* (9 h < T), "syn" to *synoptic component* (9 h < T < 10 d), "tid" to *tide*, "long" to *long-period sea-level component* (10 < T < 100 d), "mean" to *mean sea-level changes* (100 d < T). (b) Residual sea level (black), the combined series of *long-period sea-level component* and *mean sea-level changes* (grey; long + mean), *synoptic component* (purple), and *local component* (blue). The red line indicates the time 710 of occurrence of the total SL maximum.

The SL maximum occurred as the decisive cyclone crossed the Adriatic Sea (Figs. 18a and 19b), primarily due to an exceptional *synoptic component*. Although ~21.2 h oscillations are visible in *synoptic component* before the main maximum (Fig. 20b), they were weak and therefore we can say that *synoptic component* consisted mainly of the storm surge, which

was 61 cm during the total peak. This was one of the strongest SL responses at synoptic scales (compared to other extracted floods), and it can be attributed to the MSLP gradient over the Adriatic and Sirocco wind, which blew over the Adriatic for several days with extreme speeds (Fig. 18b).

Long-period sea-level variability contributed 23 cm to the overall SL maximum. The conditions for flooding began to develop about a week earlier, around 22 October, when SL started to gradually rise (Fig. 20b, long + mean) induced by a drop in MSLP (lp) (Fig. 18a) and a persistent strong southerly wind (not shown) at periods of 10–100 d. This wind blew continuously from 25 October to 9 November, reaching a peak speed of nearly 8 m/s on the day of the flood. The synchronised fluctuations of Z500 (lp), MSLP (lp) (Fig. 18a), and SL (Fig. 20b, long + mean) suggest that passages of atmospheric Rossby waves were driving changes of *long-period sea-level component*.

Mean sea-level changes (100 d < T) contributed 13 cm to this maximum (Fig. 20a, histogram). The episode occurred just before the annual SL peak, which was not particularly pronounced this year (7 cm, Figs. A1 and A2c). As with other recent episodes, the contribution of (multi)decadal changes was minimal (1 cm, Fig. A2b), while the contribution from secular change was 5 cm (Fig. A3). We note that since the episode is close to the end of the studied period, the estimation of (multi)decadal processes may have been affected by filtering effects.

In summary, this flood resulted from the positive contributions of all processes but *tide* (which had negative contribution), with *synoptic component* having the strongest effect (Fig. 20). The episode could have been much stronger (+~30 cm) if the cyclone had passed a few hours earlier when *tide* had reached its maximum.

4.6.3 Flood impacts

A review of the available daily newspapers (Jutarnji list, 29 October–1 November 2018; Novi list, 30 October–1 November 2018; Slobodna Dalmacija, 30 October–1 November 2018; Večernji list, 31 October–1 November 2018) revealed the following effects of the flood. The day before the main incident, strong winds and heavy rain wreaked havoc, toppling trees and flooding coastal roads along the Adriatic coast. The following day, the situation escalated to an even greater extent. In the northern Adriatic, the city of Rijeka (Fig. 1) was flooded due to a strong Sirocco combined with high tide, with the flooding causing water from the sewage systems to flow into the city's main market and spread to the adjacent streets and squares. Heavy rain, gale Sirocco winds and reportedly 7 m high waves halted ferry services, cutting the islands off from the mainland all along the coast. Other damage and interventions included: (i) flooding and damage to beach promenades along the northern Adriatic; (ii) damage or sinking of numerous boats along the entire coast; (iii) rescue of a woman and a child from a flooded area in the northern Adriatic.

4.7 The flood of 1 November 2012 (ID 20; rank 1)

A study by (Međugorac et al., 2016) used TG measurements from both sides of the Adriatic to empirically analyse this

episode. The findings indicated that flooding was more severe on the eastern coast, while the western side experienced
745   milder effects due to an east-to-west SL slope created by the uneven Sirocco winds, which were stronger near the eastern
shore.

4.7.1 Meteorological background
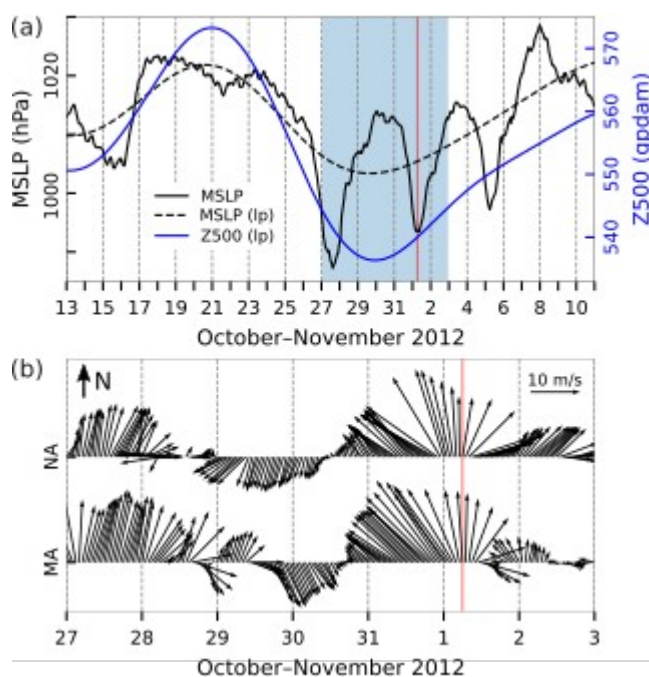
Figure 21: Series of ERA5 reanalysis data related to the flood of 1 November 2012. (a) MSLP (hourly) and MSLP (lp) (low-pass filtered with a cut-off frequency of 10 d) and Z500 (lp) (low-pass filtered with a cut-off frequency of 10 d) at a grid point near TG Bakar. (b) Hourly **W10** during the period marked in blue in the upper plot for the middle (MA) and northern (NA) Adriatic (all locations marked in Fig. 1). The red line indicates onset of SL maximum.

In the week leading up to the flood, on 27 November, a deep low-pressure system moved over the Adriatic Sea (Fig. 21a).
765   On 31 October, a well-defined surface cyclone, accompanied by a closed circulation of low pressure in the upper-level, formed in the western Mediterranean and travelled towards Italy during the day while the pressure in its centre dropped to 985 hPa (Fig. 22a). At the same time, the anticyclone gradually weakened over the Adriatic while slowly shifting eastward. The centre of the above-mentioned cyclone with a frontal system moved over the northern Adriatic on 1 November (Fig. 22b). In such synoptic conditions, a strong southeasterly wind was blowing over the Adriatic, and SL reached maximum
770   value. On 1 November, the induced precipitation was most intense in the northern Adriatic, with recorded amounts including 57 mm in Pula, 114 mm in Crikvenica (near Bakar), 36 mm at Zadar Airport, and 26 mm in Trogir (near Split). The cyclone then moved further to the east, over the land, but the wind over the Adriatic still remained mainly of a southerly direction (Fig. 21) due to MSLP gradients related to an extensive cyclone that persisted over the Atlantic for days and in the centre of which, a little south of Iceland, the pressure was exceptionally low, around 965 hPa.
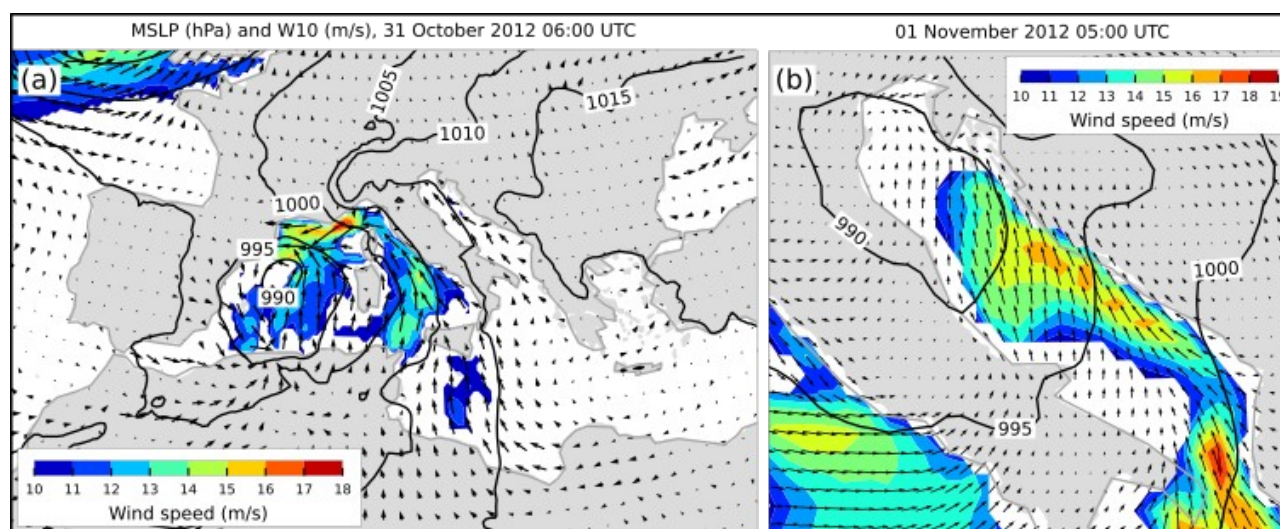
Figure 22: MSLP (black lines) and **W10** (arrows and colours) fields from the ERA5 reanalysis. Conditions (a) over the Mediterranean depicting a cyclone over the western Mediterranean that preceded the situation (b) over the Adriatic Sea (an hour before maximum SL in Bakar). Only wind speeds exceeding 10 m/s are coloured.

4.7.2 Sea-level evolution

On 1 November 2012 at 06:00 UTC, the Bakar tide-gauge station recorded the highest water level ever measured at this station. On this occasion, the sea level rose to 113 cm above the long-term average (Table 2, Fig. 23).

The maximum of the total sea level formed during the daily peak of *tide*, two days after the full moon. *Tide* therefore had a semidiurnal spring-tide character and contributed 23 cm to the maximum (Fig. 23a).

Local processes were not pronounced during the episode and contributed 6 cm.

Synoptic component was induced by a Mediterranean cyclone (Fig. 21a), which crossed rapidly from the western Mediterranean into the Adriatic (Fig. 22b). Prior to this, an atmospheric disturbance moved across the basin on 27 October (Fig. 21) and triggered basin-wide oscillations (T~21.2 h), which were, however, damped by the time of the main event (Fig. 23). Therefore, *synoptic component* consisted mainly of the storm surge, which amounted to 39 cm at the total maximum. The storm surge started to build up at the end of 30 October due to the pressure drop and the Sirocco wind blowing at high speeds along the eastern coast over most of the Adriatic Sea (Fig. 22b).

Long-period sea-level variability (10 < T < 100 d) contributed 26 cm to the overall maximum. Flood preconditions began around 21 October, marked by a rise in SL coinciding with a drop in atmospheric pressure. As shown in Fig. 21a, MSLP (lp) varied coherently with Z500 (lp) during this period, and Fig. 23b shows that SL (long + mean) mirrored these fluctuations. As demonstrated by Pasarić (2000), Pasarić et al. (2000), and Pasarić and Orlić (2001), this suggests that *long-period sea-level component* was predominantly influenced by the passage of planetary Rossby waves.
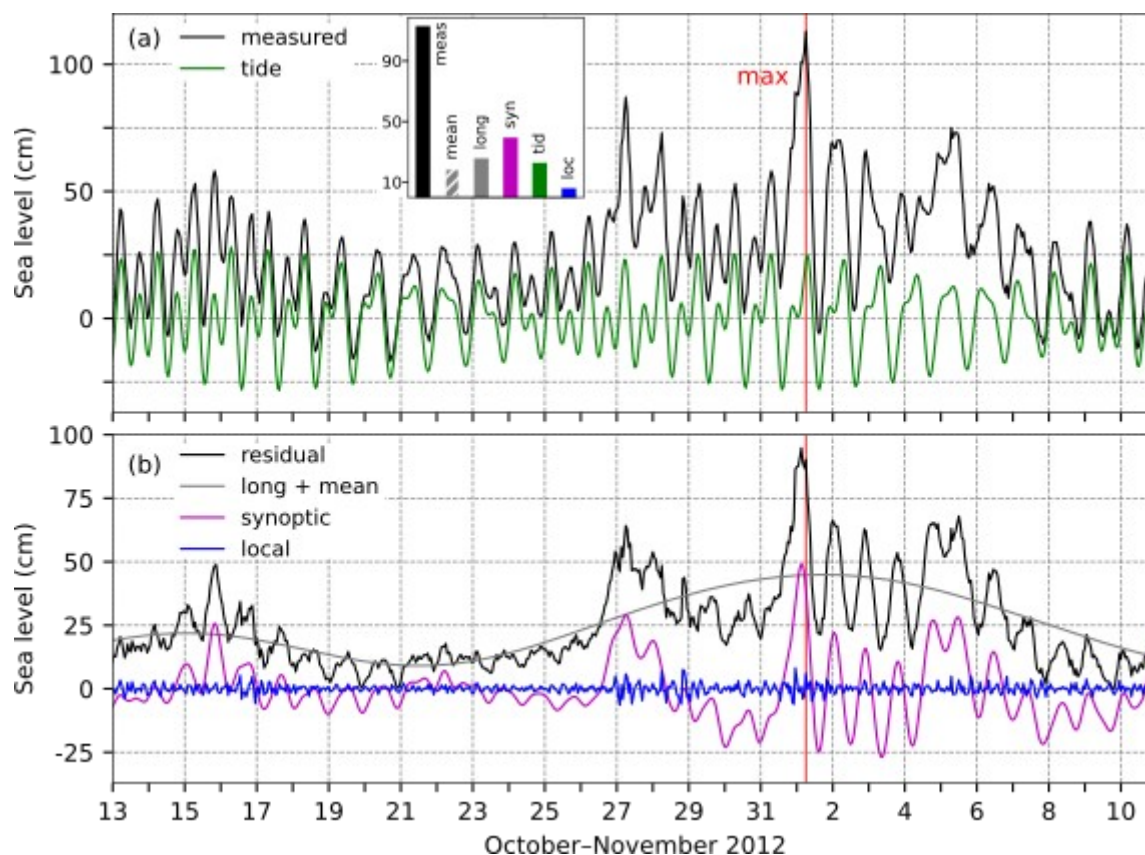
Figure 23: SL series for the flood of 1 November 2012. (a) Measured sea level (black) and *tide* (green). The inset figure shows the contributions (cm) of the five sea-level components to the maximum measured sea level ("meas"; 06:00 UTC): "loc" refers to *local component* (9 h < T), "syn" to *synoptic component* (9 h < T < 10 d), "tid" to *tide*, "long" to *long-period sea-level component* (10 < T < 100 d), "mean" to *mean sea-level changes* (100 d < T). (b) Residual sea level (black), the combined series of *long-period sea-level component* and *mean sea-level changes* (grey; long + mean), *synoptic component* (purple), and *local component* (blue). The red line indicates the time of occurrence of the total SL maximum.

Mean sea-level changes (100 d < T) contributed 19 cm to this episode (Fig. 23). This episode took place in the fall, aligning with the yearly SL peak (12 cm, Figs. A1, A2a, and A2c). During this period, sea level was further elevated by ongoing (multi)decadal variations (2 cm, Fig. A3b), and long-term secular change (5 cm, Fig. A3a).

In summary, the flood resulted from the positive superposition of all processes involved, with *synoptic component* having the strongest effect (Fig. 23a).

4.7.3 Flood impacts

The impacts of the flooding were examined using the available daily newspapers (Novi list, 2 November 2012; Slobodna

810 Dalmacija, 2 and 3 November 2012). Large parts of the coast were affected by the record-breaking high-water levels, heavy rain and strong Sirocco winds. Many coastal towns reported extensive flooding on streets and squares. Other damage and interventions included: (i) suspension of ferry services in the northern Adriatic; (ii) sewage system issues resulting with flooding in Rijeka (northern Adriatic, Fig. 1); (iii) rescue of an elderly person in the northern Adriatic; (iv) damage to cars due to fallen branches in the middle Adriatic; (v) road collapse in the middle Adriatic, with an estimated damage of several

815 tens of thousands of euros.

4.8 The flood of 3 December 2010 (ID 19; rank 13)

The flood has not been previously described in scientific literature.

4.8.1 Meteorological background
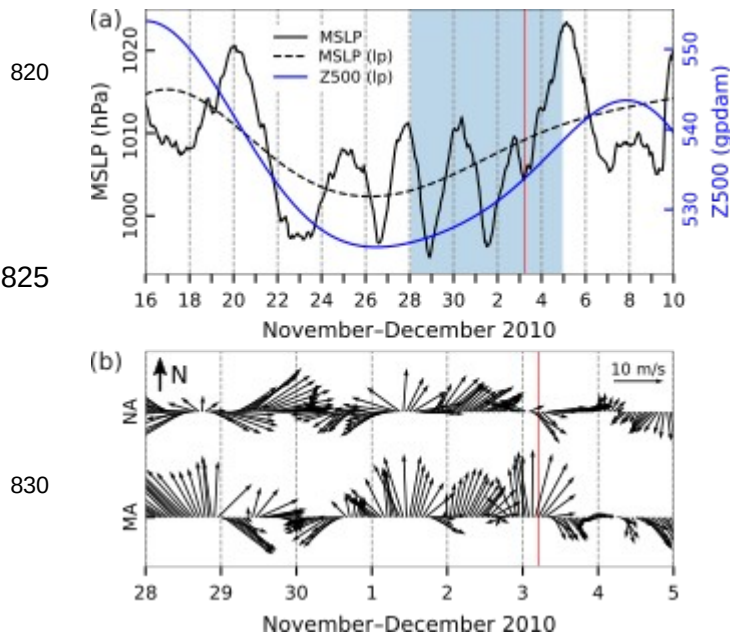
Figure 24: Series of ERA5 reanalysis data related to the flood of 3 December 2010. (a) MSLP (hourly) and MSLP (lp) (low-pass filtered with a cut-off frequency of 10 d) and Z500 (lp) (low-pass filtered with a cut-off frequency of 10 d) at a grid point near TG Bakar. (b) Hourly **W10** during the period marked in blue in the upper plot for the middle (MA) and northern (NA) Adriatic (all locations marked in Fig. 1). The red line indicates onset of SL maximum.

835 In the week leading up to the flood, the Adriatic region was on the front side of a deep upper-level trough moving from northern Europe toward the Mediterranean. This setup resulted in a strong upper-level southwestern flow, bringing warm, humid air that resulted in precipitation over the Adriatic region. A deep upper-level trough supported cyclonic activity in the western Mediterranean, causing a generation of series of cyclones which moved from the Ligurian Sea across the Adriatic in the week before the flood (Fig. 24a). In addition, the wind over the Adriatic was of a highly variable direction, although for

840 prolonged periods it had a southerly component (Fig. 24b). At 00 UTC on 3 December, the last cyclone in a series of storms

115

formed over the Adriatic (Fig. 25a) and then moved eastward. During the flood itself, a light northwesterly wind prevailed in the northern Adriatic, while the central part was affected by a strong southerly wind (Fig. 25b). The induced precipitation was light, with amounts on 3 December mostly ranging from 10 to 20 mm along the northern Adriatic and up to 15 mm along the middle Adriatic.

845
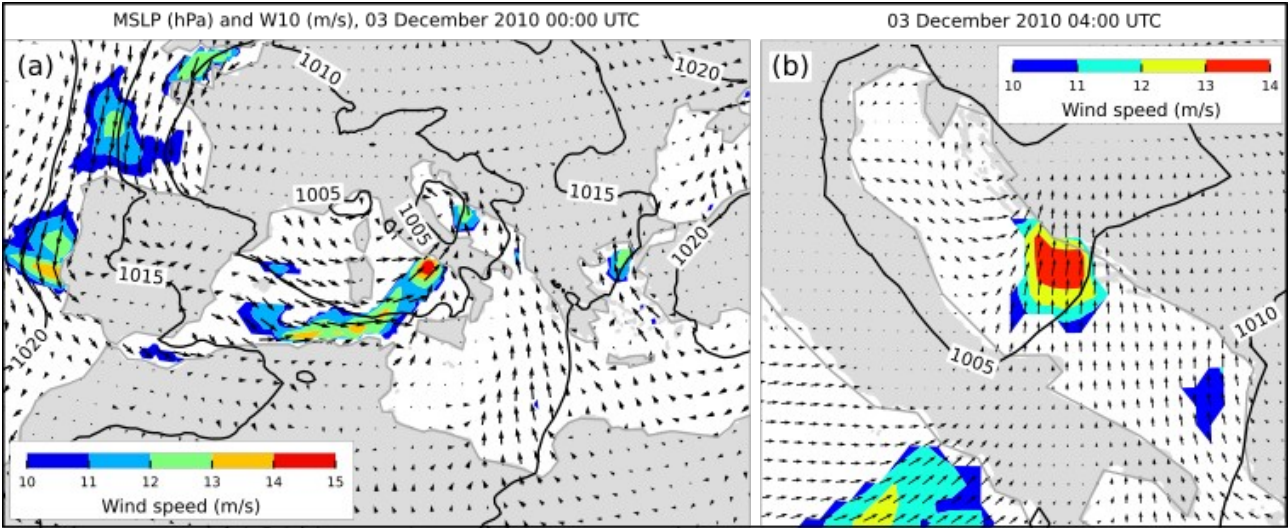
Figure 25: MSLP (black lines) and **W10** (arrows and colours) fields from the ERA5 reanalysis. Conditions (a) over the Mediterranean depicting a cyclone over the western Mediterranean that preceded the situation (b) over the Adriatic Sea (an hour before maximum SL in Bakar). Only wind speeds exceeding 10 m/s are coloured.

4.8.2 Sea-level evolution

850   In the morning hours of 3 December 2010 (05:00 UTC), the sea level in Bakar rose to 91 cm above the long-term average (Table 2, Fig. 26).

The moon was nearing the new moon phase, resulting in a semidiurnal spring *tide*. The overall SL maximum occurred during the daily tidal peak, which was notably high, contributing 28 cm to the flood level.

Local processes were not particularly pronounced during this episode and their role was negligible (they contributed -1 cm to
855   the maximum SL).

The SL maximum formed in a peak of *synoptic component* in which pre-existing seiches played a significant role. Fig. 26 shows that the ~21.2 h oscillations dominated the residual SL during the entire interval shown, which is due to a series of cyclones that crossed the Adriatic Sea before the flood (Fig. 24a). The decisive cyclone produced only weak wind and air pressure forcing in the northern Adriatic (Fig. 25), as a result, the induced storm surge was not high and, together with the
860   positive phase of pre-existing seiche, contributed 26 cm to the total maximum (less than *tide* and *mean sea-level changes*).

Long-period sea-level component contributed 9 cm to the overall SL maximum. The SL (Fig. 26b, long + mean) was raised

over the entire interval shown without significant variations in *long-period sea-level component*. This was due to unpronounced changes in MSLP (lp) (Fig. 24a) and weak wind (10–100 d) of small speeds (maximum was 2 m/s) which did not act in the same sense.

865
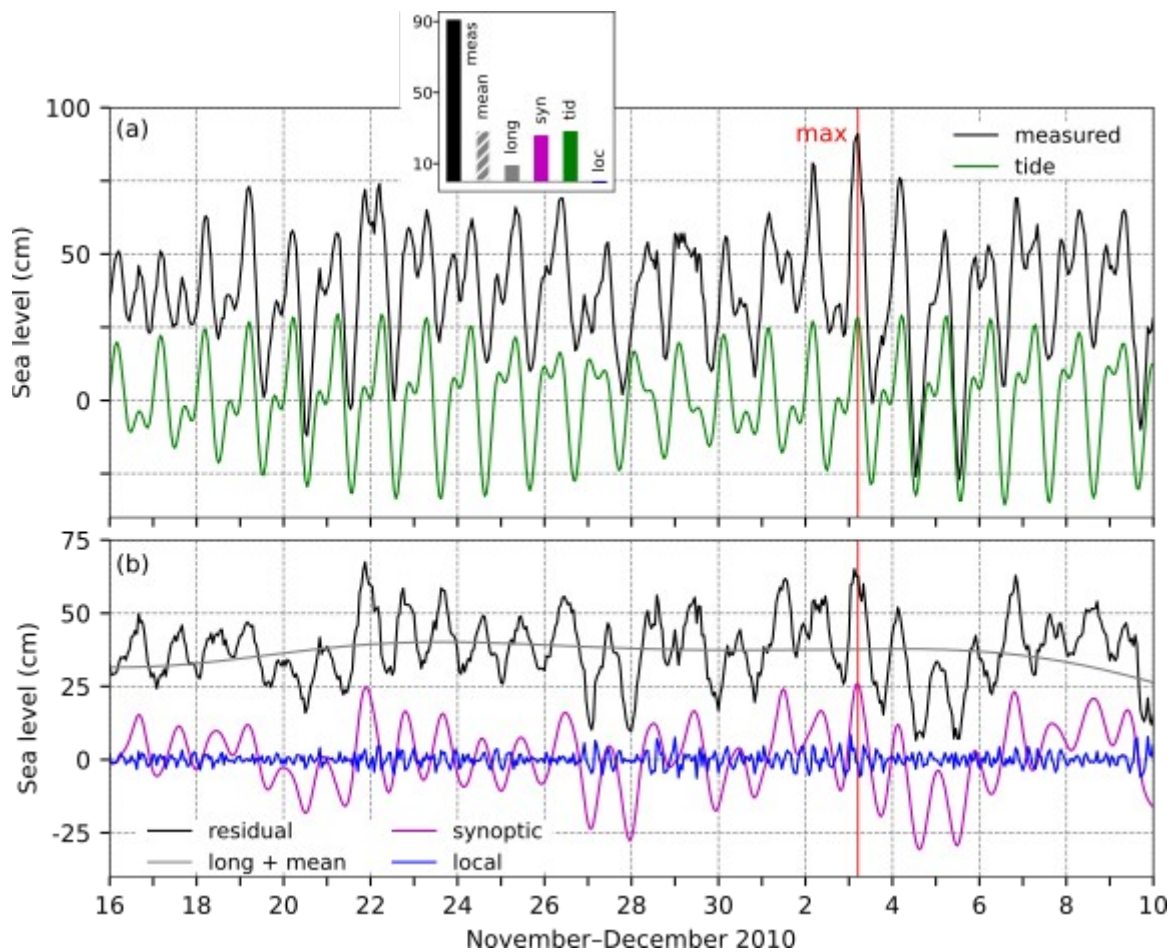
Figure 26: SL series for the flood of 3 December 2010. (a) Measured sea level (black) and *tide* (green). The inset figure shows the contributions (cm) of the five sea-level components to the maximum measured sea level ("meas"; 05:00 UTC): "loc" refers to *local component* (9 h < T), "syn" to *synoptic component* (9 h < T < 10 d), "tid" to *tide*, "long" to *long-period sea-level component* (10 < T < 100 d), "mean" to *mean sea-level changes* (100 d < T). (b) Residual sea level (black), the combined series of *long-period sea-level component* and *mean sea-level changes* (grey; long + mean), *synoptic component* (purple), and *local component* (blue). The red line indicates the time of occurrence of the total SL maximum.

870

Mean sea-level changes (100 d < T) made an exceptional contribution of 29 cm to this maximum (Fig. 26a, histogram). This episode coincided with the annual SL peak, which was unusually high this year, with an amplitude of 21 cm – one of the highest recorded (Figs. A1, A2a, and A2c). Additionally, (multi)decadal sea-level changes added 3 cm (Fig. A3b), while

875 secular change contributed 5 cm (Fig. A3a).

In summary, the flood resulted from the positive superposition of four processes, with *synoptic component*, *tide* and *mean sea-level changes* having a similar contribution (Fig. 26a).

4.8.3 Flood impacts

The following impacts of the flooding were identified through a review of daily newspapers (Slobodna Dalmacija, 4
880 December 2010; Vjesnik, 4 and 5 December 2010). Small coastal towns between Trogir and Šibenik experienced significant material damage, with the sea destroying numerous boats and flooding cellars and restaurants. In the middle Adriatic, in one small town, the sea overflowed onto the waterfront and firefighters spent the whole night pumping the water out of the flooded houses.

4.9 The floods of 23 and 25 December 2009 (IDs 17 and 18; ranks 6 and 3)

885 The flood of 25 December 2009 was studied by Bajo et al. (2019), where the authors investigated the effects of data assimilation on the reproduction of SL, which was significantly affected by the previously generated seiches.

4.9.1 Meteorological background

In the days before the SL peaks in Bakar, several cyclones moved across the Adriatic, causing spatially variable winds over the Adriatic and several episodes of strong and prolonged southeasterly and southerly winds (Fig. 27). This pronounced
890 cyclonic activity was supported by a vast upper-level through which encompassed a large part of the European mainland - stretching from Greenland in the north and North Africa in the south across the south-eastern and central Europe, all the way to the Russian borders in the east. At the leading edge of the through the upper-level flow was southwesterly, bringing unusually warm air from northern Africa towards the Adriatic.

On 23 December at 00:00 UTC, a decisive cyclone formed over the Gulf of Genoa (Fig. 28a and DWD). As a result of the
895 increasing air pressure gradient along the Adriatic, strong Sirocco wind started blowing, reaching its peak shortly before the occlusion front passed over the Adriatic (Figs. 27b and 28b; DWD for occlusion front). The wind significantly weakened after passage of the front. On 23 December, precipitation was more intense in the northern Adriatic, with recorded amounts of 110 mm in Rijeka and 67 mm in Bakar, while in the middle Adriatic, it reached up to 20 mm.

On 24 December a deep cyclone, with a minimum air pressure of 975 hPa, was located in the Bay of Biscay (Fig. 28c). On
900 25 December this cyclone moved further northeast over France and Germany. At the same time, the weather situation over Croatia and the Adriatic was under a strong influence of another cyclone positioned over northern Italy, in the centre of which the air pressure was less than 995 hPa. These conditions caused precipitation that was more intense in the northern

125

Adriatic, with 110 mm recorded in Matulji and 70 mm in Brseč (both near Rijeka), compared to the middle Adriatic, where

amounts ranged between 15 and 25 mm. These two cyclones, together with a large anticyclone in the east of the continent,

905   caused a strong pressure gradient between eastern and western Europe. As a result, there was also a strong air pressure

gradient over the Adriatic Sea, so that strong southeasterly winds blew over the Adriatic region for several days (Figs. 27b

and 28d).
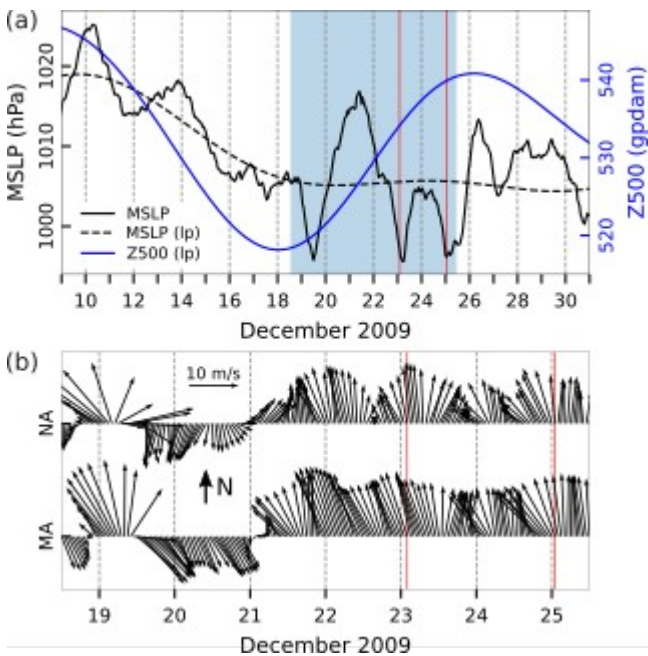
Figure 27: Series of ERA5 reanalysis data related to the floods of 23 and 25 December 2009. (a) MSLP (hourly) and MSLP (lp) (low-pass filtered with a cut-off frequency of 10 d) and Z500 (lp) (low-pass filtered with a cut-off frequency of 10 d) at a grid point near TG Bakar. (b) Hourly **W10** during the period marked in blue in the upper plot for the middle (MA) and northern (NA) Adriatic (all locations marked in Fig. 1). The red lines indicate onset of SL maxima.
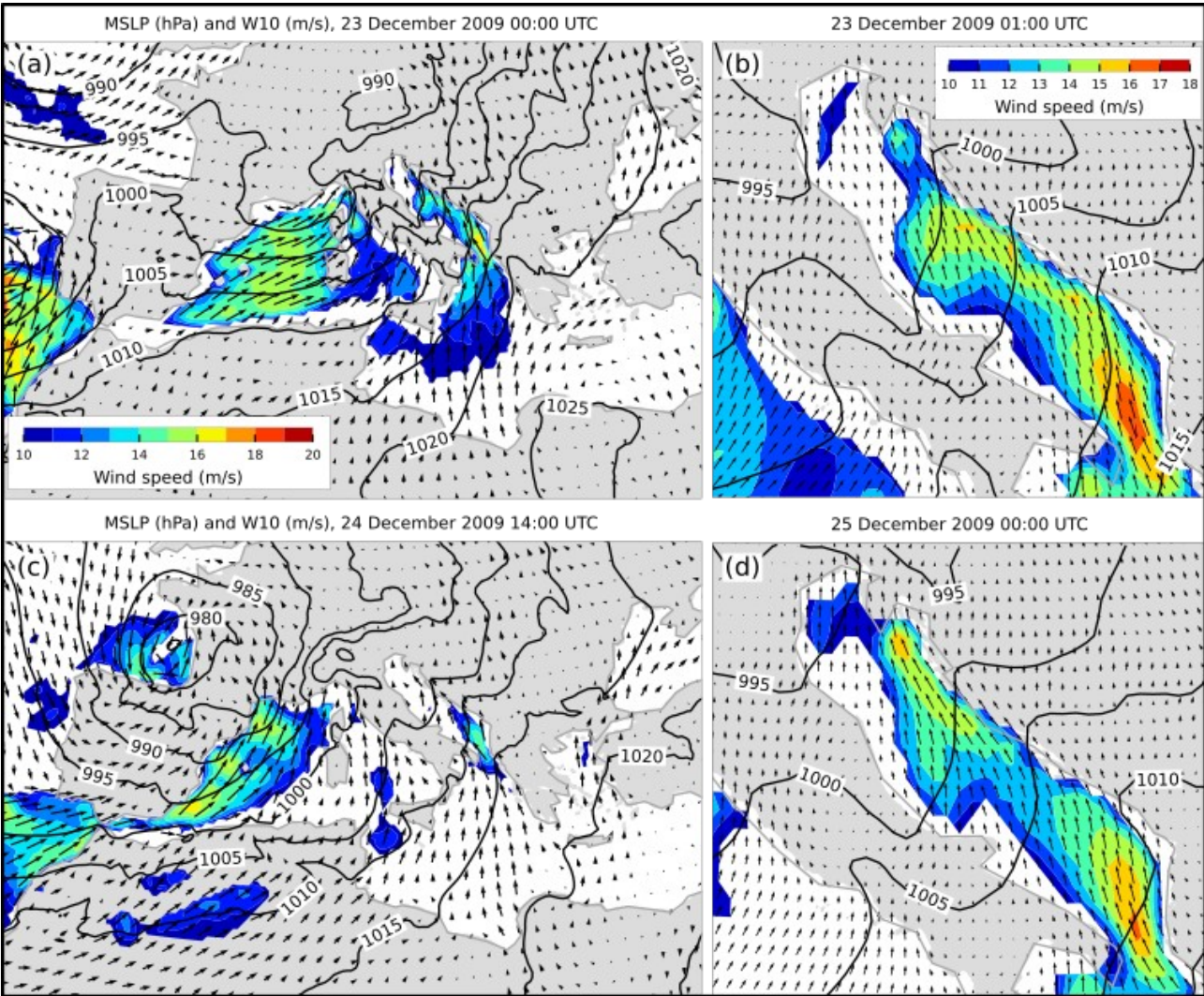
Figure 28: MSLP (black lines) and **W10** (arrows and colours) fields from the ERA5 reanalysis. Conditions (a, c) over the Mediterranean that preceded the situations (b, d) over the Adriatic Sea (an hour before maxima SL in Bakar). Only wind speeds exceeding 10 m/s are coloured. The left colourbar is for the Mediterranean and the right one is for the Adriatic.

4.9.2 Sea-level evolution

On 23 December 2009 at 02:00 UTC, the sea level in Bakar rose to 98 cm, while on 25 December 2009 at 01:00 UTC it reached 103 cm (Table 2, Fig. 29).

Between the two floods, on 24 December, the moon was in the first quarter, giving *tide* diurnal neap-tide character. The first SL maximum was reached one hour after the daily high tide, while the second was reached during the high tide. *Tide*

130

contributed 14 cm and 20 cm to the floods, respectively (Fig. 29a).
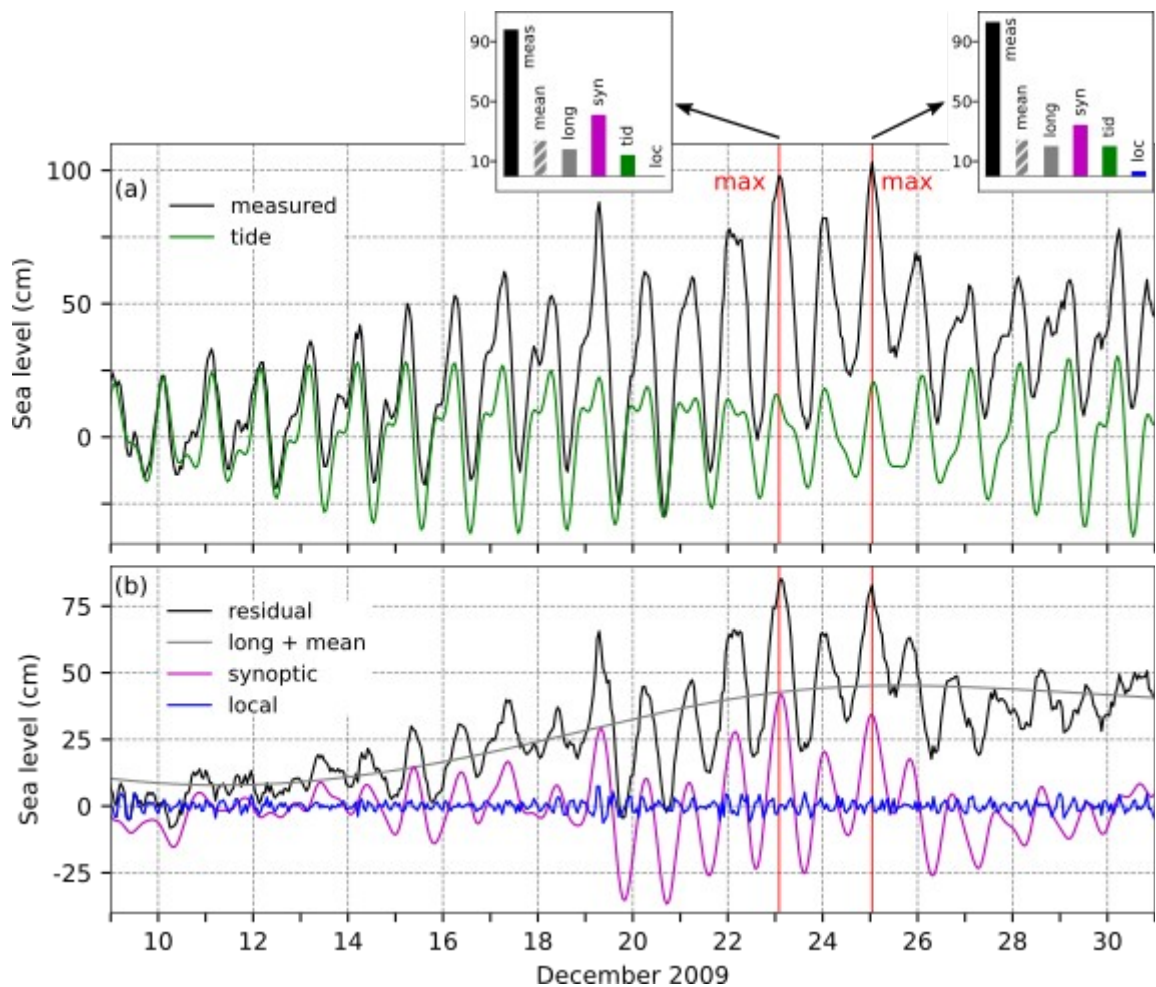
935

Figure 29: SL series for the floods of 23 and 25 December 2009. (a) Measured sea level (black) and *tide* (green). The inset figures show the contributions (cm) of the five sea-level components to the maximum measured sea levels ("meas"; left: 23 December 2009 02:00 UTC, right: 25 December 2009 01:00 UTC): "loc" refers to *local component* (9 h < T), "syn" to *synoptic component* (9 h < T < 10 d), "tid" to *tide*, "long" to *long-period sea-level component* (10 < T < 100 d), "mean" to *mean sea-level changes* (100 d < T). (b) Residual sea level

940 (black), the combined series of *long-period sea-level component* and *mean sea-level changes* (grey; long + mean), *synoptic component* (purple), and *local component* (blue). The red line indicates the time of occurrence of the total SL maximum.

Local processes were of low amplitude during both these events (Fig. 29b), so that their contribution to the total maxima amounted to 0 cm and 3 cm, respectively.

Both episodes were influenced by natural basin oscillations (Fig. 29b), which were first triggered by the passage of the

945 cyclone and sudden change of wind forcing on 19 December (Fig. 27a). Hence, *synoptic component* consisted of the storm

surges and free basin-wide oscillations (T~21.2 h). The seiches were in phase with the two storm surges and therefore amplified both of them (Fig. 29). The SL maxima formed during the peaks of *synoptic component,* which were 41 cm on 23 December and 34 cm on 25 December (Fig. 29).

Long-period sea-level component contributed 18 cm to the 23 December episode and 21 cm to the 25 December episode.
950 Figure 29b shows that the SL (long + mean) began to rise around 12 December, which can be attributed to atmospheric forcing. A comparison of Figs. 27a and 29b indicates that the SL started increasing as MSLP (lp) decreased, continuing until about 19 December. At that point, MSLP (lp) no longer supported the rise in SL, however, winds from the south or southwest (10–100 d period) started to blow, reaching speeds of nearly 6 m/s during the floods, and continued to support the SL increase.

955 M*ean sea-level component* (100 d < T) was exceptionally high during these episodes, contributing 25 cm to both events (Fig. 29a, histogram). It was largely driven by the pronounced amplitude of the seasonal signal and interannual variability, which contributed 17 cm (Figs. A1, A2a, and A2c). Smaller contributions came from (multi)decadal processes (4 cm) and secular change (4 cm, Fig. A3).

These two consecutive floods can be attributed to a positive superposition of all processes, aside from the *local processes*,
960 but above all to *synoptic component,* which was dominated by free basin oscillations, especially in the case of the second episode (Fig. 29).

4.9.3 Flood impacts

Based on daily newspapers (Novi list, 24 December 2009), the effects of the 23 December flood are listed. The flood impacts were most severe in town of Rijeka (Fig. 1) in the northern Adriatic and included: (i) turbid (cloudy) water due to intense
965 rain at night and in the morning, (ii) flooding of the city due to record-breaking rainfall (110 mm recorded in Rijeka on 23 December) and storm surge; (iii) traffic obstructions due to plant and soil debris; (iv) cracking of the road surfaces.

Based on online sources (Glas Istre, 25 and 26 December 2009; Jutarnji list, 25 December 2009; Vatrogasni portal, 25 December 2009), the effects of the 25 December 2009 flood are listed. The flood impacts were again most severe in Rijeka and its surroundings and included: (i) numerous firefighter interventions due to several days of heavy rainfall; (ii) flooding of
970 basements due to the spilling of swollen river Rječina (small river flowing through Rijeka); (iii) closure of local roads and parts of the national highway.

4.10 The flood of 1 December 2008 (ID 16; rank 2)

The meteorological and marine conditions that led to this flood have been empirically analysed (Međugorac et al., 2015; 2016), numerically modelled (Bertotti et al., 2011; Zampato et al., 2016; Bajo et al., 2019) or included in other analyses
975 (Lionello et al., 2021). The episode was particularly severe along the eastern Adriatic coast, where it flooded not only the

northern part but also large coastal stretches in the middle and southern Adriatic. The most intense flood before this episode occurred on 22 December 1979 (Table 2, ID = 9).

4.10.1 Meteorological background

The period preceding this episode was characterised by intense cyclonic activity (Fig. 30a). On 27 November a surface-based cyclone entered the Mediterranean area from the north of Africa. At the same time, the anticyclone over the Adriatic was weakening and the air temperature was gradually dropping as the upper-level ridge began to shift eastward in front of the emerging widespread trough that affected the eastern Atlantic and stretched across western and central Europe. During the day, the centre of the surface-based cyclone was deepening while shifting towards the Gulf of Genoa and then continued over northern Italy and the Adriatic further to the east.
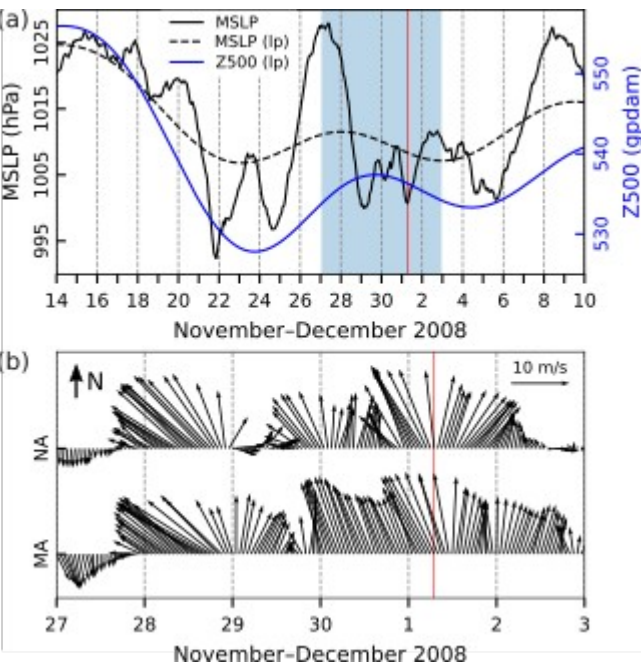
Figure 30: Series of ERA5 reanalysis data related to the flood of 1 December 2008. (a) MSLP (hourly) and MSLP (lp) (low-pass filtered with a cut-off frequency of 10 d) and Z500 (lp) (low-pass filtered with a cut-off frequency of 10 d) at a grid point near TG Bakar. (b) Hourly **W10** during the period marked in blue in the upper plot for the middle (MA) and northern (NA) Adriatic (all locations marked in Fig. 1). The red line indicates onset of SL maximum.

With the arrival of an additional amount of cold and unstable air from the northwest of the continent in the upper-levels, during the night of 28–29 November another cyclone developed in the Bay of Biscay, and the pressure in its centre dropped up to 985 hPa. During 29 November, the frontal system associated with this cyclone entered the Western European mainland causing the formation of a new cyclone in the Gulf of Lion. This new cyclone propagated quite fast eastward, and on 30 November its frontal system affected the Adriatic area. At the same time, the centre of another cyclone that originated from the Bay of Biscay moved over France, and due to the constant inflow of the cold air within the upper-level trough over

140

Western Europe and the Mediterranean, a new surface-based cyclone formed over the Western Mediterranean. The cyclone rapidly advanced toward the Gulf of Genoa, intensifying to 995 hPa, before moving across northern Italy (Fig. 31) and

1010 further over the Adriatic toward the northeast. On 1 December, an air pressure gradient of ~20 hPa developed over the Adriatic, accompanied by Sirocco that reached higher speeds near the eastern coastline (Fig. 31b). Synoptic situations like this, long-lasting low air pressure and the constant propagation of several cyclones and their frontal systems, caused quite strong southerly winds over the Adriatic for days (Fig. 30b), as well as locally heavy precipitation. On 1 December, precipitation reached up to 25 mm in the northern Adriatic and 5–20 mm in the middle Adriatic. On 2 December, amounts

1015 increased to up to 30 mm in the northern Adriatic and up to 25 mm in the middle Adriatic.
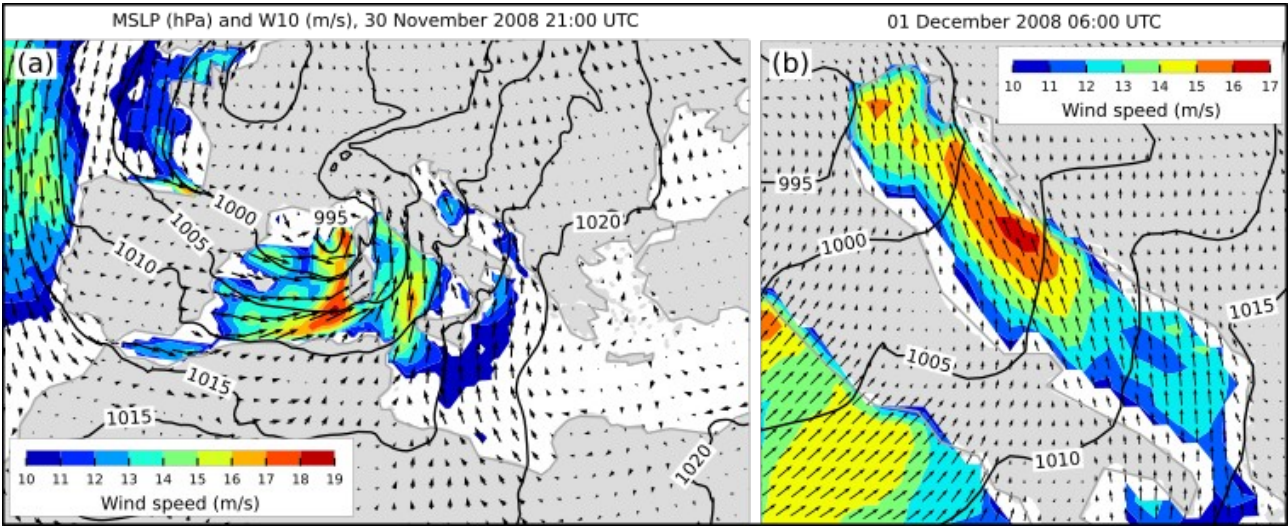
Figure 31: MSLP (black lines) and **W10** (arrows and colours) fields from the ERA5 reanalysis. Conditions (a) over the Mediterranean that preceded the situation (b) over the Adriatic Sea (an hour before maximum SL in Bakar). Only wind speeds exceeding 10 m/s are coloured.

4.10.2 Sea-level evolution

1020 In the morning hours of 1 December 2008 (07:00 UTC), the sea level in Bakar rose to 105 cm above the long-term average (Table 2, Fig. 32).

The moon was three days past the new moon, which gave *tide* a semidiurnal spring-tide character. The total SL maximum formed during the daily maximum of *tide*, which was 23 cm.

Local processes were active during the flood and their contribution amounted to 9 cm.

1025 The SL maximum formed immediately before the maximum of *synoptic component*, influenced in part by pre-existing seiches. Figure 32 shows that the natural basin oscillations of variable height were present in *synoptic component* from 21 November. They were supported by a series of cyclones that crossed the Adriatic Sea before the flood (Fig. 30a) and that caused sudden wind changes, triggering and reinforcing seiches (Fig. 30b). Considering the period of the natural oscillations

(T~21.2 h) and the timing of their amplification (strong peak of the residual SL the day before the maximum), it is obvious

1030 that they contributed positively to the flood. Due to the pre-existing oscillations and the storm surge triggered by the strong winds that developed over the entire central Adriatic, with maximum speeds closer to the eastern coast (Fig. 31b), the synoptic SL response was high and amounted to 43 cm.
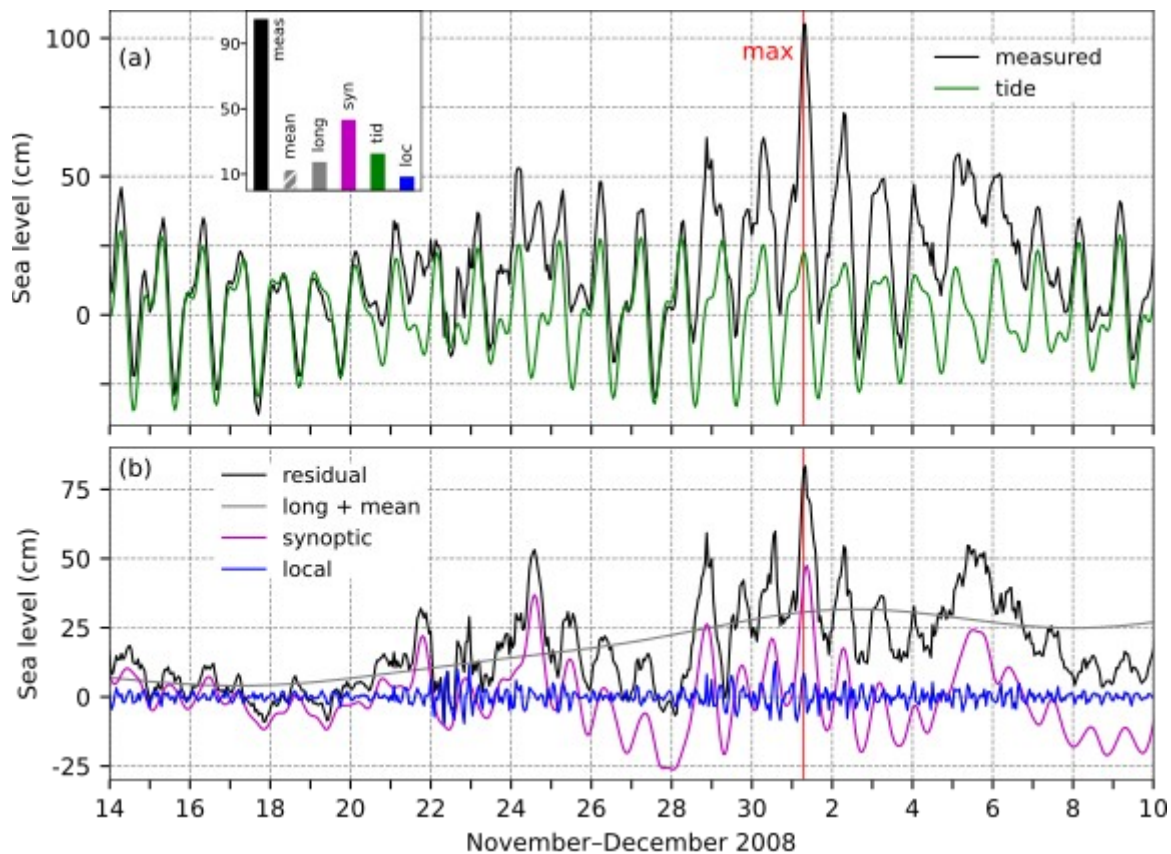
Figure 32: SL series for the flood of 1 December 2008. (a) Measured sea level (black) and *tide* (green). The inset figure shows the

1035 contributions (cm) of the five sea-level components to the maximum measured sea level ("meas"; 07:00 UTC): "loc" refers to *local component* (9 h < T), "syn" to *synoptic component* (9 h < T < 10 d), "tid" to *tide*, "long" to *long-period sea-level component* (10 < T < 100 d), "mean" to *mean sea-level changes* (100 d < T). (b) Residual sea level (black), the combined series of *long-period sea-level component* and *mean sea-level changes* (grey; long + mean), *synoptic component* (purple), and *local component* (blue). The red line indicates the time of occurrence of the total SL maximum.

1040 A planetary-scale atmospheric disturbance, closely related to passage of Rossby waves in the middle troposphere (indicated by Z500 (lp) in Fig. 30a), induced a gradual rise in SL, beginning approximately 14 days before the flood (Fig. 32b, long + mean). This SL increase was influenced by MSLP (lp) and **W10** at 10–100 d periods. MSLP (lp) drop supported SL increase until 23 November, after which MSLP (lp) began to rise. Nonetheless, SL continued to increase, supported by southerly

145

winds at 10–100 d periods with speeds of up to 3 m/s. *Long-period sea-level component* contributed 17 cm to this flood.

1045 *Mean sea-level changes* (100 d < T) contributed 13 cm to the maximum (Fig. 32a, histogram). This episode aligned with the annual peak of the seasonal cycle and interannual variability, which added 8 cm to the total SL (Figs. A1, A2a, and A2c). The contribution from (multi)decadal changes was minimal (1 cm, Fig. A3b), while secular change provided 4 cm (Fig. A3a).

In summary, the flood developed as a positive superposition of all the SL processes involved, of which *synoptic component*

1050 was the largest (Fig. 32a).

4.10.3 Flood impacts

The following impacts of the episode are listed using available daily newspapers from 2 December 2008 (Jutarnji list, Novi list, Slobodna Dalmacija, Večernji list, Vjesnik) and 3 December 2008 (Novi list). The coastal regions of the northern and middle Adriatic experienced exceptionally high sea levels. Storm surge flooded the streets and squares along the coast,

1055 roads, farmers' markets, beaches, shops, restaurants, cáfes, residential and business areas. In the northern Adriatic county of Primorje-Gorski Kotar, damage amounting to several tens of thousands of euros was reported. Additionally, the following effects were reported in the northern Adriatic: (i) exceptionally strong Sirocco (with wind gusts of up to 26 m/s in Rijeka) knocked down trees and ripped roofs off houses; (ii) local ferry and catamaran lines were disrupted; (iii) multi-ton concrete slabs at a public beach were displaced. In the middle Adriatic ferry and catamaran services were also disrupted, and several

1060 coastal towns were flooded, with water reaching highest levels in Šibenik (Fig. 1) of up to one metre in height.

4.11 The flood of 26 November 1996 (ID 15; rank 14)

This episode has not yet been studied in the scientific literature, but Lionello et al. (2006) conducted a series of numerical experiments (with data assimilation) on storm surges that occurred prior to the flood (5–14 November 1996).

4.11.1 Meteorological background

1065 The week before the flood in Bakar Bay, the Adriatic region was affected by an upper-level trough extending from Scandinavia to southern Europe. For several days, warm and humid air flowed over the region, which led to the formation of several cyclones (Fig. 33a) with frontal disturbances. These systems caused moderate precipitation as they crossed over the Adriatic Sea. The wind over the Adriatic was spatially variable in speed and direction (Fig. 33b). A low-pressure system developed over the Gulf of Genoa on the night of 25–26 November (Figure 34a), which, accompanied by a frontal system,

1070 progressed towards the northern Adriatic on 26 November (Fig. 34b). As a result, the southern and southeasterly wind was gradually strengthening along the entire basin (Fig. 33b). As the day progressed, the cyclone moved southeastward along the

Adriatic. On 26 December, precipitation in the northern Adriatic ranged from 20 to 40 mm, with locally much higher amounts, such as 69 mm recorded at Sv. Ivan na Pučini near Rovinj. In contrast, the middle Adriatic recorded up to 30 mm.
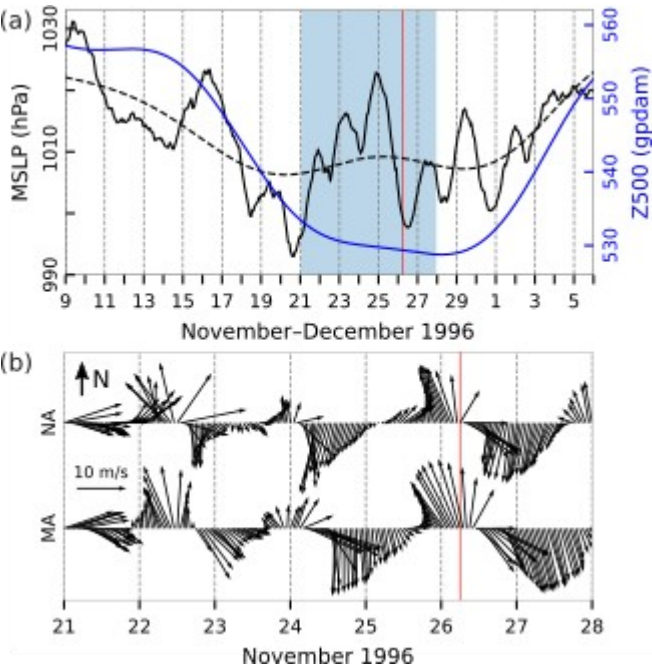
Figure 33: Series of ERA5 reanalysis data related to the flood of 26 November 1996. (a) MSLP (hourly) and MSLP (lp) (low-pass filtered with a cut-off frequency of 10 d) and Z500 (lp) (low-pass filtered with a cut-off frequency of 10 d) at a grid point near TG Bakar. (b) Hourly **W10** during the period marked in blue in the upper plot for the middle (MA) and northern (NA) Adriatic (all locations marked in Fig. 1). The red line indicates onset of SL maximum.
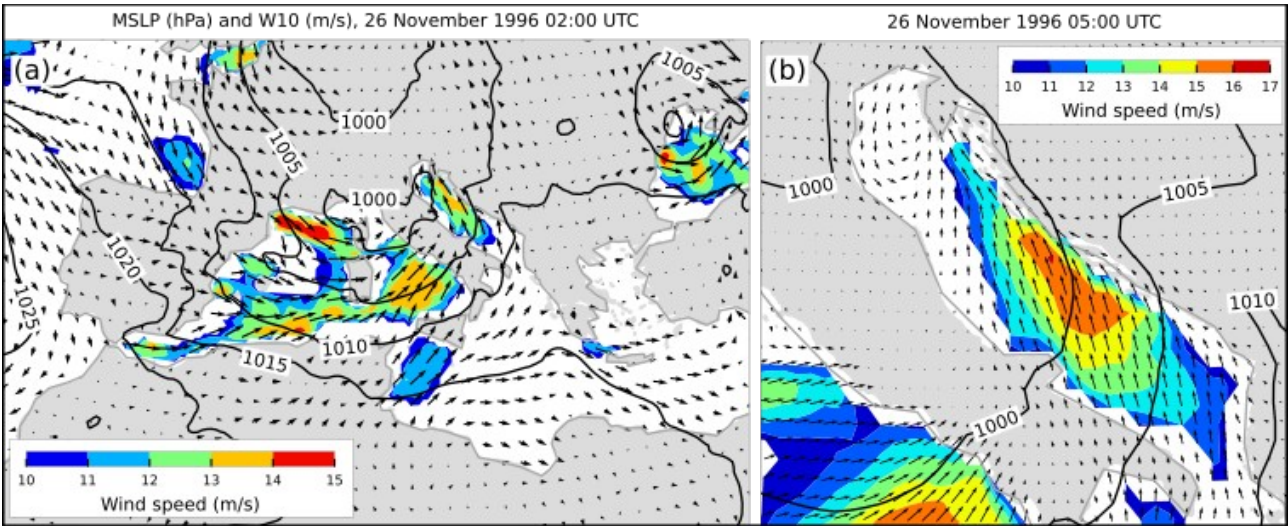
Figure 34: MSLP (black lines) and **W10** (arrows and colours) fields from the ERA5 reanalysis. Conditions (a) over the Mediterranean that preceded the situation (b) over the Adriatic Sea (an hour before maximum SL in Bakar). Only wind speeds exceeding 10 m/s are coloured.

4.11.2 Sea-level evolution

1095 On 26 November 1996, at 06:00 UTC, sea level in Bakar reached 90 cm above the long-term mean (Table 2, Fig. 35).

At that time, the moon was two days past the new moon, which meant that *tide* had semidiurnal spring-tide character. The SL maximum coincided closely with the daily tidal peak, with *tide* contributing 25 cm.

Local processes were active during the flood and added 7 cm to the total SL maximum.
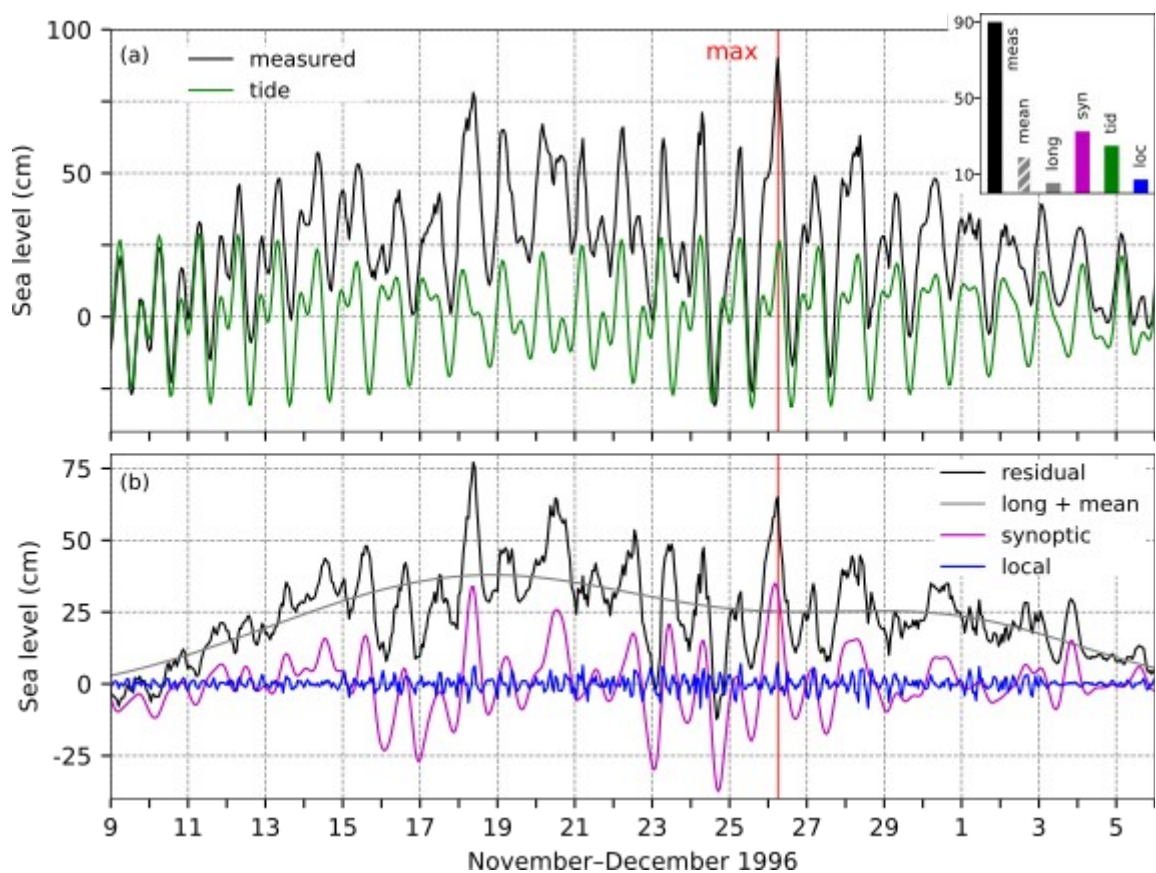
1100 **Figure 35:** SL series for the flood of 26 November 1996. (a) Measured sea level (black) and *tide* (green). The inset figure shows the contributions (cm) of the five sea-level components to the maximum measured sea level ("meas"; 06:00 UTC): "loc" refers to *local component* (9 h < T), "syn" to *synoptic component* (9 h < T < 10 d), "tid" to *tide,* "long" to *long-period sea-level component* (10 < T < 100 d), "mean" to *mean sea-level changes* (100 d < T). (b) Residual sea level (black), the combined series of *long-period sea-level component* and *mean sea-level changes* (grey; long + mean), *synoptic component* (purple), and *local component* (blue). The red line indicates the time 1105 of occurrence of the total SL maximum.

In the week leading up to the flood, several cyclones passed through the area (Fig. 33a), generating Adriatic seiches (T~21.2 h). These seiches were induced and reinforced multiple times (Lionello et al., 2006). Residual and synoptic series (Fig. 35b)

155

indicate that the last reinforcement occurred during the first half of 24 November, placing the seiche in a positive phase as the decisive storm surge developed. The main maximum occurred shortly after the peak of *synoptic component* which

1110   amounted to 33 cm.

The preconditioning (estimated by assessing *long-period sea-level component*) was weak (Fig. 35a, histogram). Sea level began to rise around 9 November (Fig. 35b, long + mean) due to a drop in air pressure (Fig. 33a, MSLP (lp)) and southeasterly winds at periods 10–100 d (not shown). However, in the days leading up to the flood around 20 November, air pressure started to increase and the wind shifted to westerly or northwesterly, resulting in a decrease of SL (Fig. 35b). This

1115   change reduced the contribution of *long-period sea-level component* to the flood to just 5 cm.

Regarding *mean sea-level changes* (100 d < T), they contributed 20 cm (Fig. 35, histogram), with the seasonal signal and interannual variability being the most significant (17 cm). This year, the seasonal signal in combination with interannual variability exhibited a large amplitude (Fig. A1, A2a and A2c), and the flood occurred at its peak. In contrast, processes with periods longer than 5 y were not prominent (Fig. A3): (multi)decadal processes made no contribution, while secular change

1120   added 3 cm.

In summary, this maximum resulted from the positive effects of all involved processes, particularly *synoptic component* and *tide* (Fig. 35).

4.11.3 Flood impacts

For this event, the available literature in the National and University Library was reviewed; however, no mentions of the

1125   event impacts were found. The reason for this is unknown.

4.12 The flood of 2 October 1993 (ID 14; rank 14)

Canestrelli et al. (2001) provided a description of the episode. Their analysis included synoptic charts, SL data from TG Venice Punta Salute (Italy), and **W10** and MSLP measurements from multiple coastal stations.

4.12.1 Meteorological background

1130   Two days before the occurrence of SL maximum in Bakar, a deep cyclone advanced from the North Atlantic towards western Europe and progressively moved further into the European continent. Under these conditions, on 1 October, the Adriatic came under the influence of upper-level southwest flow and advection of relatively warm and humid air on the front side of the trough. At the surface a moderate Sirocco was blowing along the entire Adriatic (Fig, 36b). By 2 October, much of the European continent was experiencing widespread cyclonic activity. By 06:00 UTC a secondary cyclone formed in the

1135   Gulf of Genoa (Fig. 37a) and briefly joined the cyclone over Central Europe before moving southeast from northern Italy

across the Adriatic Sea, intensifying the air-pressure gradient over the Adriatic and bringing precipitation along the Croatian coastline (along the northern Adriatic 10–40 mm, in the middle Adriatic up to 20 mm). Throughout the day, the intensity of Sirocco increased, with stronger wind observed along the eastern coast of the basin. The entire Adriatic experienced strong and severe Sirocco in the afternoon of 2 October (Figs. 36b and 37b), which peaked in intensity in the evening, coinciding with the extreme sea level in Bakar at 20:00 UTC. The wind weakened first over the northern Adriatic, followed by the central and southern regions as the cyclone continued to move towards the east.
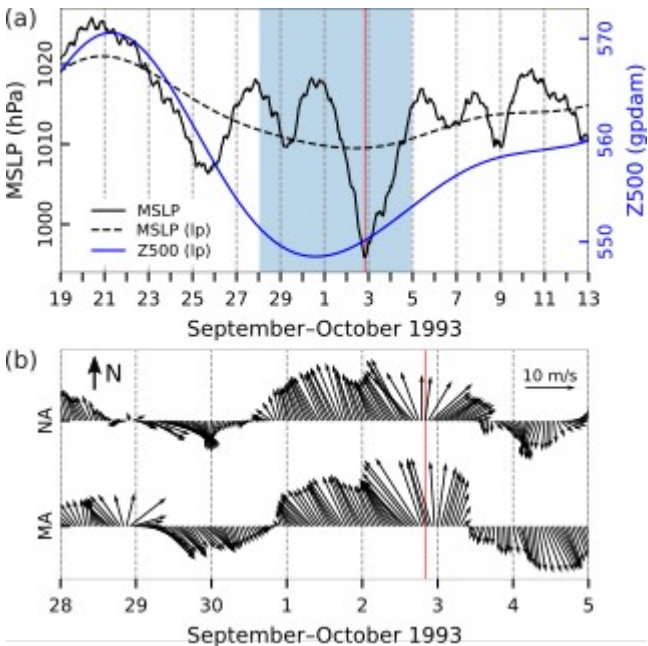
Figure 36: Series of ERA5 reanalysis data related to the flood of 2 October 1993. (a) MSLP (hourly) and MSLP (lp) (low-pass filtered with a cut-off frequency of 10 d) and Z500 (lp) (low-pass filtered with a cut-off frequency of 10 d) at a grid point near TG Bakar. (b) Hourly **W10** during the period marked in blue in the upper plot for the middle (MA) and northern (NA) Adriatic (all locations marked in Fig. 1). The red line indicates onset of SL maximum.

160
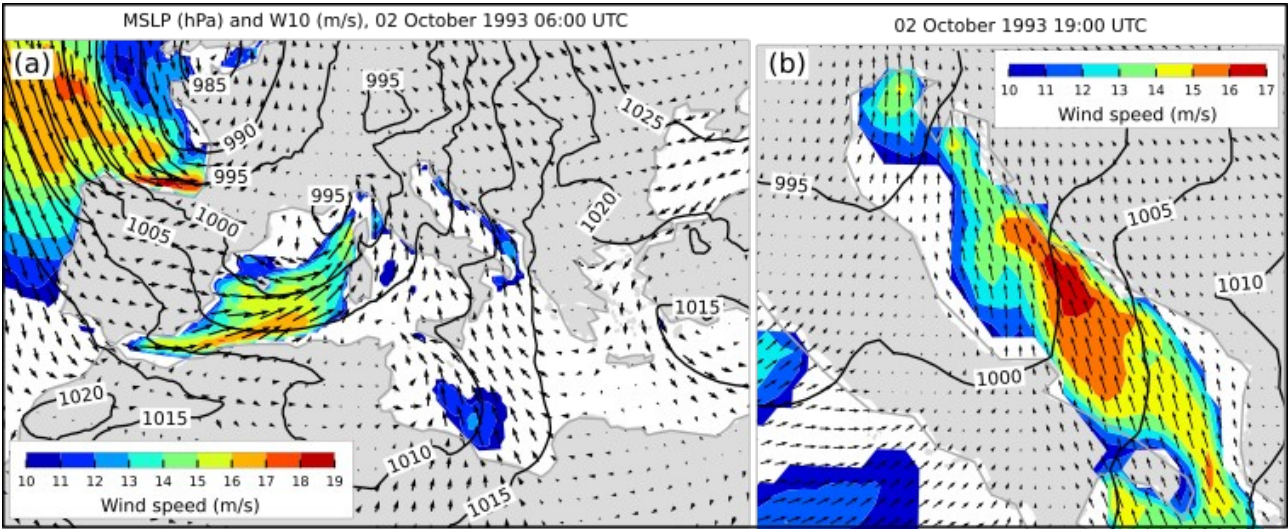
1165

Figure 37: MSLP (black lines) and **W10** (arrows and colours) fields from the ERA5 reanalysis. Conditions (a) over the Mediterranean that preceded the situation (b) over the Adriatic Sea (an hour before maximum SL in Bakar). Only wind speeds exceeding 10 m/s are coloured.

4.12.2 Sea-level evolution

On the evening of 2 October 1993 (20:00 UTC), the sea level in Bakar rose to 90 cm above the long-term mean (Table 2,
1170 Fig. 38).

The moon phase, being two days past the full moon, formed a semidiurnal spring-tide character of *tide*. The SL peak coincided with a secondary daily tidal maximum, which contributed only 5 cm to the overall maximum.

Local processes, however, contributed 20 cm to the total maximum — more than in any other event analysed in this study. As shown in Fig. 38b, a seiche in Kvarner Bay (with a period of ~6 h) was induced shortly before the main SL maximum
1175 and was the dominant process in *local component*.

In the week leading up to the event, the Adriatic was not influenced by cyclonic activity (Fig. 36a), resulting in the absence of active ~21.2 h seiches in the basin. Consequently, *synoptic component* was primarily shaped by a storm surge, which began to build in the morning of 2 October under the influence of a Mediterranean cyclone (Fig. 37a) and consequently by an air pressure gradient and Sirocco winds over the Adriatic (Figs. 36b and 37b). The developed storm surge reached its peak
1180 shortly before the SL maximum, contributing 45 cm.

Long-period sea-level component (10 < T < 100 d) was not considerable and it contributed to the flood with 9 cm (Fig. 38a, histogram). This rise was driven by a decrease in MSLP (lp) (which simultaneously changed with Z500 (lp)) (Fig. 36a), along with weak southeasterly to northeasterly winds at periods 10–100 d (not shown).

Mean sea-level changes contributed 11 cm to the overall maximum (Fig. 38a, histogram), shaped by the positive phase of the
1185 seasonal signal and interannual variability (13 cm, Figs. A1, A2a and A2c), a negative contribution from (multi)decadal

variability (-5 cm, Fig. A3b), and a positive contribution from secular change (3 cm, Fig. A3a).

In summary, his flood resulted from a positive combination of all components, particularly *synoptic* and *local processes*.
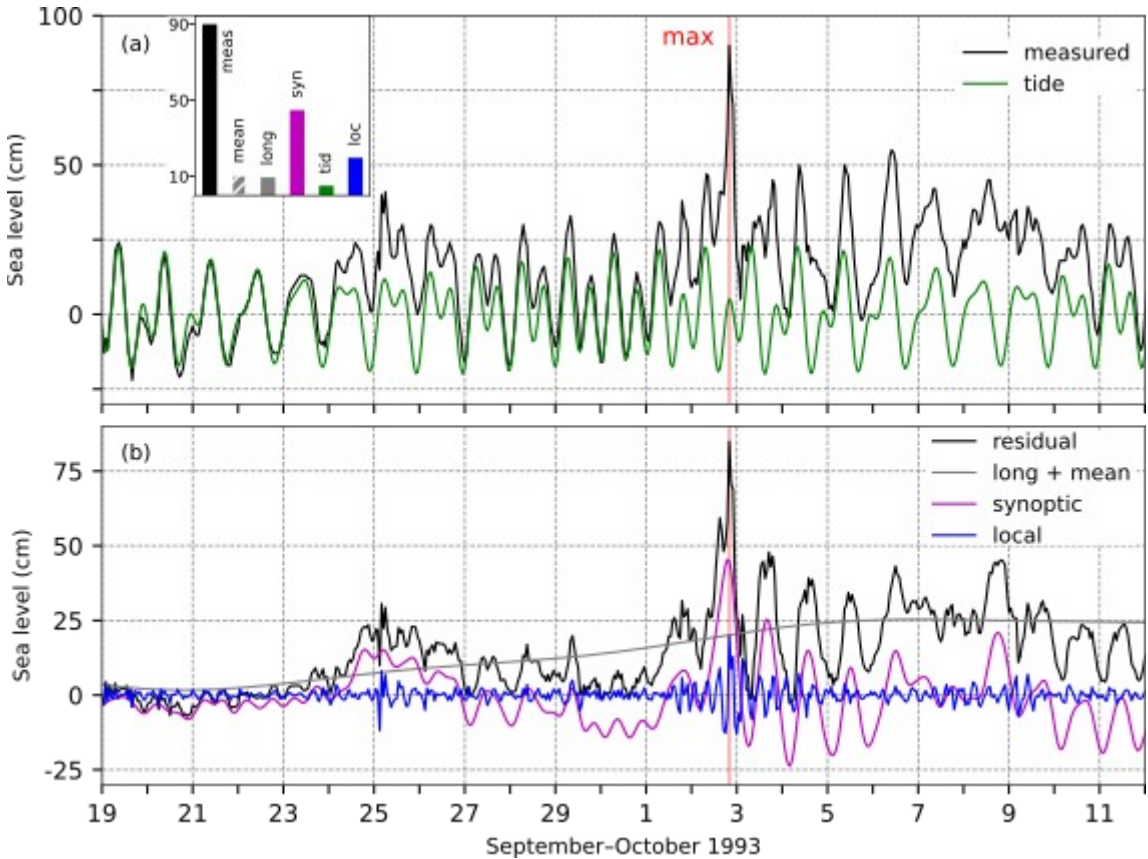
Figure 38: SL series for the flood of 2 October 1993. (a) Measured sea level (black) and *tide* (green). The inset figure shows the contributions (cm) of the five sea-level components to the maximum measured sea level ("meas"; 20:00 UTC): "loc" refers to *local component* (9 h < T), "syn" to *synoptic component* (9 h < T < 10 d), "tid" to *tide*, "long" to *long-period sea-level component* (10 < T < 100 d), "mean" to *mean sea-level changes* (100 d < T). (b) Residual sea level (black), the combined series of *long-period sea-level component* and *mean sea-level changes* (grey; long + mean), *synoptic component* (purple), and *local component* (blue). The red line indicates the time of occurrence of the total SL maximum.

4.12.3 Flood impacts

For this event, the available literature in the National and University Library was reviewed; however, no sources were found. The reason for this could be the Croatian War of Independence occurring at the time that may have caused newspapers to focus on more pressing issues.

4.13 The flood of 10 December 1990 (ID 13; rank 13)

Canestrelli et al. (2001) provided a description of the episode. Their analysis included synoptic charts, SL data from TG Venice Punta Salute, and **W10** and MSLP measurements from multiple coastal stations.

4.13.1 Meteorological background
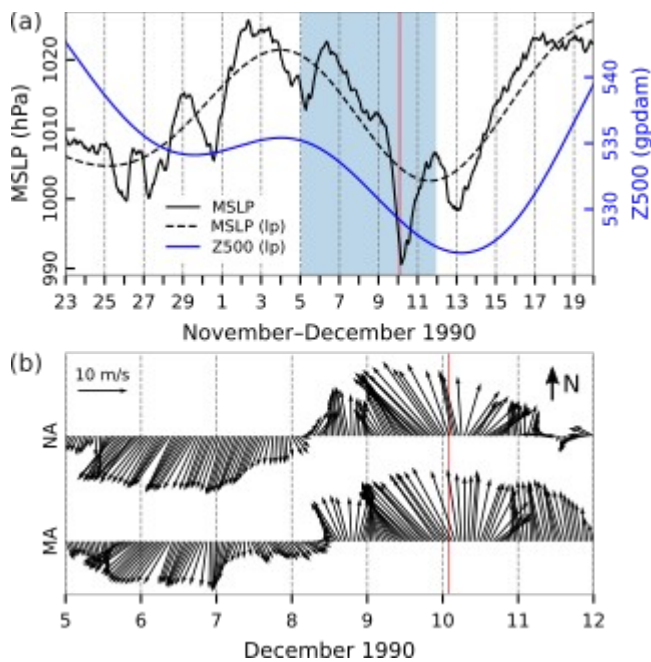
Figure 39: Series of ERA5 reanalysis data related to the flood of 10 December 1990. (a) MSLP (hourly) and MSLP (lp) (low-pass filtered with a cut-off frequency of 10 d) and Z500 (lp) (low-pass filtered with a cut-off frequency of 10 d) at a grid point near TG Bakar. (b) Hourly **W10** during the period marked in blue in the upper plot for the middle (MA) and northern (NA) Adriatic (all locations marked in Fig. 1). The red line indicates onset of SL maximum.

Period before the flood was characterised by passages of several non pronounced low-pressure systems over the Adriatic (Fig. 39a). In the week preceding the flood in Bakar, a deep upper-level trough descended from northern Europe towards the Mediterranean. Under such conditions, the entire Mediterranean was influenced by the upper-level southwest flow at the front of the trough, which supported the advection of relatively warm and humid air. At 18 UTC on 8 December, a cyclone formed over Spain and moved eastward. By the afternoon of 9 December, the cyclone with a frontal system had reached the Gulf of Genoa (Fig. 40a). With the development and deepening of the cyclone, air-pressure gradients intensified. In the afternoon of 9 December, south and southeast flow gradually strengthened over the Adriatic Sea (Fig. 39b). The winds were more intense on the eastern side than on the western side of the basin (Fig. 40a). During the night of 9–10 December, the wind reached maximum speeds, and severe Sirocco was blowing throughout the Adriatic Sea (Fig. 40b). This coincided with the onset of extreme SL recorded in Bakar on 10 December at 02:00 UTC. As the cyclone slowly moved across the Adriatic Sea, the wind weakened and changed direction to southwest first on the northern, then on the middle, and finally on the

170

1230 southern Adriatic. Considerable amounts of precipitation were recorded during this episode. On 10 December, similar amounts were observed along the entire coastline, in the northern Adriatic it was recorded mostly up to 35 mm and the middle Adriatic recorded between 10 and 40 mm.
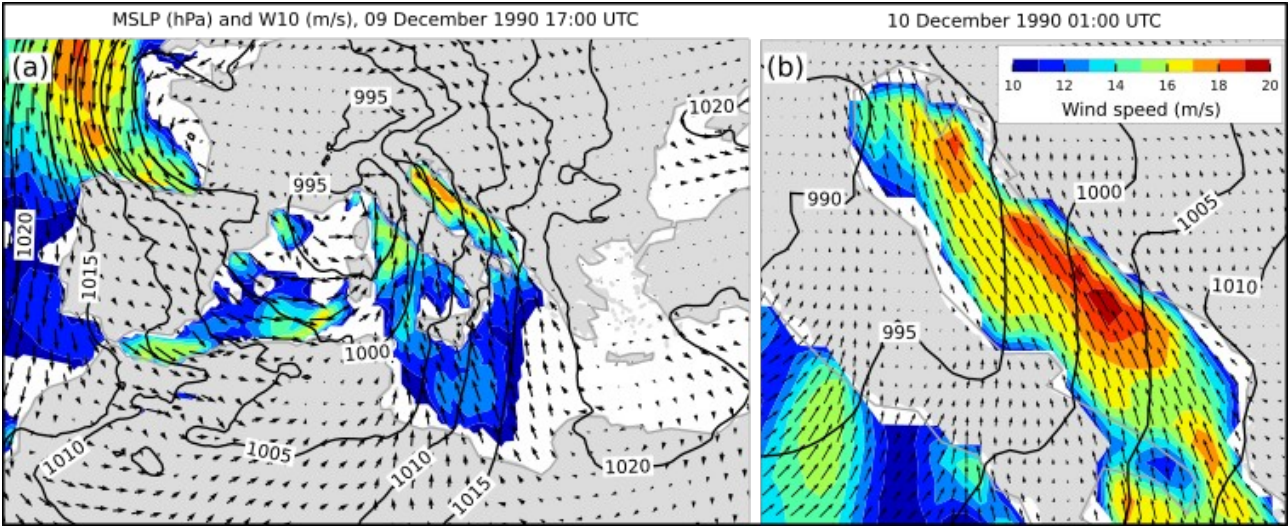
Figure 40: MSLP (black lines) and **W10** (arrows and colours) fields from the ERA5 reanalysis. Conditions (a) over the Mediterranean that
1235 preceded the situation (b) over the Adriatic Sea (an hour before maximum SL in Bakar). Only wind speeds exceeding 10 m/s are coloured. One colormap for both maps.

4.13.2 Sea-level evolution

On 10 December 1990, at 02:00 UTC, sea level in Bakar reached 91 cm above the long-term mean (Table 2, Fig. 41).

At that time, the moon was one day past the last quarter, which meant that *tide* had a diurnal neap-tide character. The SL
1240 maximum coincided with the daily tidal peak, with *tide* contributing 20 cm (Fig. 41a).

Local processes were not pronounced during the flood and added negligible 1 cm to the total SL maximum.

In the period leading up to the flood, several weak low-pressure systems moved across the Adriatic (Fig. 39a). However, these systems did not generate significant basin-wide oscillations (Fig. 41b). The residual SL series shows two peaks, on 25 November and 8 December, however, no subsequent oscillations with a period of ~21.2 h are apparent. This suggests that the
1245 episode was not influenced by a pre-existing Adriatic seiche. Instead, *synoptic component* was dominated by a storm surge, which reached a peak height of 55 cm. The total SL maximum occurred 4 h after the storm-surge peak, during the daily tidal maximum. S*ynoptic component* contributed 42 cm to the overall SL maximum.

Long-period sea-level variability contributed 21 cm to this episode. The sea level initially peaked around 26 November (Fig. 41b) but then decreased due to rising air pressure (Fig. 39a) and northeasterly winds (periods 10–100 d) from 29 November
1250 to 7 December, occasionally reaching speeds of 8 m/s. Around 4 December, as the wind conditions were still unfavorable,

the MSLP (lp) began to drop. Subsequently, the winds shifted to southeasterly, with speeds up to 4 m/s, causing the *long-period sea-level component* to rise by 21 cm at the SL peak. Throughout the shown period, SL (mean + long) varied simultaneously with MSLP (lp) (Figs. 39 and 41), while MSLP (lp) did not reflect changes in Z500 (lp) (Fig. 39a).
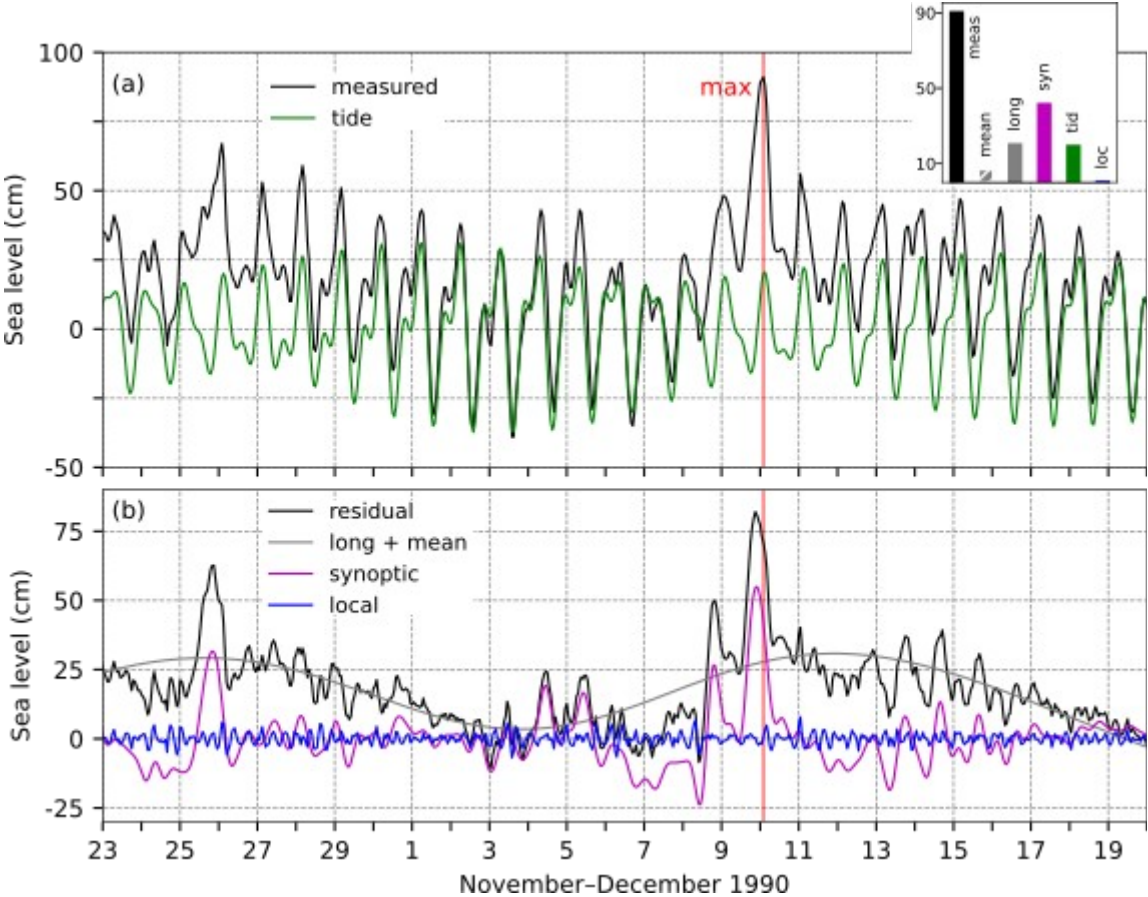
Figure 41: SL series for the flood of 10 December 1990. (a) Measured sea level (black) and *tide* (green). The inset figure shows the contributions (cm) of the five sea-level components to the maximum measured sea level ("meas"; 02:00 UTC): "loc" refers to *local component* (9 h < T), "syn" to *synoptic component* (9 h < T < 10 d), "tid" to *tide*, "long" to *long-period sea-level component* (10 < T < 100 d), "mean" to *mean sea-level changes* (100 d < T). (b) Residual sea level (black), the combined series of *long-period sea-level component* and *mean sea-level changes* (grey; long + mean), *synoptic component* (purple), and *local component* (blue). The red line indicates the time of occurrence of the total SL maximum.

Mean sea-level changes (100 d < T), contributed 7 cm to the flood (Fig. 41a, histogram), with the seasonal cycle and interannual variability being the largest contributor, amounting to 13 cm. This year, the combined series of seasonal cycle and interannual variability exhibited a pronounced amplitude (Fig. A1, A2a, and A2c); however, the flood occurred after its peak.

175

1265 In contrast, processes on (multi)decadal timescales were in a negative phase (Fig. A3b), reducing the sea level maximum by 8 cm. This represents the largest negative contribution of these processes among all the floods studied. Secular changes contributed an additional 2 cm to the maximum (Fig. A3a).

In summary, this flood was driven by the positive contributions of all involved processes, particularly *synoptic component*, *long-period sea-level variability*, and *tide* (Fig. 41).

1270 **4.13.3 Flood impacts**

A review of the available daily newspapers (Novi list, Slobodna Dalmacija, Večernji list; 11 December 1990) revealed the following effects of the episode. The strong and gale Sirocco, accompanied by heavy rain on the night of the 10 December, caused considerable disruption along the northern and middle Adriatic coast. Maritime traffic was severely affected, with numerous vessels damaged or submerged and roads flooded in the northern Adriatic. One particularly difficult incident

1275 occurred in Rijeka's port where two tugboats had to secure a tanker in the midst of strong and gale wind and waves. Many ferries and shipping lines were suspended, isolating most islands in Kvarner Bay and along the middle Adriatic coastline, where waves reached 6–7 m. Additional damage and emergency interventions included (i) damage to a breakwater in a northern Adriatic town, (ii) numerous damaged shores, especially on middle Adriatic islands, (iii) a failure in Rijeka's emergency power line, leaving it inoperative, (iv) flooded basements and first floor rooms as well as fallen power lines and

1280 uprooted trees near Šibenik.

4.14 The flood of 24 November 1987 (ID 12; rank 14)

This episode was discussed in a doctoral thesis by Pasarić (2000) (in Croatian). She concluded that in Bakar, the flood was less severe than it could have been due to a non-constructive interaction between tide and the storm surge. However, the episode was preconditioned by a gradual rise in SL, driven by the passage of atmospheric planetary waves during the week

1285 leading up to the flood.

4.14.1 Meteorological background

The conditions leading up to the flood began several days earlier, when a deep upper-level trough with its axis extending from northern Scandinavia to the African continent was visible in the field of Z500. Under these conditions, the entire Mediterranean was under the influence of upper-level southwestern flow on the front side of the trough, supporting the

1290 advection of relatively warm and humid air. On 23 November, a deep upper-level cyclone formed over the western Mediterranean, resulting in the formation of a surface cyclone over Spain that then moved northeasterly over the European continent (Figs. 42a and 43a). As a result, air-pressure gradients intensified, and there was a strengthening of southerly and

southeasterly flow over the Adriatic (Fig. 42b), which was more intense in the eastern part of the basin. Sirocco gradually intensified on 24 November (Fig. 43b), and reached severe levels along the entire Adriatic Sea. Additionally, large amounts

1295 of precipitation were recorded in the Adriatic coastal areas. In the middle Adriatic, precipitation reached up to 25 mm, while in the northern Adriatic, much higher amounts were recorded (58 mm at Pula airport, 153 mm in Rijeka, and 63 mm on the island of Cres in the northern Adriatic). The wind speeds reached their maximum values at 21:00 UTC, just an hour before the extreme SL was recorded in Bakar. Afterward, the cyclone progressed in a northeastward direction, causing the wind to gradually subside first in the northern region and later in the middle and southern parts of the Adriatic.

1300

1305
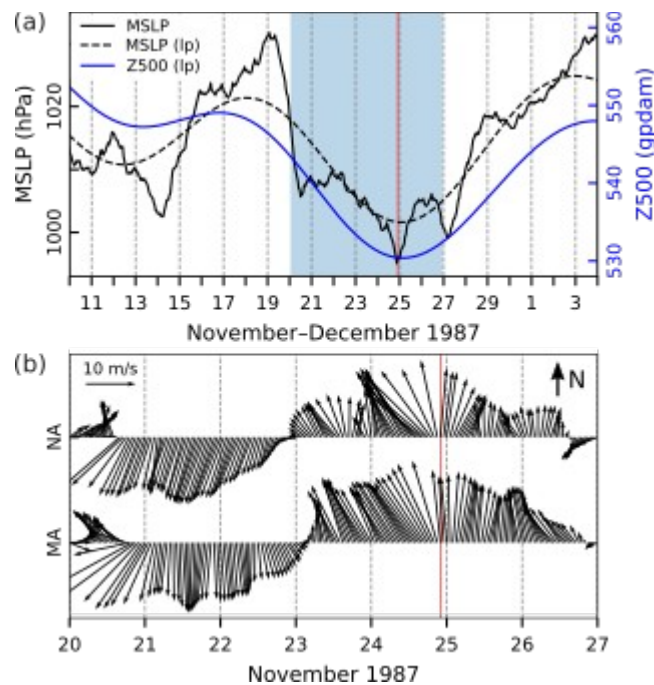
Figure 42: Series of ERA5 reanalysis data related to the flood of 24 November 1987. (a) MSLP (hourly) and MSLP (lp) (low-pass filtered with a cut-off frequency of 10 d) and Z500 (lp) (low-pass filtered with a cut-off frequency of 10 d) at a grid point near TG Bakar. (b) Hourly **W10** during the period marked in blue in the upper plot for the middle (MA) and northern (NA) Adriatic (all locations marked in Fig. 1). The red line indicates onset of SL maximum.

1310

1315
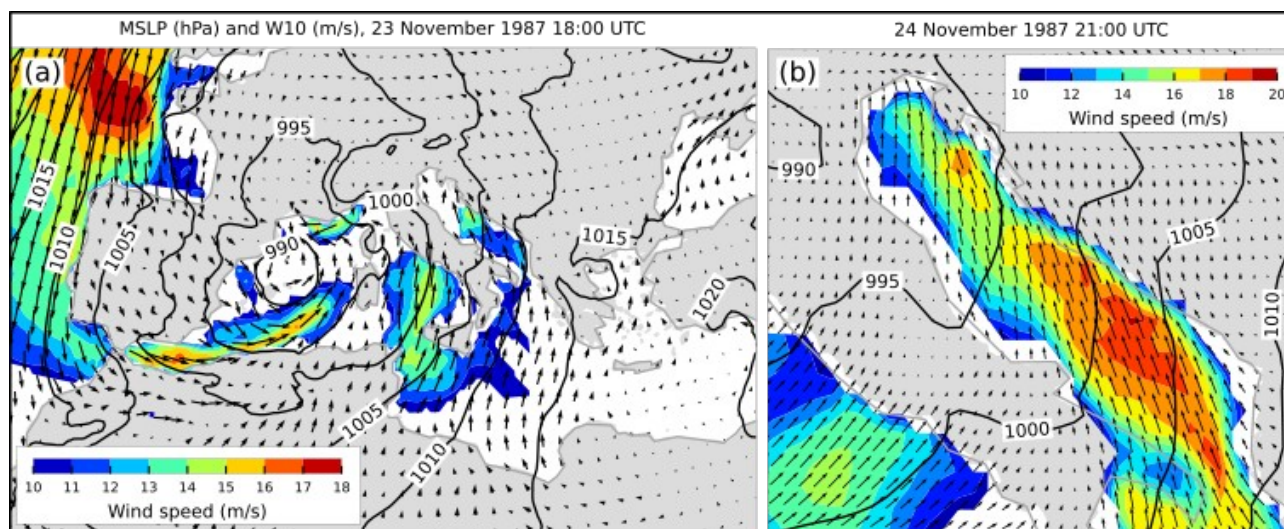
Figure 43: MSLP (black lines) and **W10** (arrows and colours) fields from the ERA5 reanalysis. Conditions (a) over the Mediterranean that preceded the situation (b) over the Adriatic Sea (an hour before maximum SL in Bakar). Only wind speeds exceeding 10 m/s are coloured.

4.14.2 Sea-level evolution

On 24 November 1987, at 22:00 UTC, the sea level in Bakar rose to 90 cm above the long-term mean (Table 2, Fig. 44). At that time, the moon was between the new moon and the first quarter, resulting in *tide* with spring-tide character. The sea-level peak occurred while *tide* was changing from negative to positive phase, therefore contributing only 5 cm to the total SL (Fig. 44a).

Local processes were relatively inactive during this period, contributing 4 cm to the overall SL maximum (Fig. 44b). Prior to the flood, there was no significant cyclonic activity in the Adriatic region (Fig. 39a), and the residual sea level or *synoptic component* did not exhibit the ~21.2 h oscillations characteristic of the Adriatic seiches. This indicates that the episode was not influenced by a pre-existing seiche. Instead, *synoptic component* was primarily a forced response, i.e., a storm surge, which peaked at 49 cm an hour before the SL maximum and contributed 48 cm to the flood. The storm surge began to develop on 23 November (Fig. 44b) as air pressure decreased (Fig. 42a) in the northern Adriatic and winds shifted to the southeast over the northern and middle parts of the basin (Fig. 42b).

Preceding conditions for the flood began several days earlier, with a gradual SL rise (Fig. 44b, long + mean) due to a consistent pressure drop (Fig. 42a) and a shift in wind direction to the southeast (10 < T < 100 d; not shown). During this period (Fig. 42a), changes in the mid-troposphere (series of Z500 (lp)) were transmitted to the lower layers (series of MSLP (lp)) and reflected in the sea level (long + mean). This suggests, as demonstrated by Pasarić (2000), Pasarić et al. (2000), and Pasarić and Orlić (2001), that *long-period sea-level component* was driven by the passage of atmospheric planetary waves, contributing 23 cm to the flood.

185

Mean sea-level changes added 10 cm to the overall maximum. The episode occurred in winter, shortly after the annual maximum, which was not particularly pronounced that year (Figs. A1, A2a, A2c). The main contribution came from the seasonal cycle and interannual variability, adding 11 cm to this component. At this time, (multi)decadal processes were in a negative phase, mitigating the flood by 3 cm (Fig. A3b). Additionally, secular change added 2 cm (Fig. A3a).

In summary, this episode resulted from a strong *synoptic component* combined with positive contributions from other processes.
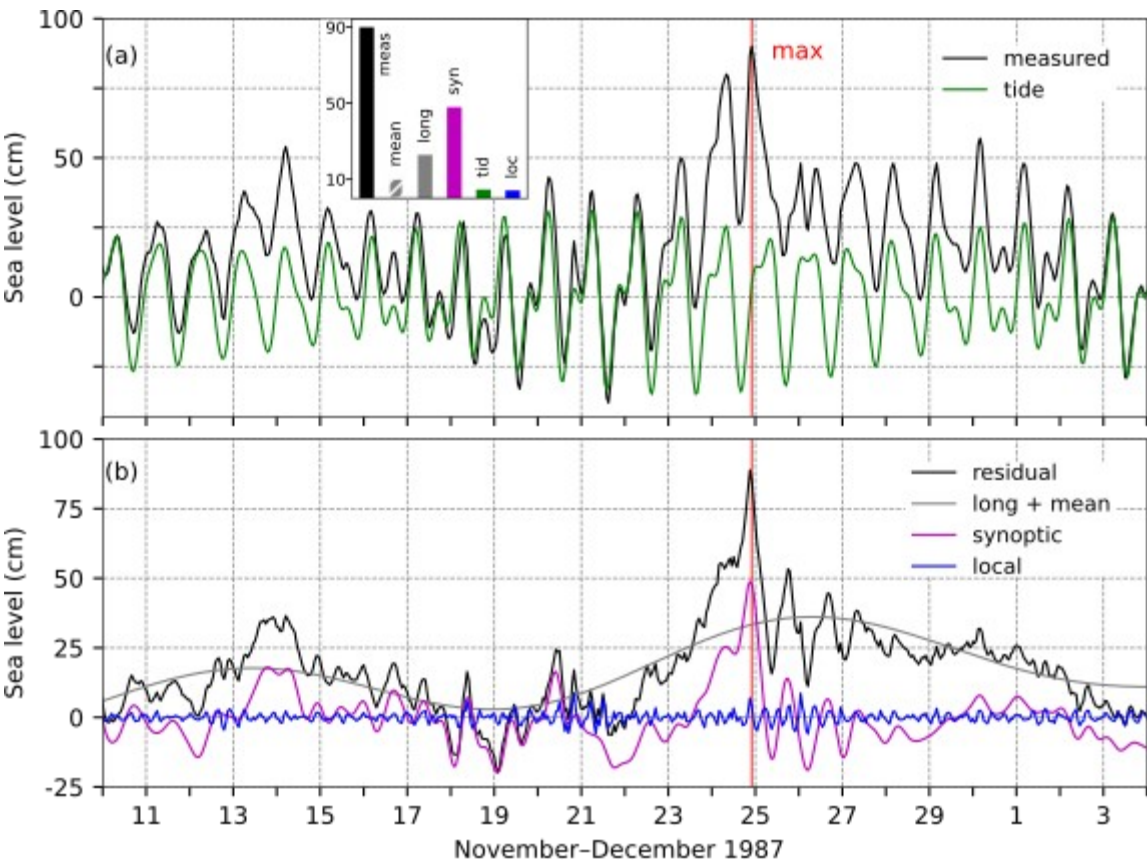
Figure 44: SL series for the flood of 24 November 1987. (a) Measured sea level (black) and *tide* (green). The inset figure shows the contributions (cm) of the five sea-level components to the maximum measured sea level ("meas"; 22:00 UTC): "loc" refers to *local component* (9 h < T), "syn" to *synoptic component* (9 h < T < 10 d), "tid" to *tide*, "long" to *long-period sea-level component* (10 < T < 100 d), "mean" to *mean sea-level changes* (100 d < T). (b) Residual sea level (black), the combined series of *long-period sea-level component* and *mean sea-level changes* (grey; long + mean), *synoptic component* (purple), and *local component* (blue). The red line indicates the time of occurrence of the total SL maximum.

4.14.3 Flood impacts

A review of the available daily newspapers (Novi list, 25 November 1987; Slobodna Dalmacija, 26 November 1987) revealed the following effects of the episode. The gale Sirocco in the northern Adriatic almost completely paralyzed ferry traffic between the mainland and the islands. High water levels, heavy rain, and strong waves caused significant flooding along many coastlines in western Istria and the Kvarner islands. In the Split area, the storm left visible consequences. The Split Riva was largely flooded, and on a local beach, debris such as shower heads, benches, beams, and other items were seen floating in the still-turbulent sea, and the concrete platform was covered with piles of seaweed. Additional damages and emergency interventions included (i) damaged boats and (ii) disruption to road traffic in the northern Adriatic.

4.15 The flood of 1 February 1986 (ID 11; rank 9)

This episode, including its meteorological background and SL components contributing to the maximum SL formation, is briefly described in Lionello et al. (2021). Also, Canestrelli et al. (2001) empirically analysed the flood taking into account synoptic charts, SL data from TG Venice Punta Salute, and **W10** and MSLP measurements from multiple coastal stations.

4.15.1 Meteorological background
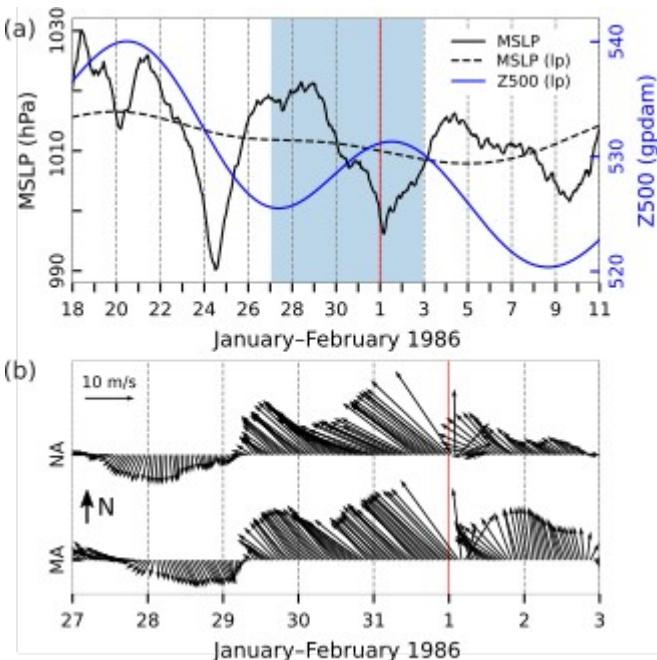
Figure 45: Series of ERA5 reanalysis data related to the flood of 1 February 1986. (a) MSLP (hourly) and MSLP (lp) (low-pass filtered with a cut-off frequency of 10 d) and Z500 (lp) (low-pass filtered with a cut-off frequency of 10 d) at a grid point near TG Bakar. (b) Hourly **W10** during the period marked in blue in the upper plot for the middle (MA) and northern (NA) Adriatic (all locations marked in Fig. 1). The red line indicates onset of SL maximum.

On 29 January, a southeast wind began to blow over the Adriatic (Fig. 45) due to a large cyclone centred over the Bay of Biscay, accompanied by a closed circulation of low pressure in the upper levels. Within this system, a secondary cyclone developed in the western Mediterranean on 30 January, where the central air pressure dropped to less than 975 hPa (Fig.

190

46a). As this cyclone moved towards the Gulf of Lion, the southeast wind over the Adriatic strengthened, turning to an easterly wind in some areas of the northern Adriatic. As the cyclone advanced towards the Gulf of Genoa, the wind over the Adriatic intensified to strong and gale on 31 January (Figs. 45b and 46b). On 1 February the cyclone advanced further northwards, resulting in gradual weakening of the wind and its shifting to southwesterly. On the day of the flood, precipitation along the coastline was mostly up to 30 mm, with locally higher amounts (55 mm on the northern Adriatic island Olib and 35 mm on the middle Adriatic island of Hvar). The following day, precipitation decreased to up to 20 mm along the coastline.
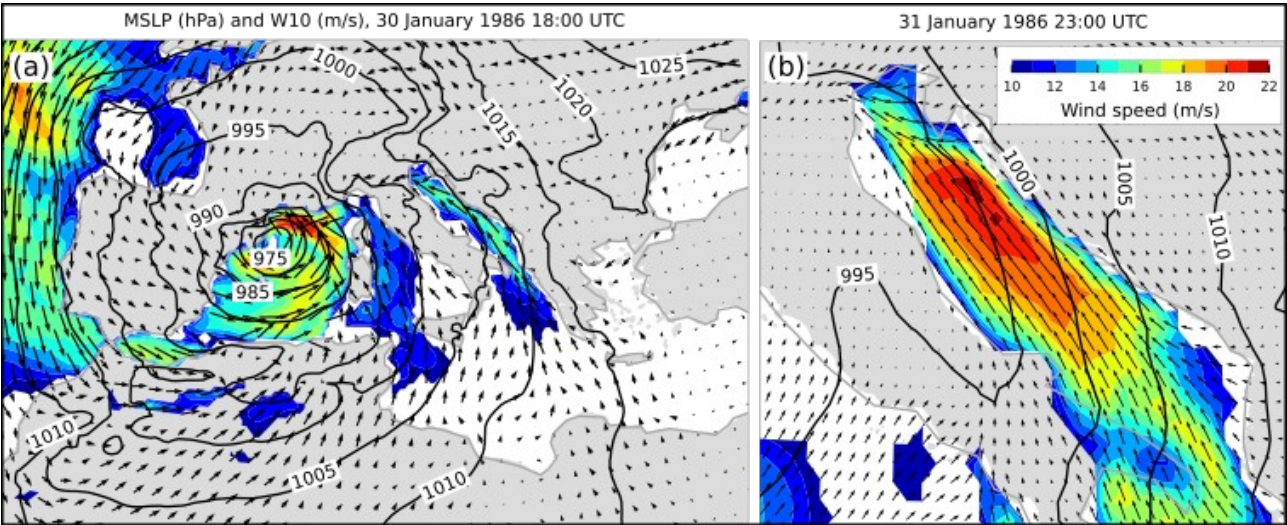
Figure 46: MSLP (black lines) and **W10** (arrows and colours) fields from the ERA5 reanalysis. Conditions (a) over the Mediterranean that preceded the situation (b) over the Adriatic Sea (an hour before maximum SL in Bakar). Only wind speeds exceeding 10 m/s are coloured. One colorbar for both maps.

4.15.2 Sea-level evolution

On 1 February 1986, at 00:00 UTC, the sea level in Bakar rose to 95 cm above the long-term average (Table 2, Fig. 47). The moon was a day before the last quarter, resulting in a diurnal neap *tide*. The sea-level peak coincided with the daily tidal maximum, contributing 21 cm to the total sea level (Fig. 47a).

Local processes had minimal impact during this event, adding 4 cm.

Synoptic component was extraordinary, peaking at 56 cm just an hour after the overall maximum. On 24 January, a deep cyclone passed over the Adriatic (Fig. 45a), raising sea level (Fig. 47b, residual) and initiating both basin-wide and local Kvarner bay (T~6h) seiches. By 1 February, however, these oscillations had dampened, so *synoptic component* primarily consisted of a storm surge. The storm surge began to develop on 29 January (Fig. 47b) as air pressure dropped and winds shifted from weak north/northwest to strong and gale southeast (Fig. 45b), contributing 54 cm to the flood.

Preconditioning for this flood, indicated by *long-period sea-level component*, was weak, with a gradual sea-level rise
1405 beginning several days prior (Fig. 47b). During the flood, this component was only 6 cm high. Comparing Z500 (lp), MSLP
(lp), and long + mean shows that these series did not change simultaneously, suggesting that the *long-period sea-level
component* was not driven by atmospheric planetary waves.

Mean sea-level component (100 d < T) added 10 cm (Fig. 47a, histogram), mainly due to the seasonal cycle and interannual
variability, as the event occurred shortly before the annual maximum (9 cm; Figs. A1, A2a, and A2c). (Multi)decadal
1410 processes did not contribute (Fig. A3b), while secular change added 1 cm (Fig. A3a).

In summary, the flood resulted from an exceptionally high storm surge superimposed on positive contributions from other
processes.
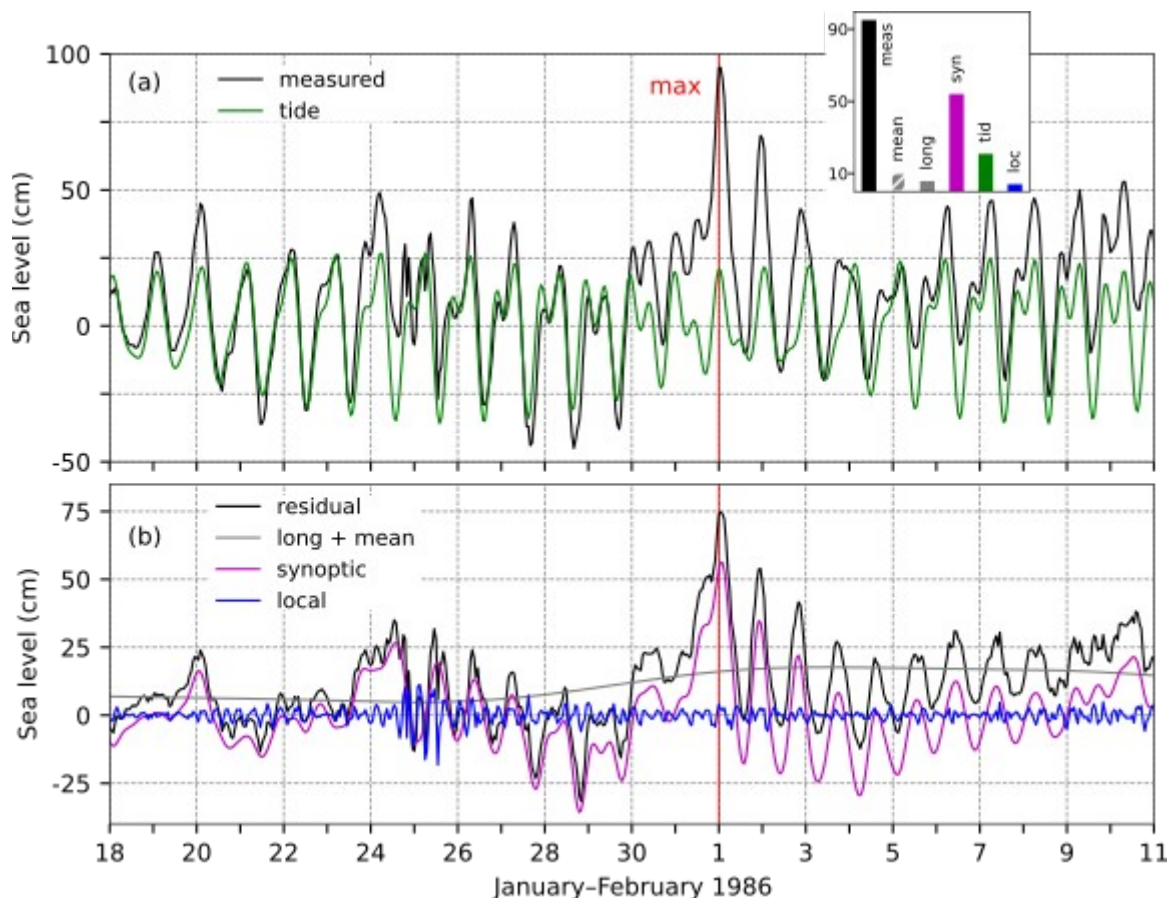
Figure 47: SL series for the flood of 1 February 1986. (a) Measured sea level (black) and *tide* (green). The inset figure shows the
1415 contributions (cm) of the five sea-level components to the maximum measured sea level ("meas"; 00:00 UTC): "loc" refers to *local
component* (9 h < T), "syn" to *synoptic component* (9 h < T < 10 d), "tid" to *tide*, "long" to *long-period sea-level component* (10 < T < 100
d), "mean" to *mean sea-level changes* (100 d < T). (b) Residual sea level (black), the combined series of *long-period sea-level component*

and *mean sea-level changes* (grey; long + mean), *synoptic component* (purple), and *local component* (blue). The red line indicates the time of occurrence of the total SL maximum.

4.15.3 Flood impacts

A review of the available daily newspapers from 3 February 1986 (Novi list, Slobodna Dalmacija) revealed the following effects of the episode. For the northern Adriatic area, the newspapers listed: (i) sinking (or ripping from their moorings) of numerous boats in the harbours; (ii) breaking and bending of antennas on the roofs; (iii) the sea washing away more than 200 crates from the fishing boats; (iv) power outages; (v) overflow of water from low-lying structures through sewer openings; (vi) disruptions of ferry traffic; (vii) flooding of properties. No flooding was reported in the middle and south Adriatic. However, in the middle Adriatic, some of the local ferry lines were suspended for up to three days due to strong Sirocco, and local power outages occurred.

4.16 The flood of 25 October 1980 (ID 10; rank 9)

This episode has not yet been studied in the scientific literature.

4.16.1 Meteorological background
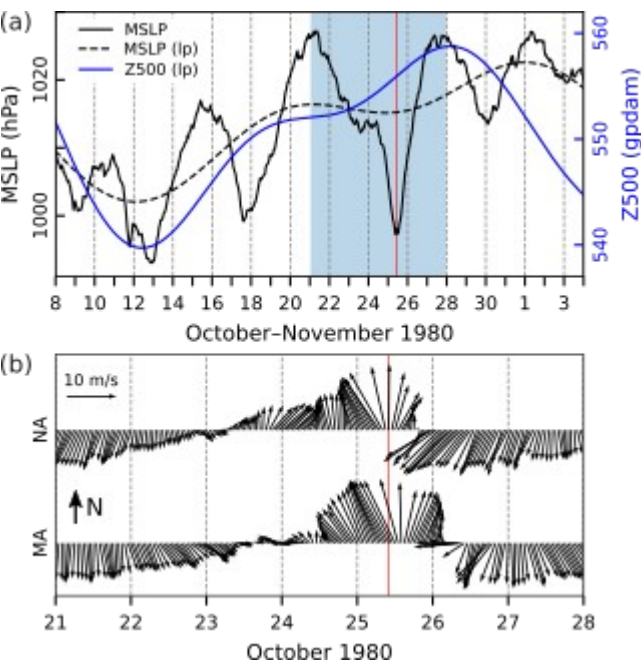
Figure 48: Series of ERA5 reanalysis data related to the flood of 25 October 1980. (a) MSLP (hourly) and MSLP (lp) (low-pass filtered with a cut-off frequency of 10 d) and Z500 (lp) (low-pass filtered with a cut-off frequency of 10 d) at a grid point near TG Bakar. (b) Hourly **W10** during the period marked in blue in the upper plot for the middle (MA) and northern (NA) Adriatic (all locations marked in Fig. 1). The red line indicates onset of SL maximum.

Two major cyclones impacted the Adriatic prior to the main SL maximum in Bakar (Fig. 48). On 24 December, i.e., at a day

before the extreme SL in Bakar, the Z500 distribution indicated the descent of an upper-level trough from northern Europe, extending southwards up to the Mediterranean, where an upper-level cyclone formed. During this period, a warm and humid air mass, transported by an upper-level southwest flow, was situated over the Adriatic Sea. At the surface, a cyclone developed over the Gulf of Genoa (Fig. 49a). On 25 October, this cyclone deepened rapidly as it moved southeast, bringing light precipitation to the northern Adriatic (up to 15 mm). The development and intensification of the cyclone reinforced air-pressure gradients, leading to stronger south and southeast winds over the eastern Adriatic Sea (Fig. 49b). During the night and morning of 25 December, a strong Sirocco wind affected the northern and middle Adriatic (Fig. 48b). Just before the sea level peaked in Bakar, wind speeds reached their maximum at 09:00 UTC (Fig. 49b). By the end of the day, the cyclone had moved southeast towards Italy, with a moderate northeasterly wind over the northern Adriatic, while southeasterly winds weakened over the rest of the Adriatic (Fig. 48b).
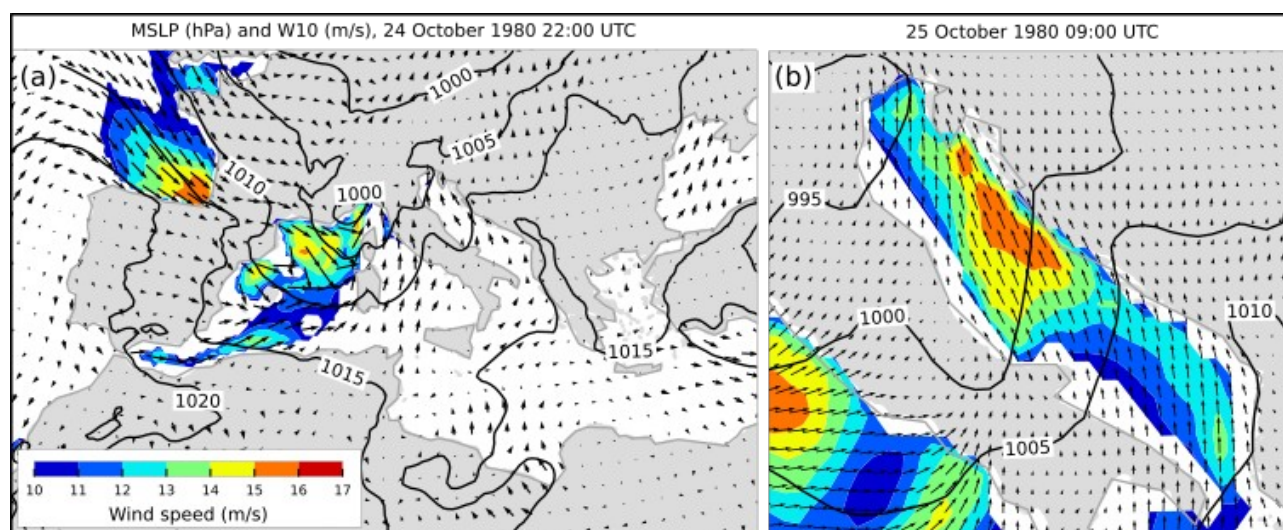
Figure 49: MSLP (black lines) and **W10** (arrows and colours) fields from the ERA5 reanalysis. Conditions (a) over the Mediterranean that preceded the situation (b) over the Adriatic Sea (an hour before maximum SL in Bakar). Only wind speeds exceeding 10 m/s are coloured.

4.16.2 Sea-level evolution

On 25 October 1980 (10:00 UTC), the sea level in Bakar rose to 95 cm above the long-term average (Table 2, Fig. 50).
The lunar phase was two days after the full moon, giving *tide* a semidiurnal spring-tide character. The overall maximum occurred after the daily tidal maximum, and *tide* contributed 13 cm.
Local processes were triggered shortly before the total maximum, peaking simultaneously with it. Their contribution was significant, amounting to 16 cm.
Before the decisive cyclone passed over the Adriatic on 25 October (Fig. 48a), two earlier disturbances (on 11–12 and 17 October) raised water level in the northern Adriatic (Fig. 50b), triggering ~21.2 h oscillations, especially pronounced during

the first event. These basin-wide seiches dissipated before the main SL peak on 25 October. Consequently, *synoptic component* during this episode was not influenced by pre-existing seiches and was mainly driven by a storm surge. The SL

1470   maximum coincided with the storm-surge peak, which reached a height of 49 cm.
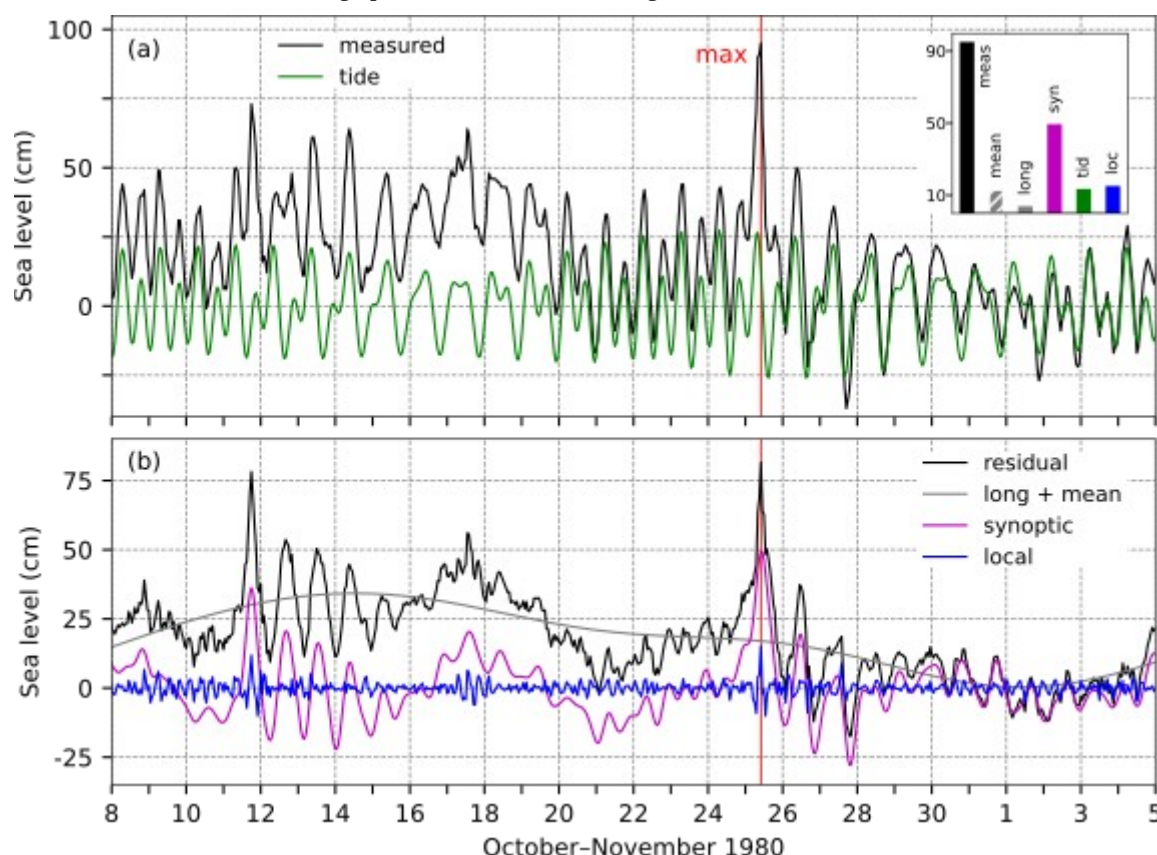
Figure 50: SL series for the flood of 25 October 1980. (a) Measured sea level (black) and *tide* (green). The inset figure shows the contributions (cm) of the five sea-level components to the maximum measured sea level ("meas"; 10:00 UTC): "loc" refers to *local component* (9 h < T), "syn" to *synoptic component* (9 h < T < 10 d), "tid" to *tide*, "long" to *long-period sea-level component* (10 < T < 100

1475   d), "mean" to *mean sea-level changes* (100 d < T). (b) Residual sea level (black), the combined series of *long-period sea-level component* and *mean sea-level changes* (grey; long + mean), *synoptic component* (purple), and *local component* (blue). The red line indicates the time of occurrence of the total SL maximum.

Long-period sea-level component contributed 4 cm to the overall SL maximum (Fig. 50a, histogram). The preconditioning was weak, explained by mild atmospheric forcing on a planetary scale. In the weeks preceding the flood, MSLP (lp) over

1480   Bakar rose (Fig. 48a), while wind speeds over periods of 10 d < T < 100 d (not shown) were low (maximum speeds of 4 m/s). Additionally, starting a week before the flood, winds in the northern Adriatic shifted to east and northeast directions.

Mean sea-level changes (100 d < T) contributed 13 cm to the maximum SL (Fig. 50a, histogram). This episode occurred

205

shortly before the annual SL peak, which was not particularly pronounced that year (Figs. A1, A2a, and A2c). Major contributions here came from seasonal and interannual variability (11 cm), while (multi)decadal and secular changes added 1 cm each (Fig. A3).

This episode resulted from a constructive superposition of all contributing processes, with the greatest influence coming from the storm surge (Fig. 50). *Local processes, tide* and *mean sea-level changes* had similar effects, while *long-period sea-level variability* had the smallest impact.

4.16.3 Flood impacts

A review of the available daily newspapers from 27 October 1980 (Slobodna Dalmacija; Novi list; Večernji list) revealed the following impacts of the event. In the northern Adriatic, and especially in Kvarner (Fig. 1), strong Sirocco wind, combined with a storm surge led to: (i) suspension of numerous ferry services in Kvarner, (ii) floodings in Rijeka (Fig. 1) and other towns along the Kvarner coast; (iii) a collision between a ferry and a smaller ship; (iv) traffic obstructions and traffic accidents due to heavy precipitation. Near Rovinj (Fig. 1), a 13 m yacht had set sail just a few hours earlier when heavy weather conditions and high waves made sailing impossible. The crew, who were forced to abandon ship, fortunately survived. Similar weather conditions prevailed in the northern parts of the middle Adriatic, where at least one local ferry line was suspended, and floodings were reported.

4.17 The flood of 22 December 1979 (ID 9; rank 7)

This episode has been studied in several papers. Bertotti et al. (2011) analysed the accuracy of deterministic and ensemble-based forecasts of meteorological conditions and sea state during the flood. Canestrelli et al. (2001) described the episode using synoptic charts, SL measured at TG Venice Punta Salute, and **W10** and MSLP measured at several coastal stations. Cavaleri et al. (2010) demonstrated that modern forecasting systems based on hydrodynamic models could have accurately predicted the storm, waves, and storm surge several days in advance. Lionello et al. (2021) briefly outlined the meteorological background and SL components that contributed to the formation of the overall SL maximum.

4.17.1 Meteorological background

A series of low-pressure systems affected the Adriatic in the period preceding this flood (Fig. 51a). On 18 and 19 December, an upper-level trough containing cold air descended from the north of the continent. By 20 December, the axis of this trough extended from the Scandinavian Peninsula across western Europe to northwestern Africa. Under these synoptic conditions, a surface flow with a pronounced southerly component became established over the Adriatic (Fig. 51b) and other parts of the Mediterranean. A surface-based cyclone developed in the lee of the Atlas Mountains, deepened, and moved northeast until

its centre reached the western Mediterranean on 21 December (Fig. 52a). This extensive cyclone continued to deepen to less than 985 hPa at its centre as it proceeded towards Corsica. As it approached Corsica, the cyclone's influence over the Adriatic became more pronounced: a southeast wind began to blow, strengthening to strong and very strong on 21 December and reaching gale on 22 December (Fig. 52b). On 23 December, the cyclone's centre shifted further northeast, with the southeast wind persisting over the Adriatic but gradually weakening. On the day of the flood, precipitation amounts were modest, with up to 15 mm recorded along the coastline. However, higher amounts were recorded the following day, including 22 mm in Bakar and 33 mm in Split.
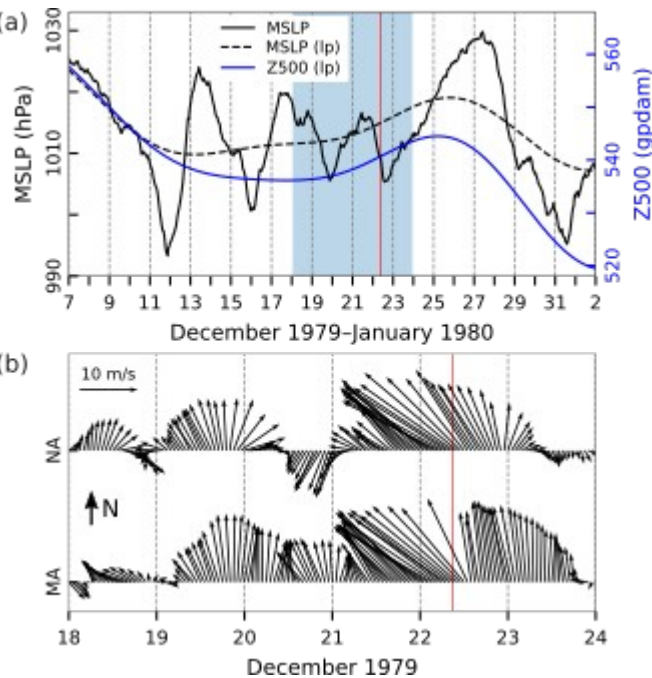
Figure 51: Series of ERA5 reanalysis data related to the flood of 22 December 1979. (a) MSLP (hourly) and MSLP (lp) (low-pass filtered with a cut-off frequency of 10 d) and Z500 (lp) (low-pass filtered with a cut-off frequency of 10 d) at a grid point near TG Bakar. (b) Hourly **W10** during the period marked in blue in the upper plot for the middle (MA) and northern (NA) Adriatic (all locations marked in Fig. 1). The red line indicates onset of SL maximum.
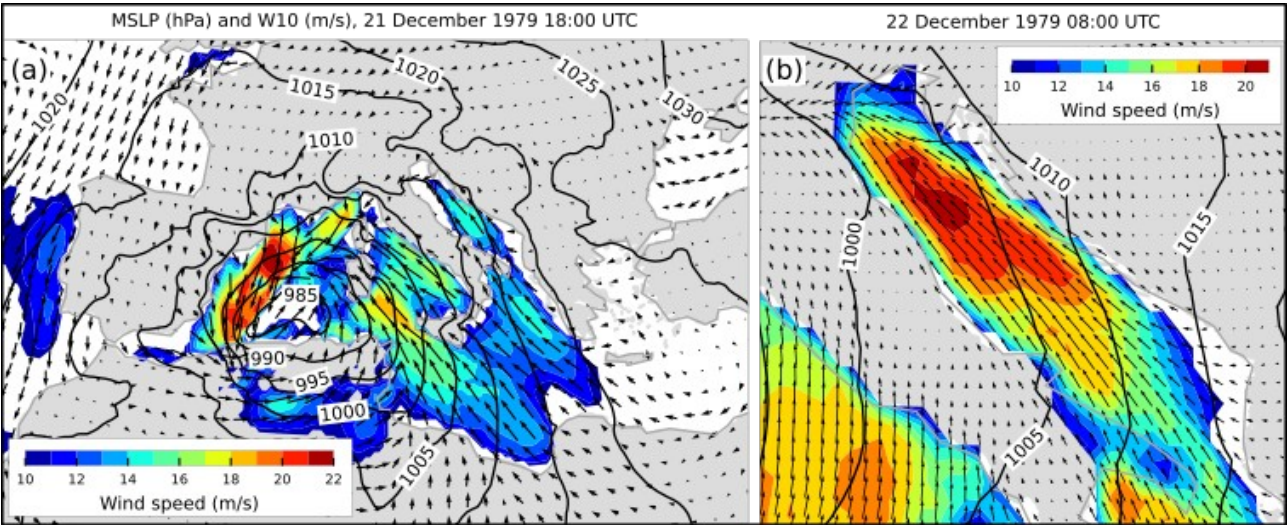
Figure 52: MSLP (black lines) and **W10** (arrows and colours) fields from the ERA5 reanalysis. Conditions (a) over the Mediterranean that preceded the situation (b) over the Adriatic Sea (an hour before maximum SL in Bakar). Only wind speeds exceeding 10 m/s are coloured.

4.17.2 Sea-level evolution

1540   In the morning hours of 22 December 1979, at 09:00 UTC, the sea level in Bakar rose to 97 cm above the long-term average (Table 2, Fig. 53). The moon was between the new moon and the first quarter, producing a semidiurnal spring *tide*. The sea-level peak occurred shortly after the daily *tidal* maximum, which contributed 20 cm (Fig. 53).

Local processes were active during this episode, but the overall maximum occurred before their peak; therefore, their contribution was minimal (1 cm).

1545   Several pronounced disturbances crossed the Adriatic in the weeks preceding the flood (Fig. 51a), causing basin-wide seiches visible in synoptic *component* as ~21.2 h oscillations (Fig. 53b). These oscillations largely dissipated before the decisive cyclone affected the Adriatic. As a result, *synoptic component* was mainly a forced response to synoptic conditions, primarily a storm surge. The storm surge began to develop on 21 December when a very strong Sirocco started accumulating water at the closed end of the basin. Notably, the origin and trajectory of the cyclone (which was atypical for Adriatic storm

1550   surges) induced southeasterly winds with higher velocities near the western coast. This likely caused a stronger SL response along the western coastline, where the basin is shallower (Fig. 1), compared to the eastern side, where depths are greater. To confirm this hypothesis, a numerical experiment would be needed. Indicatively, this flood ranked third at TG Venice Punta Salute station (1936–2019; Venice Municipality; Canestrelli et al., 2001), whereas in Bakar, for the same period, it ranked sixth (Table 2). The induced storm surge was extraordinary, peaking at 67 cm just two hours after the overall maximum and

1555   contributing 61 cm to the overall sea-level maximum. This was one of the strongest *synoptic components* among the extracted flood events, attributed to the MSLP gradient over the Adriatic and extreme Sirocco, which persisted for over a day

215

(Fig. 51b).

Preconditioning for this flood, indicated by *long-period sea-level component*, was weak (Fig. 53a) and contributed only 7 cm. This was due to stable MSLP (lp), which in fact, had been slightly rising in the 10 days preceding the flood (Fig. 51a).

1560 For the same time interval, wind at these temporal scales blew from the southwest, reaching a maximum speed of 4.5 m/s. A comparison of Z500 (lp), MSLP (lp), and long + mean series suggests that they did not vary coherently, indicating that *long-period sea-level variations* were not dominated by planetary atmospheric waves.
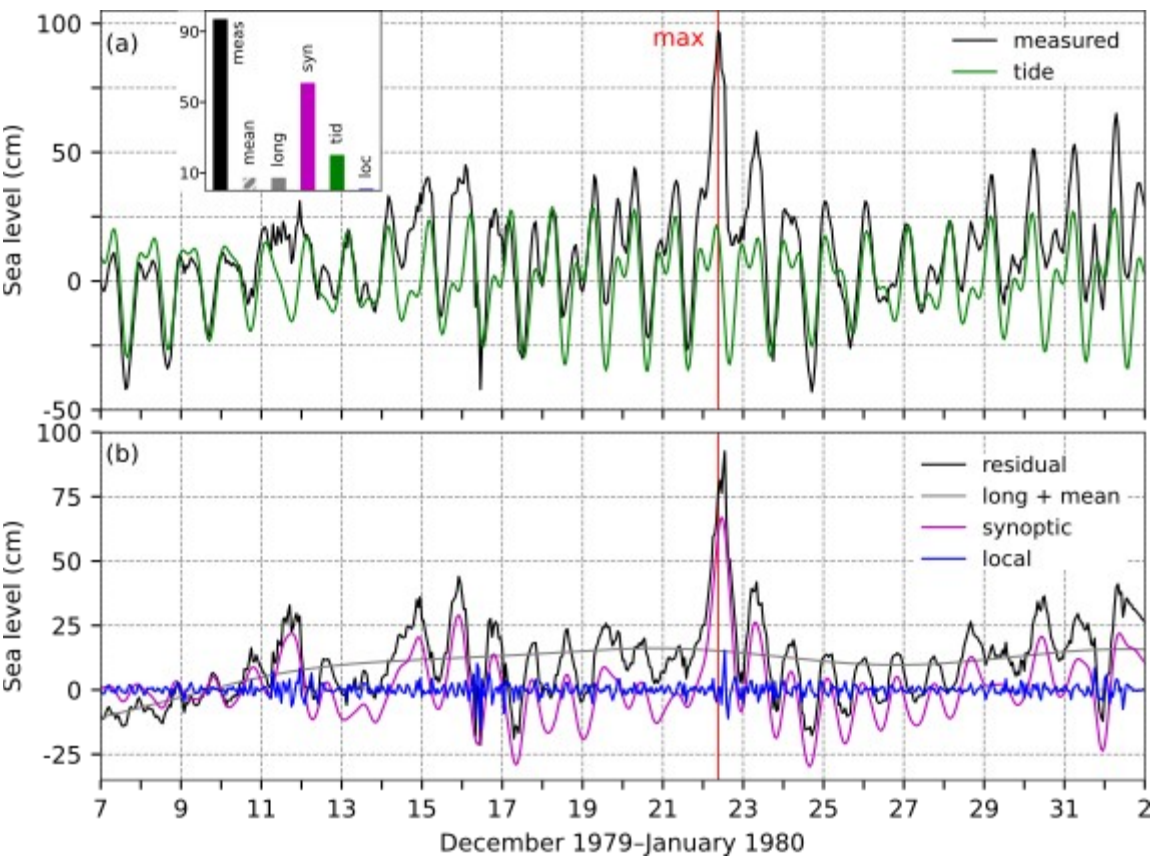
Figure 53: SL series for the flood of 22 December 1979. (a) Measured sea level (black) and *tide* (green). The inset figure shows the
1565 contributions (cm) of the five sea-level components to the maximum measured sea level ("meas"; 09:00 UTC): "loc" refers to *local component* (9 h < T), "syn" to *synoptic component* (9 h < T < 10 d), "tid" to *tide*, "long" to *long-period sea-level component* (10 < T < 100 d), "mean" to *mean sea-level changes* (100 d < T). (b) Residual sea level (black), the combined series of *long-period sea-level component* and *mean sea-level changes* (grey; long + mean), *synoptic component* (purple), and *local component* (blue). The red line indicates the time of occurrence of the total SL maximum.

1570 *Mean sea-level component* (100 d < T) added 8 cm to the overall maximum (Fig. 53a, histogram). The episode occurred after

the annual SL peak, which was not pronounced that year (Figs. A1, A2a, A2c). The seasonal cycle and interannual variability contributed 6 cm to this component, (multi)decadal processes added 2 cm (Fig. A3b), while secular change was negligible (Fig. A3a).

In summary, this flood resulted from an exceptionally high storm surge superimposed on smaller positive contributions from other processes.

4.17.3 Flood impacts

The effects of the flooding are outlined using reports from various daily newspapers (Novi list, 24, 25 and 26 December 1979; Slobodna Dalmacija, 24 and 25 December 1979; Večernji list, 24 December 1979). Coastal regions along the Croatian side of Adriatic experienced severe Sirocco wind and flooding due to storm surge. The impact of the event was especially severe in the northern Adriatic, where: (i) the western coast of Istria and islands of Kvarner (Fig. 1) experienced flooding on the streets and coastal properties, along with damage to boats, cars, shores and piers; (ii) water overflowed from lower-lying structures through sewer openings; (iii) the staff and their families had to be evacuated from two lighthouses due to water intrusion; (iv) breakwater wall was demolished on one of the islands; (v) numerous ferry lines were suspended.

In the middle Adriatic: (i) ferry lines were disrupted; (ii) inland, many villages were left without electricity as the severe Sirocco toppled utility poles and live transmission lines, with the damaged transmission line causing a minor wildfire; (iii) in a coastal town, powerful waves lifted hundreds of cubic metres of seabed stones onto the shore, and shifted massive stone blocks, some weighing up to two tons, from the breakwater.

4.18 The flood of 25 November 1969 (ID 8; rank 8)

Despite causing severe flooding along the eastern Adriatic coastline and setting a record for the highest total SL at TG Trieste (182.7 cm above the long-term mean for 1956–2020; Šepić et al., 2022), and despite the substantial storm surge generated during the episode (as demonstrated in this paper), no scientific studies have been found that specifically analyse this episode. Only a brief empirical analysis about this flood is available in the report by Canestrelli et al. (2001).

4.18.1 Meteorological background

On 21 November, the anticyclone over the Adriatic gradually weakened, while a deep surface-based cyclone formed over the Celtic Sea, accompanied by an upper-level closed low-pressure circulation. Over the next two days (22 and 23 November), this extensive cyclone deepened further, with its centre moving southwest and exerting an increasing influence over western and central Europe. Consequently, an upper-level southwesterly flow was established over the Adriatic, and surface air pressure began to decrease (Fig. 54). On 24 November, a new cyclone developed in the Bay of Biscay and advanced

220

northeast through France and Germany, deepening to 995 hPa at its centre. Simultaneously, an anticyclonic field

1600 strengthened over the eastern Mediterranean. Under these conditions, on 24 November, south and southeast winds over the

Adriatic increased to moderate and strong, subsequently shifting to south and southwest winds. However, during the night of

24–25 November, another cyclone formed in the western Mediterranean (Fig. 55a) and rapidly advanced towards the Gulf of

Genoa during the day, where it deepened and continued northeast. As it passed over the northern Adriatic, MSLP in its

centre dropped to less than 980 hPa (Fig. 55b). As a result, on 25 November, strong to gale southeasterly winds developed

1605 over the Adriatic, shifting to strong to gale southwesterly winds by the morning of the following day, accompanied by

westerly winds in the northern Adriatic (Fig. 54b). The cyclone brought moderate precipitation. On 25 November, up to 30

mm was recorded along the entire coastline. On 26 November, precipitation in the northern Adriatic ranged from 20 to 40

mm, while in the middle Adriatic it was up to 20 mm.
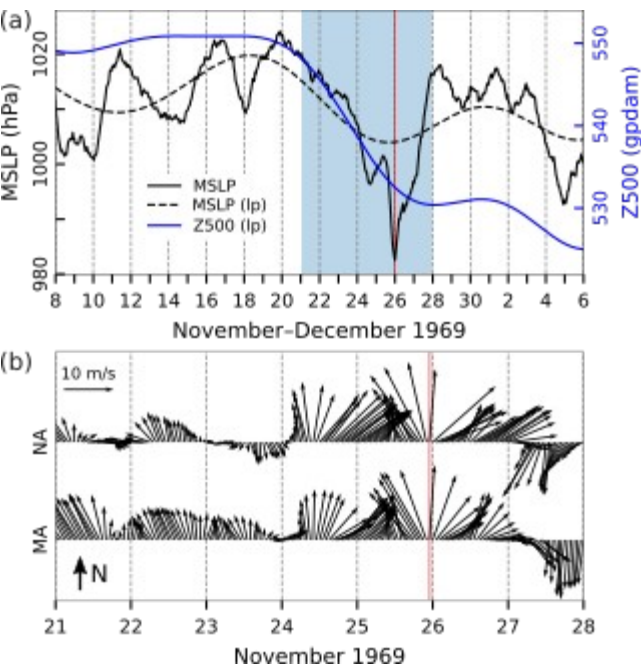
Figure 54: Series of ERA5 reanalysis data related to the flood of 25 November 1969. (a) MSLP (hourly) and MSLP (lp) (low-pass filtered with a cut-off frequency of 10 d) and Z500 (lp) (low-pass filtered with a cut-off frequency of 10 d) at a grid point near TG Bakar. (b) Hourly **W10** during the period marked in blue in the upper plot for the middle (MA) and northern (NA) Adriatic (all locations marked in Fig. 1). The red line indicates onset of SL maximum.
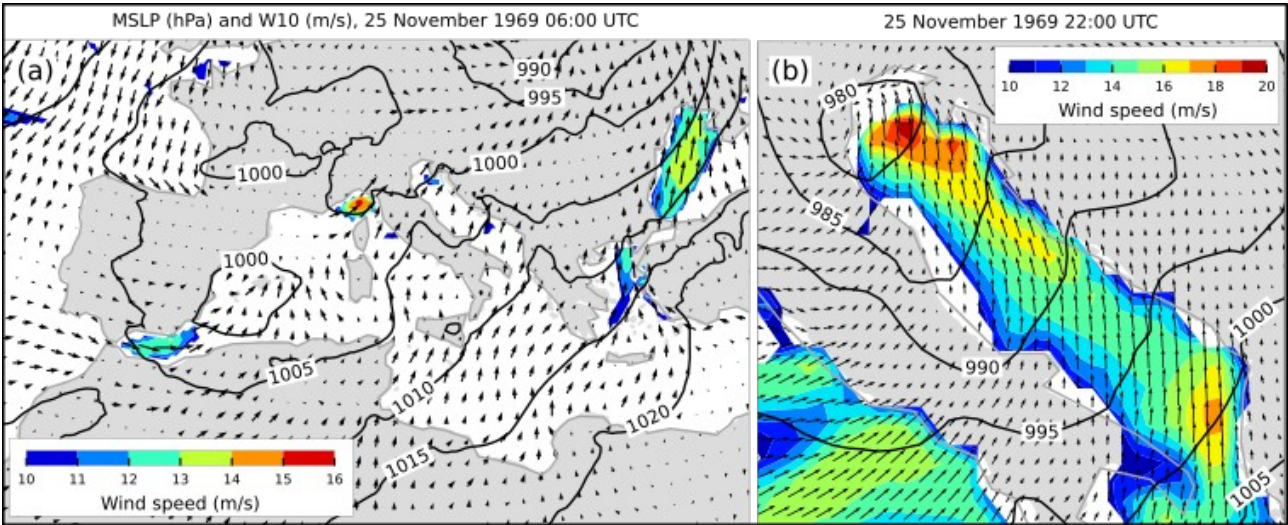
Figure 55: MSLP (black lines) and **W10** (arrows and colours) fields from the ERA5 reanalysis. Conditions (a) over the Mediterranean that preceded the situation (b) over the Adriatic Sea (an hour before maximum SL in Bakar). Only wind speeds exceeding 10 m/s are coloured.

4.18.2 Sea-level evolution

On 25 November 1969, at 23:00 UTC, the sea level in Bakar rose to 96 cm above the long-term average (Table 2, Fig. 56). The moon, two days past the full moon, produced a semidiurnal spring *tide*. The overall maximum occurred during the tidal rise, with *tide* contributing just 6 cm.

During the episode, *local processes* were active (Fig. 56b), but the overall maximum did not align with their peak, contributing only 1 cm. It should be mentioned that an exceptional local activity was recorded at TG Trieste during this event, with a record-setting sea level of 183 cm above the long-term mean. Šepić et al. (2022) reported that local processes, primarily driven by the Trieste Bay seiche (with periods of 2.7–4.2 h), contributed 40 cm to Trieste's maximum.

In the weeks leading up to the flood, several low-pressure systems influenced the Adriatic (Fig. 54a), inducing basin-wide seiches with a ~21.2 h period visible in *synoptic component* (Fig. 56b). However, these oscillations weakened by the time when the decisive cyclone crossed the Adriatic, and *synoptic component* was primarily driven by a storm surge. The surge began building on 24–25 November as winds with a pronounced southern component fluctuated between southwest and southeast directions (Fig. 54b). For several days, the wind blew more directly toward the eastern coastline, likely causing a stronger SL response along that side than the western. This probably led to a record-breaking sea level in Trieste. *Synoptic component* contributed 61 cm, and it was one of the highest among studied floods.

Preconditioning for the event was moderate, starting a week prior (Fig. 56b, long + mean) as SL rose under the influence of a drop in MSLP (lp) (Fig. 54a) and southeasterly winds (10 < T < 100 d). Winds at these periods blew from the south (at maximum speeds of around 6 m/s) starting in early December and continuing for several days after the flood. *Long-period*

sea-level variability contributed 16 cm to the total sea level.

Mean sea-level changes added 12 cm (Fig. 56a, histogram). The flood occurred before the annual SL peak (Figs. A1, A2a, A2c). Contributions from the seasonal cycle and interannual variability were 10 cm, while (multi)decadal processes accounted for 2 cm (Fig. A3b). Secular change (linear trend) was negligible during this flood (Fig. A3a).

1650 In summary, this flood resulted from an exceptional contribution by *synoptic component*, amplified by raised sea level driven by positive contributions from other components.
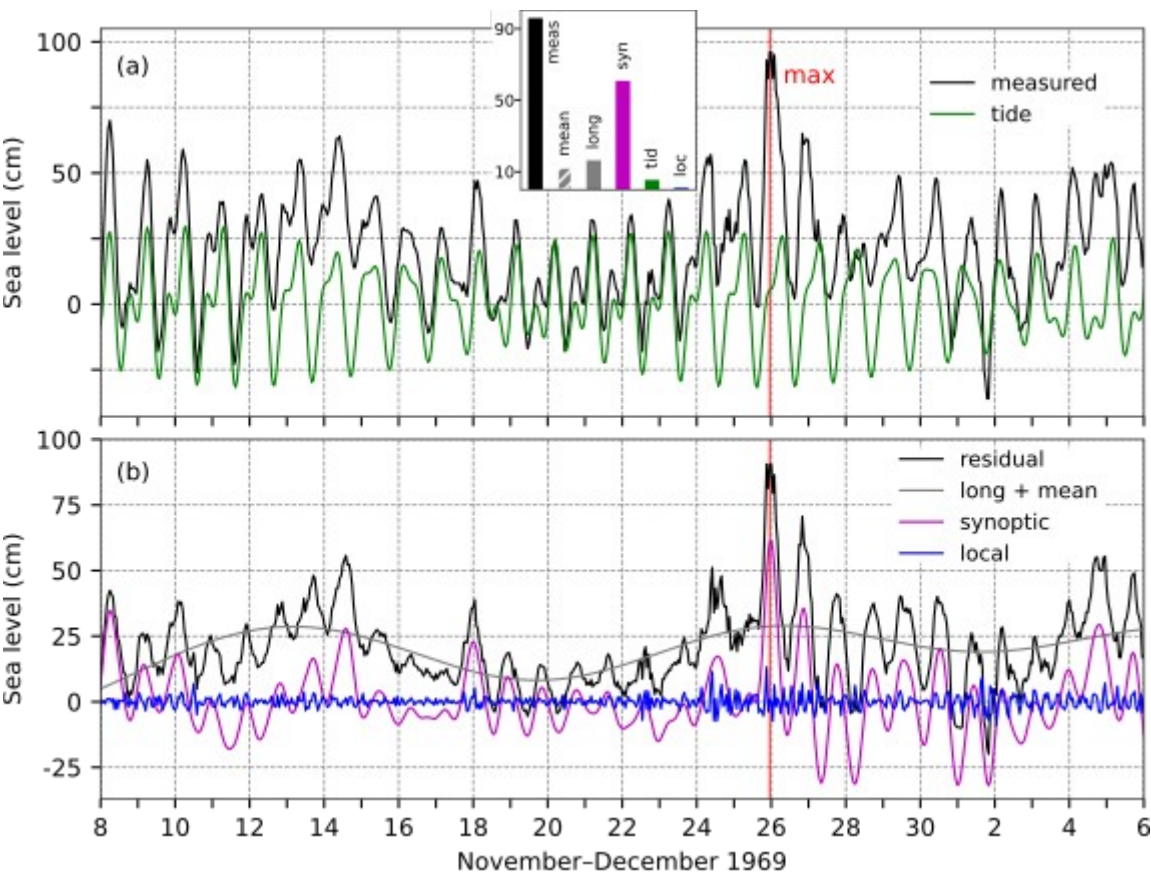
Figure 56: SL series for the flood of 25 November 1969. (a) Measured sea level (black) and *tide* (green). The inset figure shows the contributions (cm) of the five sea-level components to the maximum measured sea level ("meas"; 23:00 UTC): "loc" refers to *local component* (9 h < T), "syn" to *synoptic component* (9 h < T < 10 d), "tid" to *tide*, "long" to *long-period sea-level component* (10 < T < 100 d), "mean" to *mean sea-level changes* (100 d < T). (b) Residual sea level (black), the combined series of *long-period sea-level component* and *mean sea-level changes* (grey; long + mean), *synoptic component* (purple), and *local component* (blue). The red line indicates the time of occurrence of the total SL maximum.

4.18.3 Flood impacts

230

A review of the available daily newspapers (Novi list, 25–27 November 1969; Slobodna Dalmacija, 27 November 1969; Večernji list, 28–30 November 1969) revealed the following effects of the event. The impact of the event was strongest in the northern Adriatic, where: (i) strong waves, reaching destructive heights, damaged and destroyed many boats, including a 13 m long research vessel (BIOS) that sank in Rovinj; (ii) numerous tourist resorts and houses were damaged; (iii) local breakwaters were damaged; (iv) many towns were flooded (v) the salt stores of Pag island were flooded, dissolving a considerable amount of transportable salt.

In the middle Adriatic: (i) in Zadar, the waves flooded roads and damaged around twenty boats; (ii) localised flooding and (iii) power outages were reported.

4.19 The flood of 3 November 1968 (ID 7; rank 14)

Canestrelli et al. (2001) provided a description of the episode. Their analysis included synoptic charts, SL data from TG Venice Punta Salute, and **W10** and MSLP measurements from multiple coastal stations.

4.19.1 Meteorological background
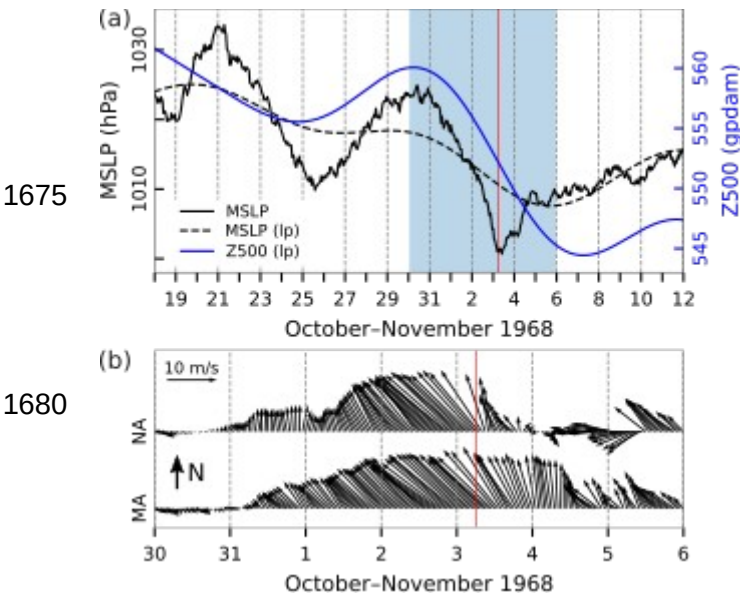
Figure 57: Series of ERA5 reanalysis data related to the flood of 3 November 1968. (a) MSLP (hourly) and MSLP (lp) (low-pass filtered with a cut-off frequency of 10 d) and Z500 (lp) (low-pass filtered with a cut-off frequency of 10 d) at a grid point near TG Bakar. (b) Hourly **W10** during the period marked in blue in the upper plot for the middle (MA) and northern (NA) Adriatic (all locations marked in Fig. 1). The red line indicates onset of SL maximum.

On 31 October, the weather over the Mediterranean and the Adriatic was characterised by the upper-level ridge accompanied by surface air pressure around 1020 hPa (Fig. 57). At the same time, an upper-level trough was present over the Atlantic, with a surface-based cyclone in the centre of which the pressure dropped to 985 hPa. In the next three days, the above-mentioned trough and surface-based cyclone slowly made their way towards the east, and on 3 November, the upper-level

flow over the Adriatic was from the south, while the surface-based secondary cyclone from the Gulf of Lion propagated to the east (Fig. 58a). Consequently, a moderate southeasterly wind, which started blowing over the Adriatic on 31 October, was intensifying day by day, becoming strong and gale on 2 November in the night and morning hours of 3 November (Figs. 57b and 58b). During the episode, precipitation along the coastline was not heavy. On 3 November, amounts were mostly below 20 mm, while on 4 November, they generally reached up to 30 mm.
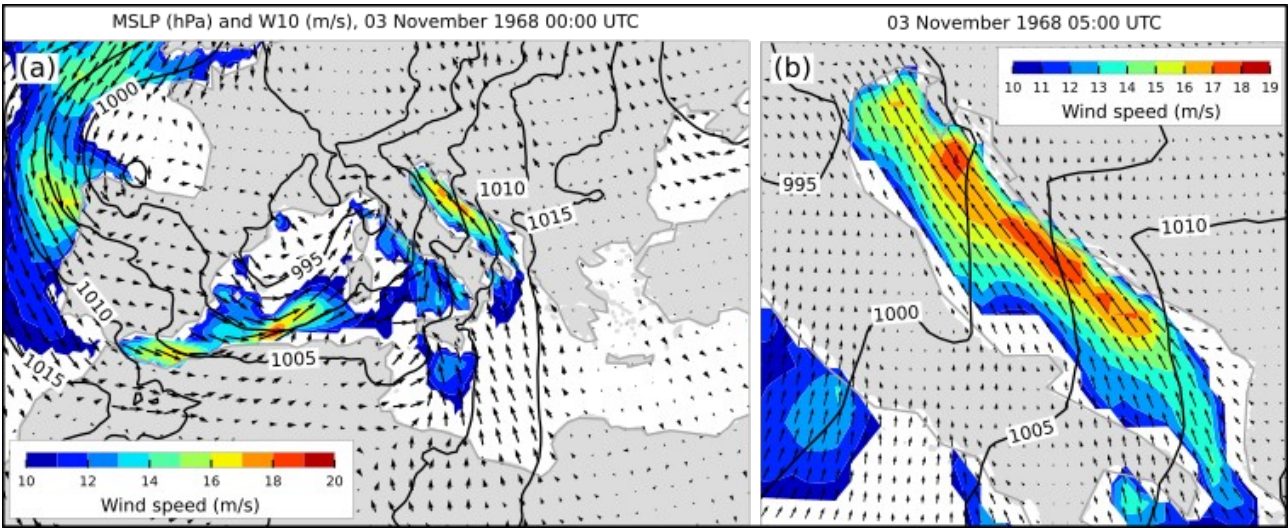
Figure 58: MSLP (black lines) and **W10** (arrows and colours) fields from the ERA5 reanalysis. Conditions (a) over the Mediterranean that preceded the situation (b) over the Adriatic Sea (an hour before maximum SL in Bakar). Only wind speeds exceeding 10 m/s are coloured.

4.19.2 Sea-level evolution

On 3 November 1968, at 06:00 UTC, the sea level in Bakar reached 90 cm above the long-term average (Table 2, Fig. 59). The moon phase, two days before the full moon, resulted in a semidiurnal spring *tide*. The overall SL maximum coincided with the daily *tidal* peak, which contributed 25 cm.

Local processes were triggered just around SL peak and added another 9 cm (Fig. 59b).

Since the period before the flood was calm and the final cyclone was an isolated event (Fig. 57a), no previously triggered seiches were present in the basin. Therefore, *synoptic component* was mainly driven by a storm surge driven by several days of Sirocco wind (Fig. 57b). The wind started to accumulate water into the closed end of the basin around 31 October (Figs. 59b and Fig. 58) when moderate southeasterly wind started to blow over the greater portion of the basin. Overall SL maximum developed in the maximum of *synoptic component*, contributing 34 cm.

Long-period sea-level variability contributed 15 cm to the flood. This rise began two weeks prior to the episode (Fig. 59b, mean + long), but it started from a negative phase, diminishing a more significant positive contribution. The rise was linked

235

to a drop in MSLP (lp) and a corresponding decrease in Z500 (lp) (Fig. 57b). After 28 October, wind (10 < T < 100 d) began
to support this rise, gradually shifting from northwest to southeast. As shown by Pasarić (2000) and Pasarić et al. (2000;
1710   2001), this pattern indicates that *long-period sea-level variability* was primarily influenced by the passage of planetary
Rossby waves.
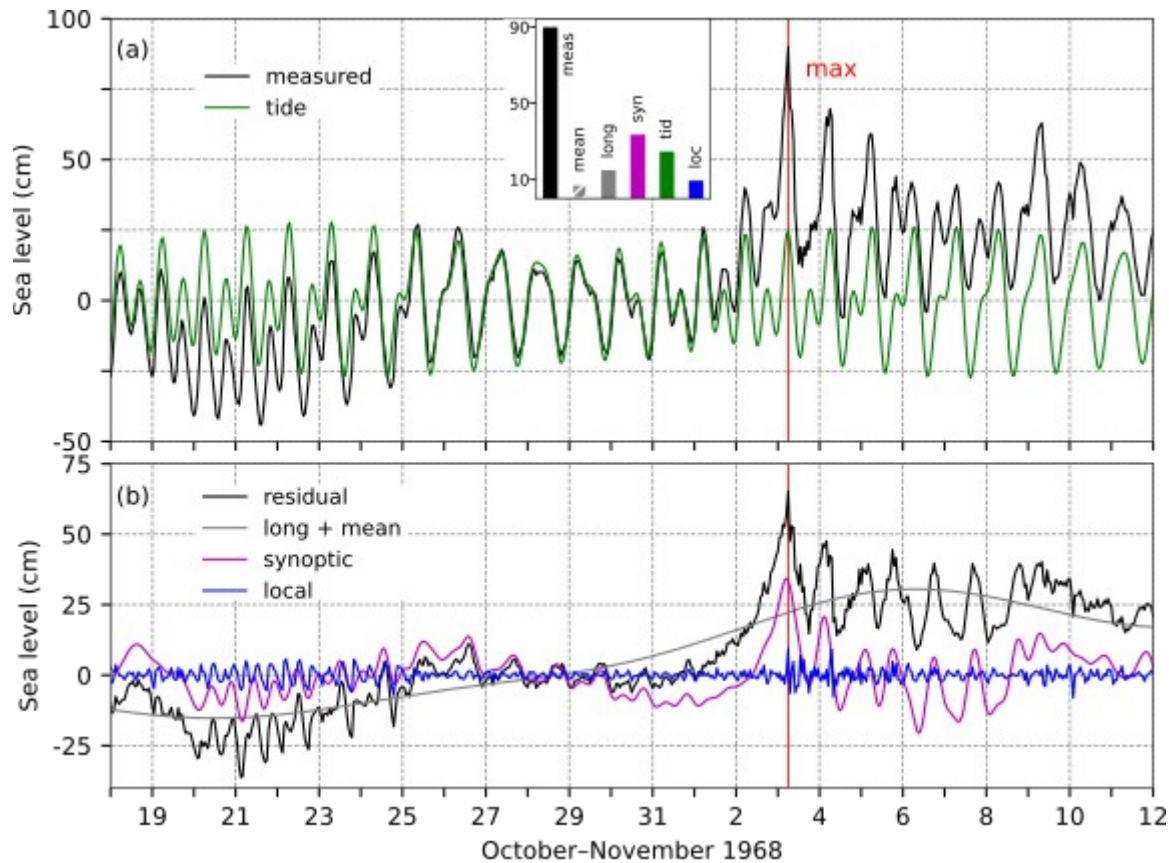
Figure 59: SL series for the flood of 3 November 1968. (a) Measured sea level (black) and *tide* (green). The inset figure shows the
contributions (cm) of the five sea-level components to the maximum measured sea level ("meas"; 06:00 UTC): "loc" refers to *local*
1715   *component* (9 h < T), "syn" to *synoptic component* (9 h < T < 10 d), "tid" to *tide*, "long" to *long-period sea-level component* (10 < T < 100
d), "mean" to *mean sea-level changes* (100 d < T). (b) Residual sea level (black), the combined series of *long-period sea-level component*
and *mean sea-level changes* (grey; long + mean), *synoptic component* (purple), and *local component* (blue). The red line indicates the time
of occurrence of the total SL maximum.

Mean sea-level changes during this period were not pronounced, contributing 7 cm to the flood (Fig. 59a, histogram). The
1720   episode occurred before the annual sea-level peak, which was relatively low that year (Figs. A1, A2a, A2c). Contributions
from the seasonal cycle and interannual variability accounted for 6 cm, while (multi)decadal processes added 1 cm (Fig.
A3b), and secular change was negligible (Fig. A3a).

In summary, the flood was caused by a combination of storm surge and *tide*, amplified by smaller positive contributions from other processes.

1725 **4.19.3 Flood impacts**

A review of available daily newspapers from 4 November 1968 (Novi list and Večernji list) revealed the following effects of the flood. The flood affected the northern part of the Adriatic. The stormy Sirocco brought ferry and catamaran traffic to a standstill and damaged harbors, industrial facilities and parks along the coast. In many Kvarner towns, numerous streets were flooded, with seawater entering stores and warehouses near the shore. In Rijeka, lower parts of the city were inundated –

1730 partly due to rain and waves, and partly because strong winds scattered large quantities of leaves, clogging the sewers. Large waves also washed away a floating beacon near Kraljevica (northern Adriatic). In Crikvenica (near Bakar), the waves damaged several beaches and destroyed part of the protective wall of the harbor breakwater.

4.20 The flood of 4 November 1966 (ID 6; rank 10)

The flood has been extensively studied in numerous papers and is considered a 'century' flood due to the severe damage it

1735 caused throughout the wider Venice region. During this episode, SL at the TG Venice Punta Salute reached its highest recorded level in the station's operational history, which dates back to 1872 (Corsini and Ferla, 2009). Research has explored various aspects of the flood, including oceanographic analyses and meteorological studies (Finizio et al., 1972; Accerboni and Manca, 1973; Stravisi and Marussi, 1973; Mosetti, 1985; Canestrelli et al., 2001; Malguzzi et al., 2006; Cavaleri et al., 2010; Bertotti et al., 2011; Lionello et al., 2021). Trincardi et al. (2016) reviewed the 1966 flood with modern scientific

1740 insights, emphasising factors contributing to flooding, current monitoring and forecasting systems, and engineering measures implemented since then to protect Venice. Međugorac et al. (2015) compared it with the 2008 flood to show differences in atmospheric forcings and SL responses along the western and eastern coastlines. Roland et al. (2009) and De Zolt et al. (2006) used a model incorporating wave-current interactions, resulting in SL predictions that closely matched observations in the northern Adriatic and in Venice.

1745 **4.20.1 Meteorological background**

On 3 November, air pressure over the Adriatic began to decrease (Fig. 60) as the influence of an anticyclonic field from northeastern Europe weakened due to an approaching surface-based cyclone from the western Mediterranean (Fig. 61a), associated with an upper-level trough containing a closed low slightly shifted to the west. On 4 November, the cyclone impacted the Adriatic region as its centre moved over the northern Adriatic, causing a pressure drop to less than 995 hPa

1750 before continuing northeast (Fig. 61b). Meanwhile, the anticyclone remained present further east, resulting in a pronounced

air pressure gradient over the Adriatic. Consequently, conditions for a southeasterly wind were established on 3 November. By the morning of 4 November, the southeasterly wind became strong and gale, shifting to a southwest wind in the afternoon as the cyclone advanced northeast (Fig. 60b). Precipitation recorded along the coastline on 4 November was mostly up to 10 mm, with higher amounts at some locations. On 5 November, precipitation in the northern Adriatic was generally up to 30

1755   mm, while the middle Adriatic experienced heavier amounts, with 45 mm recorded in Split and 73 mm in Starigrad near Zadar.
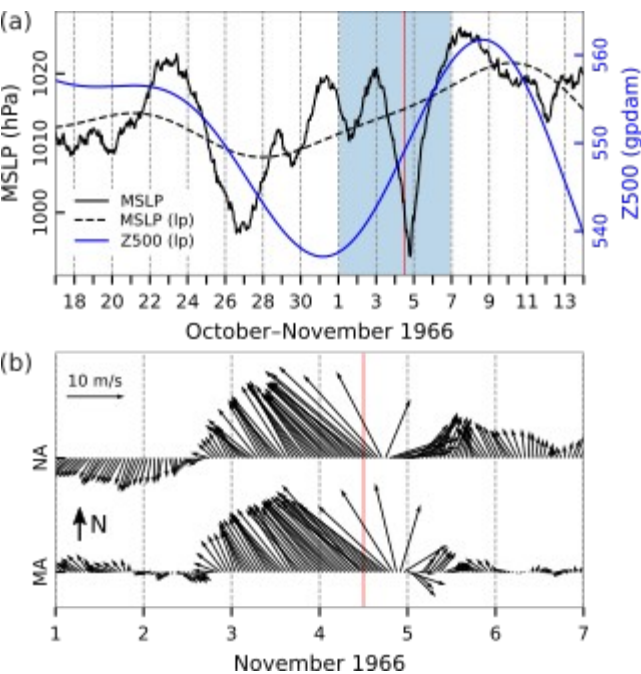
Figure 60: Series of ERA5 reanalysis data related to the flood of 4 November 1966. (a) MSLP (hourly) and MSLP (lp) (low-pass filtered with a cut-off frequency of 10 d) and Z500 (lp) (low-pass filtered with a cut-off frequency of 10 d) at a grid point near TG Bakar. (b) Hourly **W10** during the period marked in blue in the upper plot for the middle (MA) and northern (NA) Adriatic (all locations marked in Fig. 1). The red line indicates onset of SL maximum.

245

1775
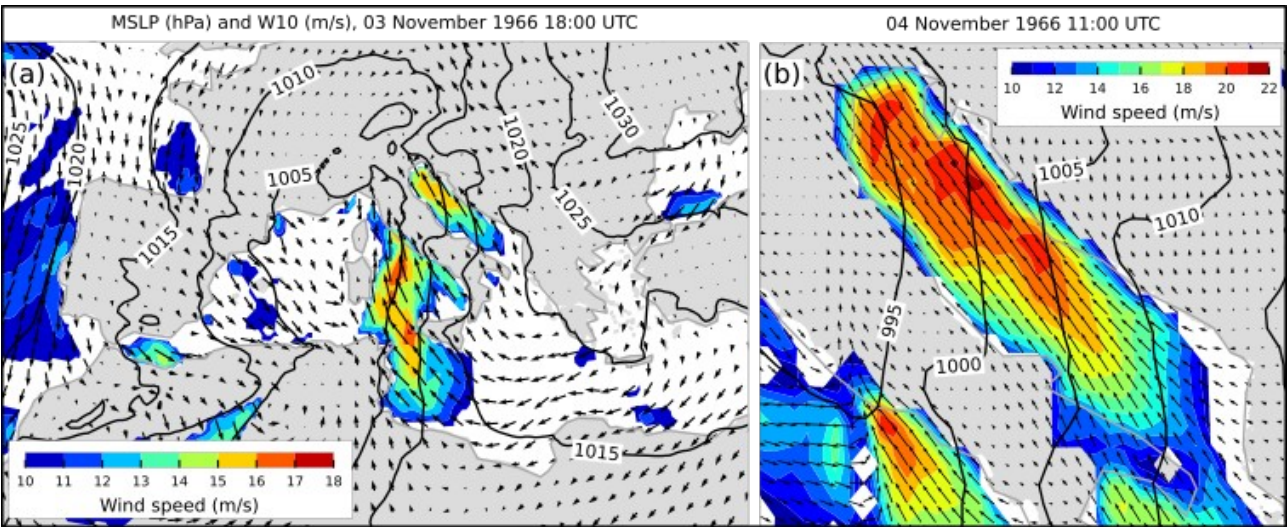
Figure 61: MSLP (black lines) and **W10** (arrows and colours) fields from the ERA5 reanalysis. Conditions (a) over the Mediterranean that preceded the situation (b) over the Adriatic Sea (an hour before maximum SL in Bakar). Only wind speeds exceeding 10 m/s are coloured.

4.20.2 Sea-level evolution

On 4 November 1966, at 12:00 UTC, the sea level in Bakar reached 94 cm above the long-term average, followed by a
1780 second peak of 92 cm at 20:00 UTC (Table 2, Fig. 62).

The moon, one day before the last quarter, created a diurnal neap *tide*. The first maximum occurred after the daily *tidal* peak, as *synoptic component* was still building, resulting in a positive *tidal* contribution of 9 cm. In contrast, the evening peak coincided with the passage of a weather front over the Adriatic, when *synoptic component* reached its maximum, but *tide*, in a negative phase, reduced the level by 19 cm (Fig. 62a).

1785 *Local processes* activated later in the day, contributing 3 cm to the first peak and 14 cm to the second (Fig. 62b).

Synoptic component was an isolated storm-surge event, with no evidence of pre-existing seiches (Fig. 62b). Sea-level and meteorological data (Fig. 60) confirm this, indicating that *synoptic component* was entirely driven by storm-surge activity. The storm surge was fueled by a strong, persistent Sirocco wind blowing uniformly along the Adriatic for over a day (Figs. 60b, 61b), accumulating water into the basin's closed end. *Synoptic component* contributed 48 cm to the first peak and 63 cm
1790 to the second.

Preconditioning for the flood, indicated by *long-period sea-level component*, began well before the event (Fig. 62, long + mean). Interestingly, the weeks leading up to the flood did not feature significant decreases in MSLP (lp) (Fig. 60a), but winds (10 d < T < 100 d) during this period consistently blew from southern directions. *Long-period sea-level component* added 14 cm to the events.

1795 *Mean sea-level changes* contributed 20 cm to the maximum (Fig. 62a, histogram), aligning with an annual peak that was

particularly pronounced that year (Figs. A1, A2a, A2c). The seasonal cycle and interannual variability added to this component 19 cm. Meanwhile, (multi)decadal processes were in a positive phase, but their contribution was minimal (1 cm, Fig. A3b), while secular changes slightly offset this, reducing the component by 1 cm (Fig. A3a).

In summary, this episode involved two events: the first aligned with the tidal daily peak, and the second coincided with the

1800   storm-surge maximum. The flood was the result of an exceptional storm surge superimposed on an elevated background sea level due to other SL processes.
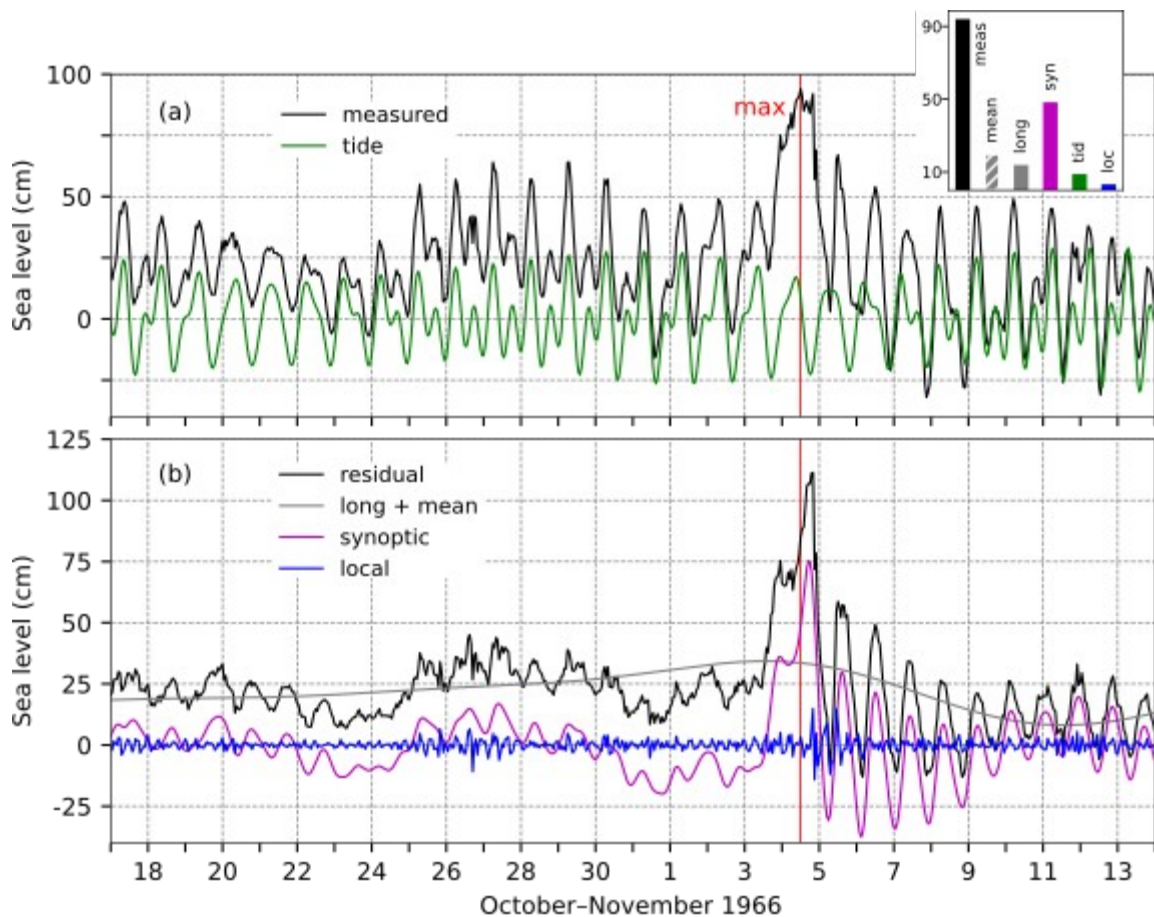
Figure 62: SL series for the flood of 4 November 1966. (a) Measured sea level (black) and *tide* (green). The inset figure shows the contributions (cm) of the five sea-level components to the maximum measured sea level ("meas"; 12:00 UTC): "loc" refers to *local*

1805   *component* (9 h < T), "syn" to *synoptic component* (9 h < T < 10 d), "tid" to *tide*, "long" to *long-period sea-level component* (10 < T < 100 d), "mean" to *mean sea-level changes* (100 d < T). (b) Residual sea level (black), the combined series of *long-period sea-level component* and *mean sea-level changes* (grey; long + mean), *synoptic component* (purple), and *local component* (blue). The red line indicates the time of occurrence of the total SL maximum.

4.20.3 Flood impacts

250

The following effects of the flood were identified through a review of daily newspapers (Večernji list and Novi list, 5, 6 and 7 November 1966; Vjesnik, 5 November 1966). The event was most impactful in the northern Adriatic, especially in Istria and Kvarner (Fig. 1). Strong Sirocco, combined with wind waves and surge caused property damage amounting to over 10 million new Yugoslavian dinars (equivalent to around USD 7.7 million today's). Coastal regions, beaches, and harbours were flooded, with boats, residential buildings, warehouses, breakwaters, restaurants, and shops severely damaged. Furthermore, there were localised power losses. In Istria several families had to evacuate their homes due to the extensive damage, and one of these homes was beyond repair. In the city of Rijeka, a shipyard sustained significant damage, while the wind also harmed multiple roofs, tearing down antennas and trees. Furthermore, numerous ferry lines in the northern Adriatic were suspended.

In the middle and southern Adriatic, no severe flooding was recorded, but the reported damage, primarily due to Sirocco, exceeded a million new Yugoslavian dinars (equivalent to around USD 770 000 today's). Severe impacts included: (i) disruption of ferry lines; (ii) power outages; (iii) collapse of several roofs and chimneys; and (iv) sinking of the sailing ship, which tragically resulted in the loss of one passenger's life.

4.21 The flood of 23 January 1966 (ID 5; rank 10)

This event has not yet been addressed in the scientific literature.

4.21.1 Meteorological background

From 15 to 22 January, the Adriatic was positioned between two air masses: a colder air mass from the north of the continent associated with a surface-based anticyclone centred over Russia, and a warmer air mass over the southern and middle Adriatic, within which nonintense cyclones propagated eastward one after another (Fig. 63). On 22 January, a cyclone originating from the Bay of Biscay moved onto the European mainland, causing the aforementioned anticyclone to retreat northward. Simultaneously, a secondary cyclone developed in the Gulf of Genoa (Fig. 64a) which led to southeasterly wind over the Adriatic (Figs. 63b and 64a). On 23 January, the newly formed cyclone from the Gulf of Genoa advanced to the northern Adriatic from where it propagated southeast along the Adriatic, leading to MSLP dropping to less than 995 hPa (Fig. 64b), followed by the strengthening influence of an anticyclonic ridge from the west. As a result, the southeast wind over the Adriatic was strong and gale during the night and morning of 23 January (Figs. 63b and 64b), gradually shifting to a west wind and, by the afternoon, to a northwest wind. On 23 January, the induced precipitation was more intense in the northern Adriatic, with 56 mm recorded in Rovinj and 51 mm in Rijeka, while in the middle Adriatic, amounts ranged from 10 to 30 mm.

1840

1845
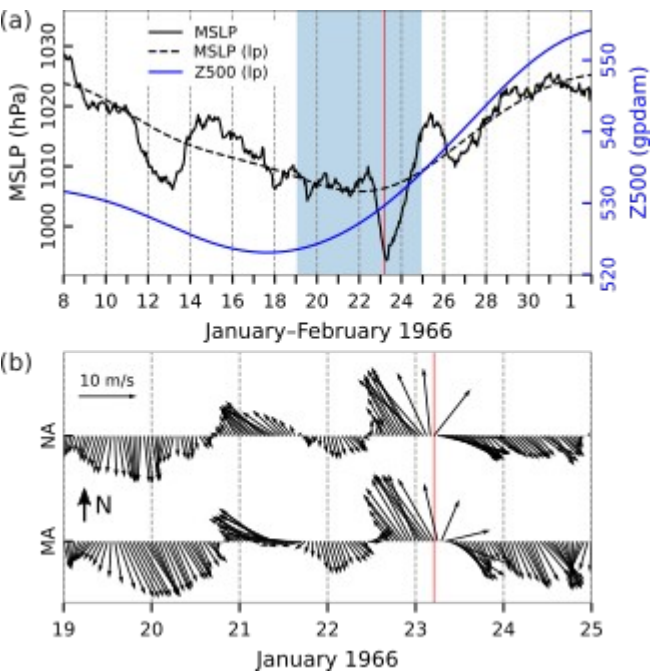
Figure 63: Series of ERA5 reanalysis data related to the flood of 23 January 1966. (a) MSLP (hourly) and MSLP (lp) (low-pass filtered with a cut-off frequency of 10 d) and Z500 (lp) (low-pass filtered with a cut-off frequency of 10 d) at a grid point near TG Bakar. (b) Hourly **W10** during the period marked in blue in the upper plot for the middle (MA) and northern (NA) Adriatic (all locations marked in Fig. 1). The red line indicates onset of SL maximum.

1850

1855

1860

1865
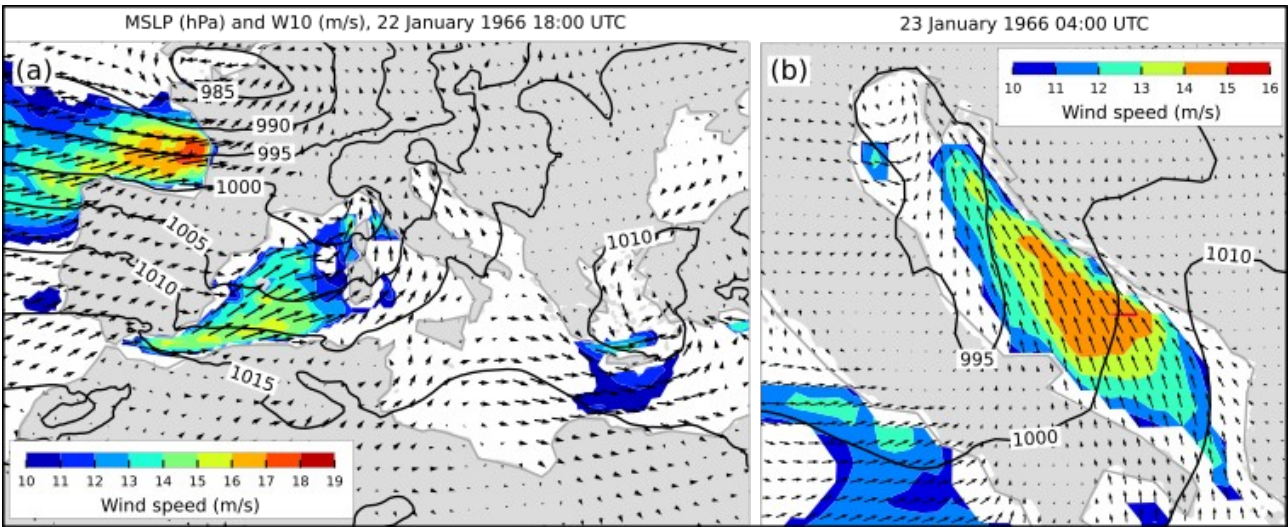
Figure 64: MSLP (black lines) and **W10** (arrows and colours) fields from the ERA5 reanalysis. Conditions (a) over the Mediterranean that preceded the situation (b) over the Adriatic Sea (an hour before maximum SL in Bakar). Only wind speeds exceeding 10 m/s are coloured.

4.21.2 Sea-level evolution

1870 On 23 January 1966, at 05:00 UTC, the sea level in Bakar rose to 94 cm above the long-term average (Table 2, Fig. 65). The moon, two days past the new moon, created a semidiurnal spring *tide*. The overall maximum occurred two hours before the daily *tidal* peak, with *tide* contributing 16 cm.
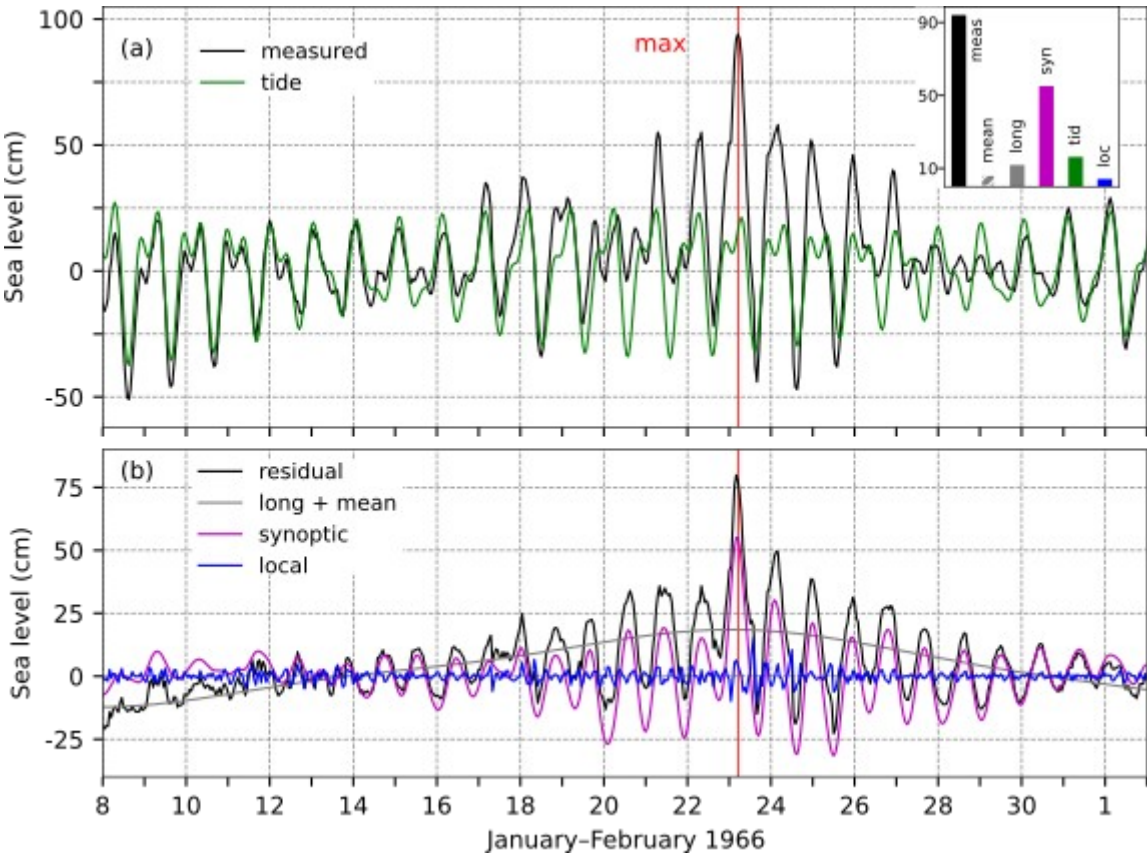
Figure 65: SL series for the flood of 23 January 1966. (a) Measured sea level (black) and *tide* (green). The inset figure shows the
1875 contributions (cm) of the five sea-level components to the maximum measured sea level ("meas"; 05:00 UTC): "loc" refers to *local component* (9 h < T), "syn" to *synoptic component* (9 h < T < 10 d), "tid" to *tide*, "long" to *long-period sea-level component* (10 < T < 100 d), "mean" to *mean sea-level changes* (100 d < T). (b) Residual sea level (black), the combined series of *long-period sea-level component* and *mean sea-level changes* (grey; long + mean), *synoptic component* (purple), and *local component* (blue). The red line indicates the time of occurrence of the total SL maximum.

1880 *Local processes* were weak during the storm, adding only 4 cm to the total SL.

Synoptic component was influenced by pre-existing seiches that were gradually induced and reinforced, likely driven by atmospheric forcings visible in the meteorological data (Fig. 63), including subtle air-pressure variations and rapidly shifting winds with a ~24-h period. The main event occurred as a cyclone approached the Adriatic, bringing southeasterly winds that pushed water into the basin's closed end. *Synoptic component*, combining a positive phase of pre-existing seiches and a

260

1885   newly induced storm surge, contributed 55 cm to the flood.

Flood preconditioning was modest (Fig. 65b, long + mean), with *long-period sea-level component* adding 12 cm to the maximum. This rise was primarily due to a drop in MSLP (lp) (Fig. 63a), while winds (10 < T < 100 d) were mainly from the northeast.

Mean sea-level changes contributed 7 cm (Fig. 65a, histogram), as the episode followed an annual peak that was not

1890   significant that year (Figs. A1, A2a, A2c). The seasonal cycle and interannual variability added 6 cm, while (multi)decadal processes in a positive phase added 2 cm (Fig. A3b). Secular change slightly offset this, reducing the component by 1 cm (Fig. A3a).

In summary, the flood resulted from an exceptional storm surge superimposed on an elevated background sea level caused by other involved processes.

1895   **4.21.3 Flood impacts**

According to reports from daily newspapers (Novi list, Večernji list; 24 January 1966), the flood had the most severe impact in Rovinj, a town on the west coast of the Istrian peninsula. The flooding, caused by a strong Sirocco and rough sea, resulted in extensive damage. A massive stone wall, over 200 m long, was completely swept away. A section of railroad track between the northern outskirts of Rovinj and the train station was buried. In the northern port, everything that had been

1900   repaired and modernized since the last devastation by the sea was completely destroyed. Other damages and emergency responses included buried beaches and flooded basements of residential buildings and ground-level stores.

4.22 The floods of 17, 18 and 24 December 1958 (IDs 2, 3 and 4; ranks 8, 12, 11)

These episodes have not yet been addressed in the scientific literature.

4.22.1 Meteorological background

1905   From 10 to 25 December, the weather over Europe was characterized by a wide upper-level trough that encompassed most of the European mainland. At the same time, surface air pressure ranged from 990 hPa over the British Isles to approximately 1010 hPa over the Balkans and eastern Europe. Such low air pressure over Great Britain was the result of the constant cyclonic activity in the Atlantic. The center of one of those cyclones moved on 15 December over the Celtic Sea, while the air pressure dropped up to 970 hPa, and remained nearby for the next few days.

1910   As a part of the above-mentioned wide upper-level trough, short-wave troughs moved one after another over the Adriatic, supporting the unstable weather, while the surface air pressure was low for days and ranged mostly from 990 to 1005 hPa (Fig. 66a). The gradients in the air pressure over the Adriatic Sea were especially pronounced on 17 December (Fig. 67b),

because the upper-level ridge started to penetrate from northwest Africa towards the eastern Mediterranean accompanied by air pressure increase in the low levels, and as a result, strong southeast, south and southwest winds blew over the Adriatic
1915 (Fig. 66b, Fig. 67).

On 18 December, the upper-level ridge shifted further to the east of the Mediterranean, while a new short-wave upper-level trough was propagating over the Adriatic, and at the same time, an intense cyclone deepened over the Atlantic, in the center of which the air pressure dropped up to 960 hPa. All this caused strong air pressure gradients over Europe (Figs. 67c and 67d).

1920
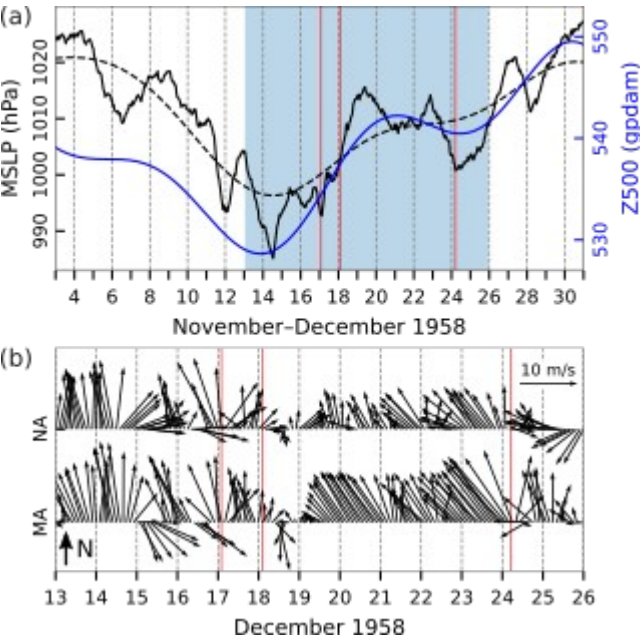
Figure 66: Series of ERA5 reanalysis data related to the floods of 17, 18 and 24 December 1958. (a) MSLP (hourly) and MSLP (lp) (low-pass filtered with a cut-off frequency of 10 d) and Z500 (lp) (low-pass filtered with a cut-off frequency of 10 d) at a grid point near TG Bakar. (b) Hourly **W10** during the period marked in blue in the upper plot for the middle (MA) and northern (NA) Adriatic (all locations marked in Fig. 1). Every third value is plotted. The red lines indicate onset of SL maxima.

On 23 December, the influence of a large anticyclone field centered in the north, over the Barents Sea, gradually weakened over the Adriatic, as a surface-based cyclone approached from the western Mediterranean (Fig. 67e) accompanied by a closed low at upper-levels. As this system approached the Adriatic, southeasterly wind started to blow in the evening of 23 December, gradually increasing by the end of the day (Fig. 66b). On 24 December, the center of the cyclone shifted over the
1940 Adriatic (Fig. 67f) where the cyclone gradually filled during 25 and 26 December. On 24 December, the wind was turning to a strong and very strong southwesterly, then westerly, and on 25 December it gradually weakened. During each of these three episodes, precipitation was higher along the northern Adriatic compared to the middle or southern Adriatic. On 17 December, 55 mm was recorded in Bakar and 32 mm in Rijeka, while the middle Adriatic recorded up to 15 mm. On 18 December, the middle Adriatic recorded almost no precipitation, while in the northern Adriatic it was measured between 5
1945 and 25 mm. On 24 December, larger amounts of precipitation were measured along the entire coastline, with 40 mm in

265

Rovinj, 21 mm in Bakar, and 36 mm on Lastovo, an island in the southern Adriatic.

1950

1955

1960

1965
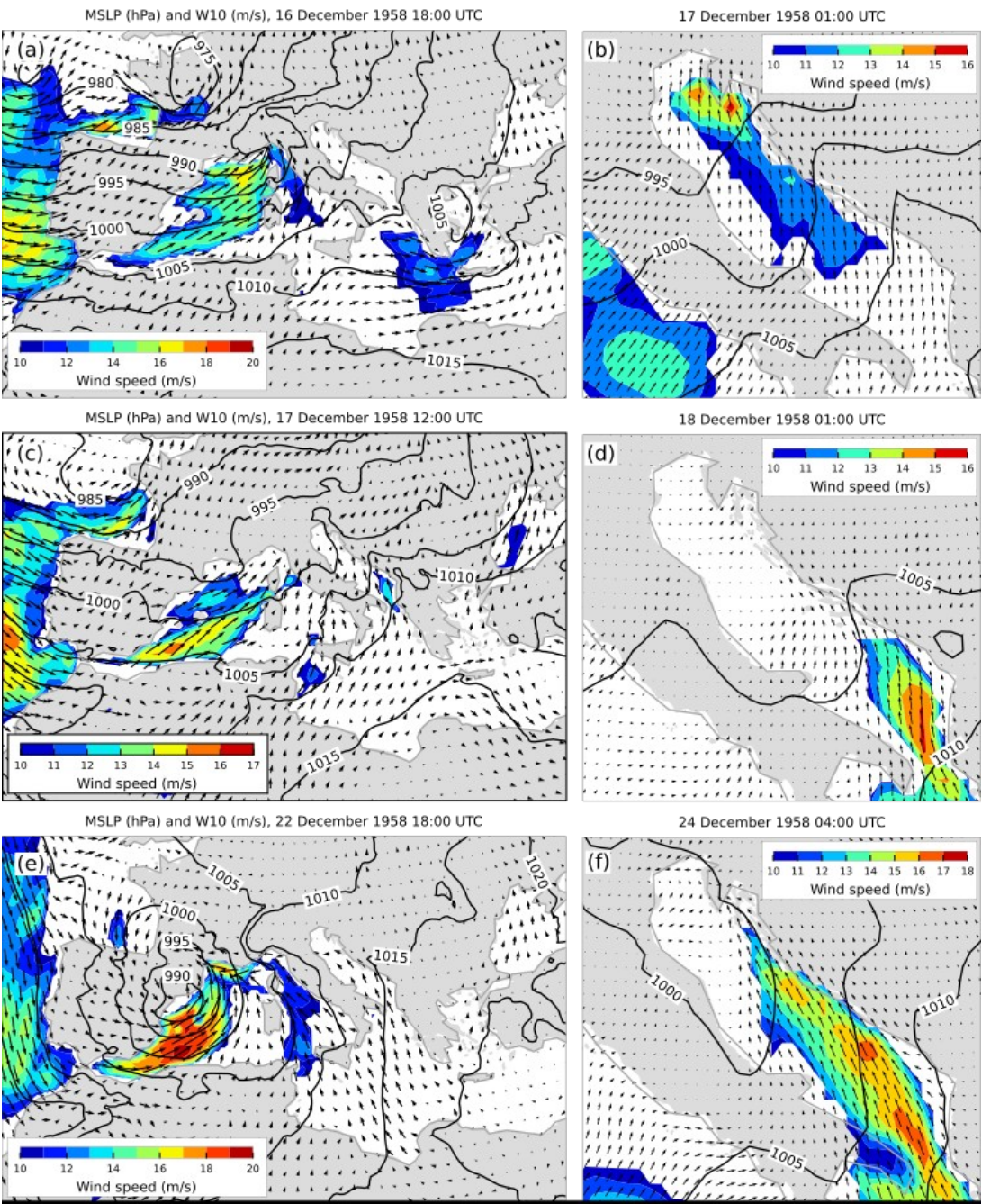
Figure 67: MSLP (black lines) and **W10** (arrows and colours) fields from the ERA5 reanalysis. Conditions (a, c, e) over the Mediterranean that preceded the situations (b, d, f) over the Adriatic Sea (an hour before maxima SL in Bakar). Only wind speeds

1970 exceeding 10 m/s are coloured.

4.22.2 Sea-level evolution

In December 1958, three flooding episodes occurred in Bakar: on 17 December (02:00 UTC), the sea level rose to 96 cm; on 18 December (02:00 UTC), it reached 92 cm; and on 24 December (05:00 UTC), it peaked at 93 cm above the long-term mean (Table 2, Fig. 68).

1975
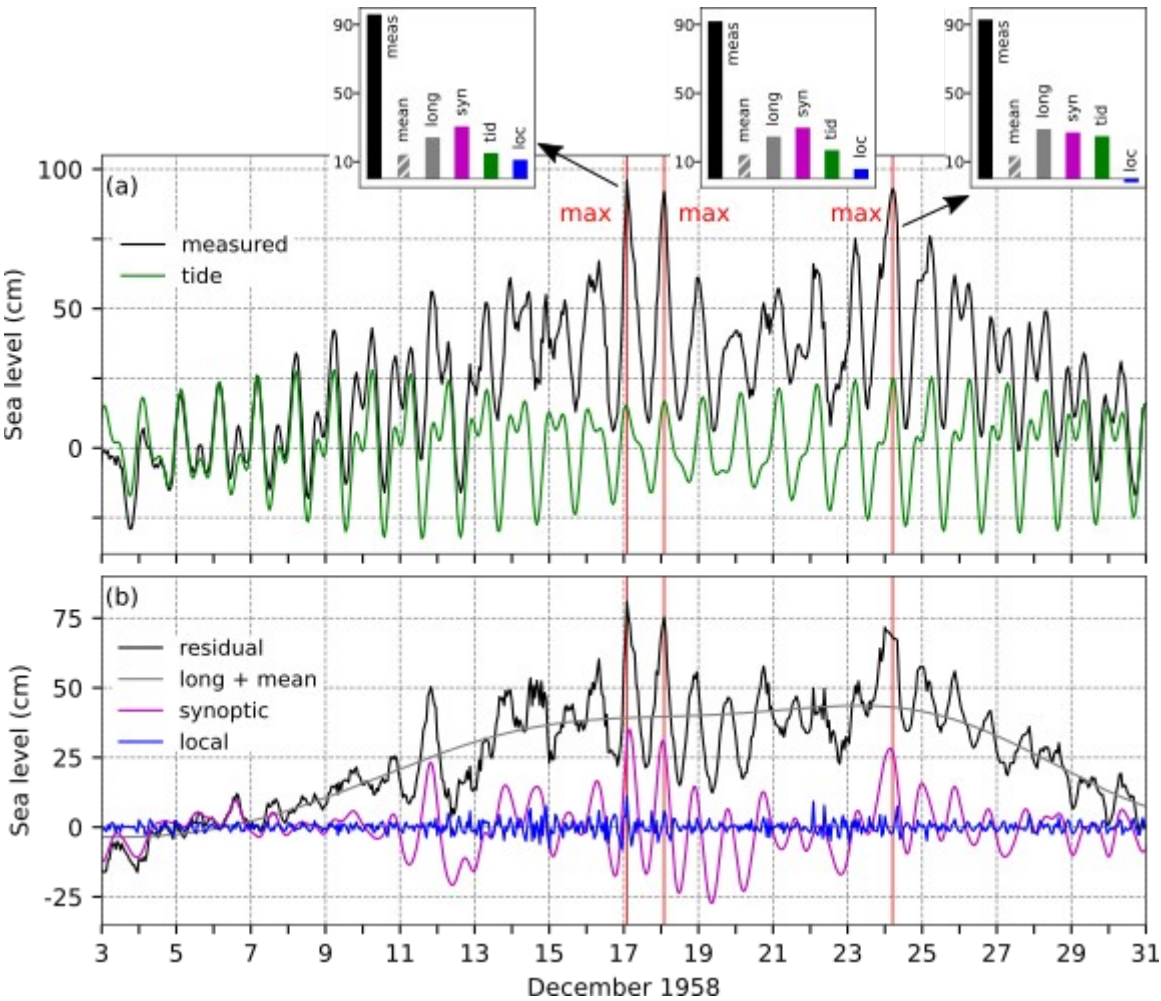
Figure 68: SL series for the floods 17, 18 and 24 December 1958. (a) Measured sea level (black) and *tide* (green). The inset figures show the contributions (cm) of the five sea-level components to the maximum measured sea levels ("meas"; left: 17 December 1958 02:00 UTC, middle: 18 December 1958 02:00 UTC, right: 24 December 1958 05:00 UTC): "loc" refers to *local component* (9 h < T), "syn" to *synoptic component* (9 h < T < 10 d), "tid" to *tide*, "long" to *long-period sea-level component* (10 < T < 100 d), "mean" to *mean sea-level changes* 1980 (100 d < T). (b) Residual sea level (black), the combined series of *long-period sea-level component* and *mean sea-level changes* (grey;

long + mean), *synoptic component* (purple), and *local component* (blue). The red line indicates the time of occurrence of the total SL maximum.

The moon was in its first quarter on 17 December, causing *tide* to shift from a diurnal neap-tide to a semidiurnal spring-tide during this period. All three floods coincided with daily tidal maxima, with *tide* contributing 15 cm, 17 cm, and 25 cm on 17, 18, and 24, respectively.

Local processes amplified the first episode by 11 cm, contributed 6 cm during the second, and slightly reduced the third by 2 cm.

Basin-wide oscillations were evident throughout much of the period (Fig. 68b), initially triggered on 11 December and reinforced for the last time on 16 December, just before the first flood. The first two floods were strongly influenced by pre-existing seiches, while the third was predominantly driven by a storm surge. The ~21.2 h period of seiches, combined with the timing of storm surge setups, positively impacted the first two floods, especially the second. The 18 December flood was mainly driven by the seiche since atmospheric forcing that day was minimal (Figs. 66, 67cd). *Synoptic components* contributed 31 cm, 30 cm, and 27 cm to the floods, respectively.

Preconditioning for these events was notable, with *long-period sea-level variability* contributing 24 cm to the first two floods and 28 cm to the third (Fig. 68b, long + mean). The sea level began to rise gradually about ten days before the first flood, coinciding with a drop in MSLP (lp) (Fig. 66a) and a shift in wind direction from northwest to southeast. Although MSLP (lp) began rising several days before the first peak, persistent southerly winds (10–100 d periods) with sustained speeds of 2–6 m/s for over two weeks, drove a continuous sea level rise that persisted beyond the third flood.

Mean sea-level changes accounted for 15 cm of the maximum (Fig. 68a, histogram), coinciding with the annual peak that was particularly pronounced that year (Figs. A1, A2a, A2c). The seasonal cycle and interannual variability added 16 cm to this component. During this time, (multi)decadal processes were negligible, amplifying the component by only 1 cm (Fig. A3b), while secular changes slightly offset this effect, reducing the component by 2 cm (Fig. A3a).

In summary, the floods resulted from the constructive interplay of all contributing processes, except for *local processes* in the third episode, which had a mitigating effect. *Synoptic component* was not particularly dominant, but strong preconditioning played an important role, with all episodes coinciding with the daily tidal maximum.

4.22.3 Flood impacts

For episodes 17 and 18 December 1958 the available literature in the National and University Library was reviewed; however, no mentions of the event impacts were found. The reason for this remains unclear. The flood of 25 December was described in Slobodna Dalmacija (26 December 1958) where following effects of the flood are listed, all in the middle Adriatic: (i) damaged beaches, uprooted trees, water entrance into buildings; (ii) damaged local roads resulting with traffic obstructions; (iii) damage to power plant; (iv) flooding of Trogir (town near Split, Fig. 1).

275

4.23 The flood of 15 December 1937 (ID 1; rank 13)

This episode has not yet been addressed in the scientific literature.

4.23.1 Meteorological background

2015   In the days leading up to this episode, weather conditions over the Adriatic were characterised by air pressure around 1010 hPa and predominantly southerly winds (Fig. 69). In the upper levels, a southwesterly flow prevailed at the leading edge of a vast trough extending from the Atlantic across western and central to southeastern Europe. Within this trough, as colder air descended from the north towards the British Isles, a surface-based cyclone intensified over Great Britain on 13 and 14 December, with central air pressure dropping to 985 hPa. At the same time, an upper-level ridge was present over the eastern

2020   Mediterranean, accompanied by surface air pressure of around 1020 hPa. During the night of 14 to 15 December (Fig. 70a), a new cyclone developed in the Gulf of Lion, quickly moving towards the Tyrrhenian Sea and entering the Adriatic Sea in the early hours of 15 December (Fig. 70b). This led to the MSLP gradient over the Adriatic. On 14 December, a strong southeast wind began to blow (Fig. 69b), which shifted to a strong and gale southwest and west wind in the evening and during the night of 15 December. Precipitation along the coast was heavier in the northern Adriatic compared to the south:

2025   on 15 December, 37 mm was recorded in Rijeka-Trsat, 11 mm in Novalja (at island near Zadar), and 6 mm in Hvar (an island near Split).
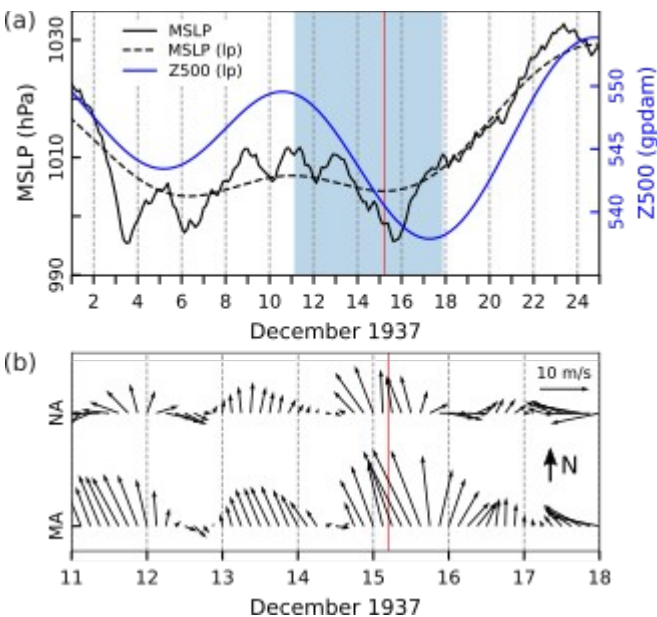
Figure 69: Series of NOAA-CIRES-DOE reanalysis data related to the flood of 15 December 1937. (a) MSLP (every 3 h) and MSLP (lp) (low-pass filtered with a cut-off frequency of 10 d) and Z500 (lp) (low-pass filtered with a cut-off frequency of 10 d) at a grid point near TG Bakar. (b) **W10** (every 3 h) during the period marked in blue in the upper plot for the middle (MA) and northern (NA) Adriatic (all locations marked in Fig. 1). The red line indicates onset of SL maximum.
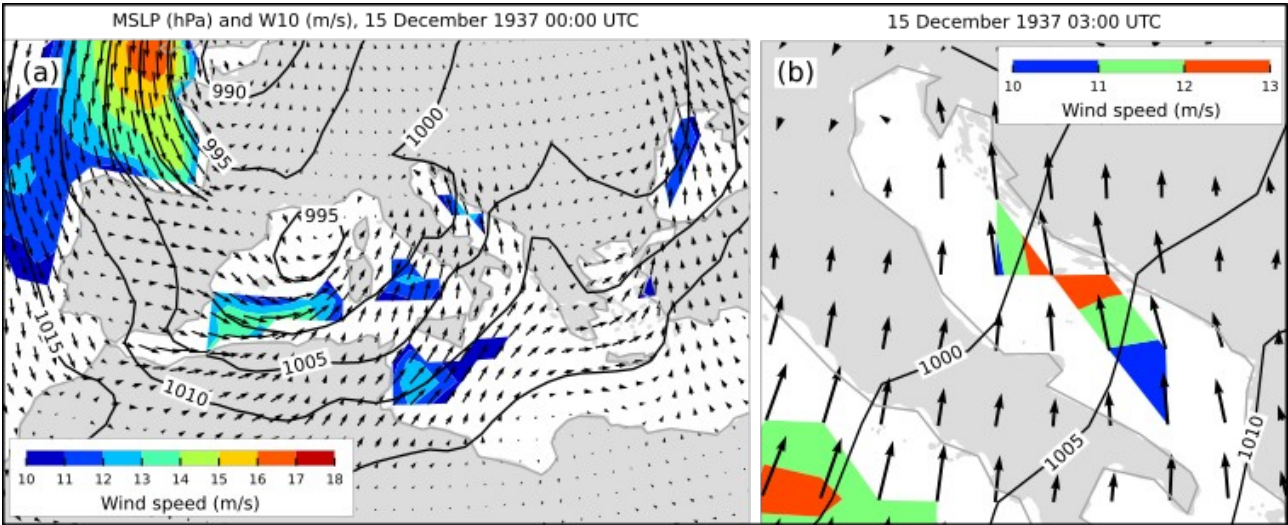
Figure 70: MSLP (black lines) and **W10** (arrows and colours) fields from the NOAA-CIRES-DOE reanalysis. Condition (a) over the Mediterranean that preceded the situation (b) over the Adriatic (an hour before maximum SL in Bakar). Only wind speeds exceeding 10 m/s are coloured.

4.23.2 Sea-level evolution

On 15 December 1937, at 05:00 UTC, the sea level in Bakar rose to 91 cm above the long-term mean (Table 2, Fig. 71). The moon was just two days before the full moon, resulting in a semidiurnal spring *tide*. The SL maximum coincided with the primary daily tidal peak, with *tide* contributing 29 cm.

Local processes were not pronounced during the episode and they mitigated the flood by 3 cm.

Before the main event, several mild atmospheric disturbances impacted the Adriatic (Fig. 69a), generating basin-wide oscillations (Fig. 71b). The most notable episode of seiches occurred from 6 to 11 December, although these oscillations were dampened before the main event. Consequently, *synoptic component* during the flood was primarily driven by a storm surge. Atmospheric forcing during the episode was relatively brief, producing only a weak SL response, which was less pronounced than the response to planetary forcing or the tidal influence (Fig. 71a, histogram). *Synoptic component* contributed 22 cm to the total maximum.

Significant preconditioning for the flood had developed well in advance (Fig. 71b). *Long-period sea-level component*, which contributed 27 cm to the maximum sea level, started rising at the beginning of the month as MSLP (lp) (Fig. 69a) dropped and winds ($10 < T < 100$ d) shifted to a southerly direction. While MSLP (lp) varied in the lead-up to the flood, southerly winds persisted throughout this period, reaching speeds of up to 8 m/s in the middle Adriatic and up to 4 m/s in the northern Adriatic.

Mean sea-level changes accounted for 16 cm of the maximum, coinciding with an annual peak that was particularly

280

prominent that year (Figs. A1, A2a, A2c). The seasonal cycle and interannual variability added 15 cm to this component. During this time, (multi)decadal processes were in a positive phase, amplifying the component by 5 cm (Fig. A3b), while secular change slightly offset this effect, reducing the component by 4 cm (Fig. A3a).

In summary, the flood resulted from a moderate storm surge superimposed on a background sea level that had been elevated by a combination of *tide*, *long-period sea-level variability* and *mean sea-level changes*.
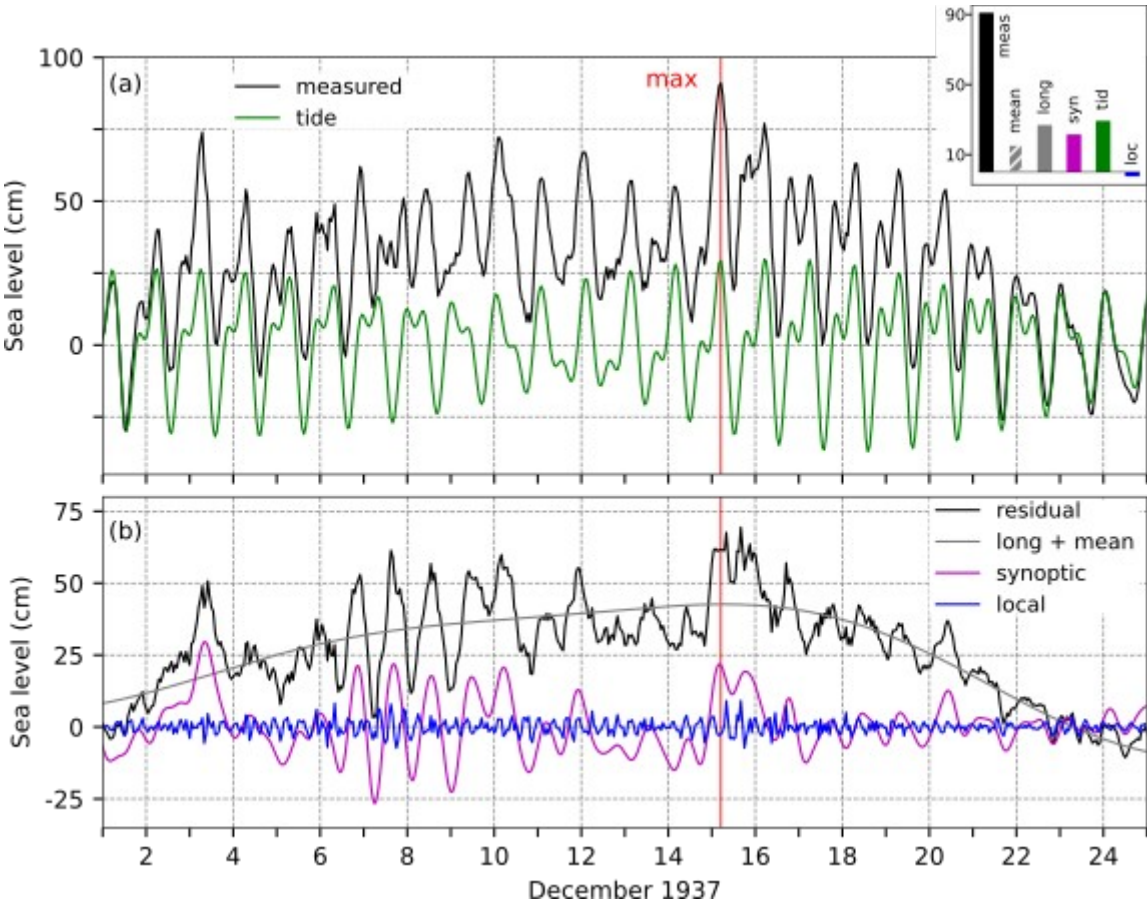
Figure 71: SL series for the flood of 15 December 1937. (a) Measured sea level (black) and *tide* (green). The inset figure shows the contributions (cm) of the five sea-level components to the maximum measured sea level ("meas"; 05:00 UTC): "loc" refers to *local component* (9 h < T), "syn" to *synoptic component* (9 h < T < 10 d), "tid" to *tide*, "long" to *long-period sea-level component* (10 < T < 100 d), "mean" to *mean sea-level changes* (100 d < T). (b) Residual sea level (black), the combined series of *long-period sea-level component* and *mean sea-level changes* (grey; long + mean), *synoptic component* (purple), and *local component* (blue). The red line indicates the time of occurrence of the total SL maximum.

4.23.3 Flood impacts

The newspapers Obzor (16 December 1937) and Primorske novine (17 December 1937) reveal that the effects of the episode were particularly strong in the middle and the southern Adriatic. These effects include: (i) winds peaking at 30 m/s (Split, Fig. 1); (ii) waves up to 10 m high that flooded coastal areas; (iii) submerging of coastal roads; (iv) disruptions in maritime 2080 traffic; (v) significant damage to windows and roofs.

5 Summary and conclusion

In this paper, we analyzed 27 flooding episodes defined as occasions when the hourly SL measured at TG Bakar (northern Adriatic) exceeded a threshold of 89 cm. The study included an empirical analysis of the meteorological background and sea-level evolution for each episode, along with a review of previous scientific literature examining these episodes and a 2085 review of daily newspaper and online sources describing impacts of floods on the natural and built environment along the Croatian coastline.
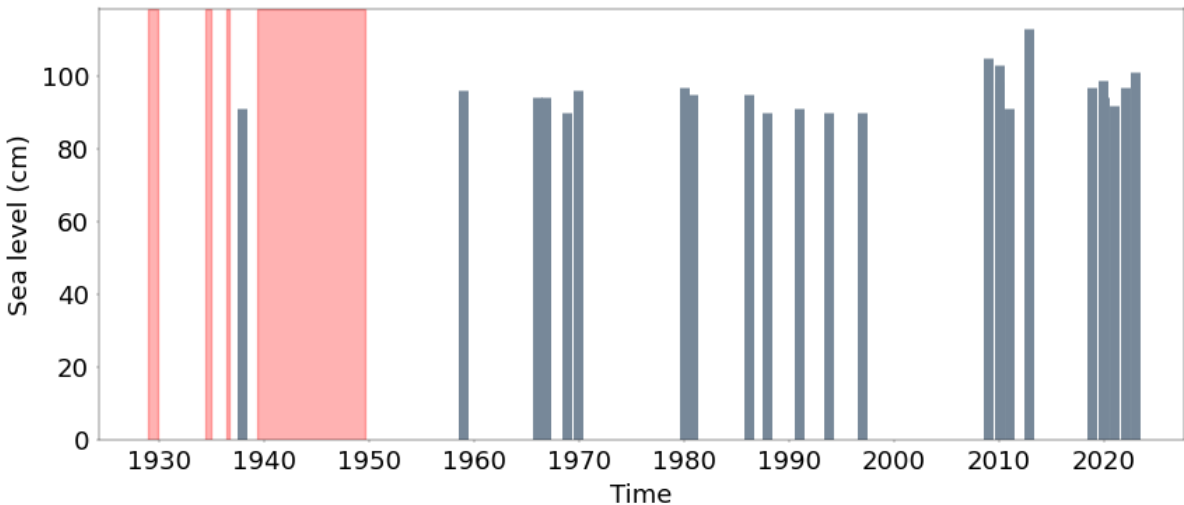
Figure 72: Temporal distribution of floods in the northern Adriatic between 1929 and 2022. The grey bars represent the maximum SL recorded at TG Bakar during the 27 episodes. Red areas mark periods with data gaps of more than 30 days.

2090 The temporal distribution of the episodes (Fig. 72) reveals that they do not occur uniformly over time, with a notable increase in frequency toward the end of the studied period. Since 2018, at least one episode has occurred each year. In some years, multiple episodes were observed, such as December 1958 (three episodes), January and November 1966 (two episodes), December 2009 (two episodes), and December 2019 (three episodes). However, Fig. 72 does not indicate that the intensity of episodes has increased over time. The highest hourly SL at TG Bakar was recorded on 1 November 2012. 2095 Seasonally, these episodes occur in the colder months, from October to February, especially in November and December.

The contributions of various components to the extracted episodes (Fig. 73) highlight key factors influencing extreme SL in

Bakar. During northern Adriatic extremes, all components were generally in a positive phase, with the exception of *local processes* and *tide* on a few occasions. This is expected since extremely high SLs occur when independent processes overlap constructively. Among the contributors, *local processes* had the least impact, *synoptic component* often played a major role,

2100 and other components typically made smaller contributions to the total SL maxima. Toward the end of the studied period, *synoptic component's* influence became less dominant, while contributions from *long-period* and *mean sea-level changes* increased. Several episodes, especially those of 1966, 2018 and 2022, could have been much stronger if they had occurred during maxima of *synoptic component* or *tide* or both (Fig. 73).

Although these conclusions are generally true, each episode is the result of a unique combination of factors. For example,

2105 during the 2 October 1993 episode (Fig. 38), *local processes* – which are typically weak – made a significant contribution. Although still smaller than *synoptic component*, the contribution from *local processes* surpassed the other three components due to the presence of a Kvarner Bay seiche (T~6 h) that peaked simultaneously with the total SL maximum. Similarly, during the 24 December 1958 and 8 December 2020 episodes, *long-period sea-level component* was strong, comparable to *synoptic component.* This preconditioning resulted from a gradual MSLP (lp) drop, but more importantly from prolonged

2110 winds (10 < T < 100 d) blowing from the south at speeds of up to 7 m/s for a week (2020) or two (1958).

The analysis also underlined the role of pre-existing seiches in flooding events. On 11 occasions, a pre-existing seiche was present during flooding and positively overlapped with the newly induced storm surge. Particularly notable events occurred on 18 December 1958 and 23 December 2019, when oscillations triggered a day earlier significantly amplified the subsequent flooding. Despite weak direct forcing during the total SL maxima (Figs. 12, 66, and 67d), the total SL exceeded

2115 the threshold due to the constructive overlap of the seiche with the tidal daily maxima.

From Fig. 73, it is clear that the largest SL responses to synoptic forcing occurred during floods in 1966, 1969, 1979, and 2018. These events were unaffected by pre-existing seiches (Table 2, Figs. 20, 53, 56, 62), meaning they were primarily driven by storm surges. Most of these episodes were particularly pronounced along the northwestern coast (in front of Venice Lagoon), which likely explains why they have been extensively studied in the scientific literature. The most studied

2120 floods include those on 4 November 1966, 22 December 1979, 1 December 2008, 29 October 2018, and 13 and 15 November 2019.

The analysis of meteorological conditions showed that most floods were associated with cyclones approaching from the west, often forming in the western Mediterranean (e.g., the Gulf of Lion, the Ligurian Sea, or further west) or the Gulf of Genoa. These cyclones typically deepened over the Gulf of Genoa before moving eastward across the northern Adriatic. In

2125 some cases, the cyclones originated in the Atlantic or western Europe, then traveled to the western Mediterranean before heading toward the northern Adriatic (e.g., 22 November 1987, 10 December 1990, 2 October 1993).

In several cases, cyclones followed atypical trajectories. Two notable examples are the floods of 22 December 1979 and 13 December 2019. In 1979, a cyclone formed in the lee of the Atlas Mountains, moved northeast across Corsica, and then continued northward without crossing the Adriatic. In 2019, a cyclone originating in the western Mediterranean crossed the

290

2130 Tyrrhenian Sea and entered the Adriatic farther south than usual (Fig. 16ab), generating southerly winds with hurricane gusts over the southern and middle Adriatic (Sect. 4.5.1). The storm surges resulting from these two floods were among the most significant on record (Fig. 73d).
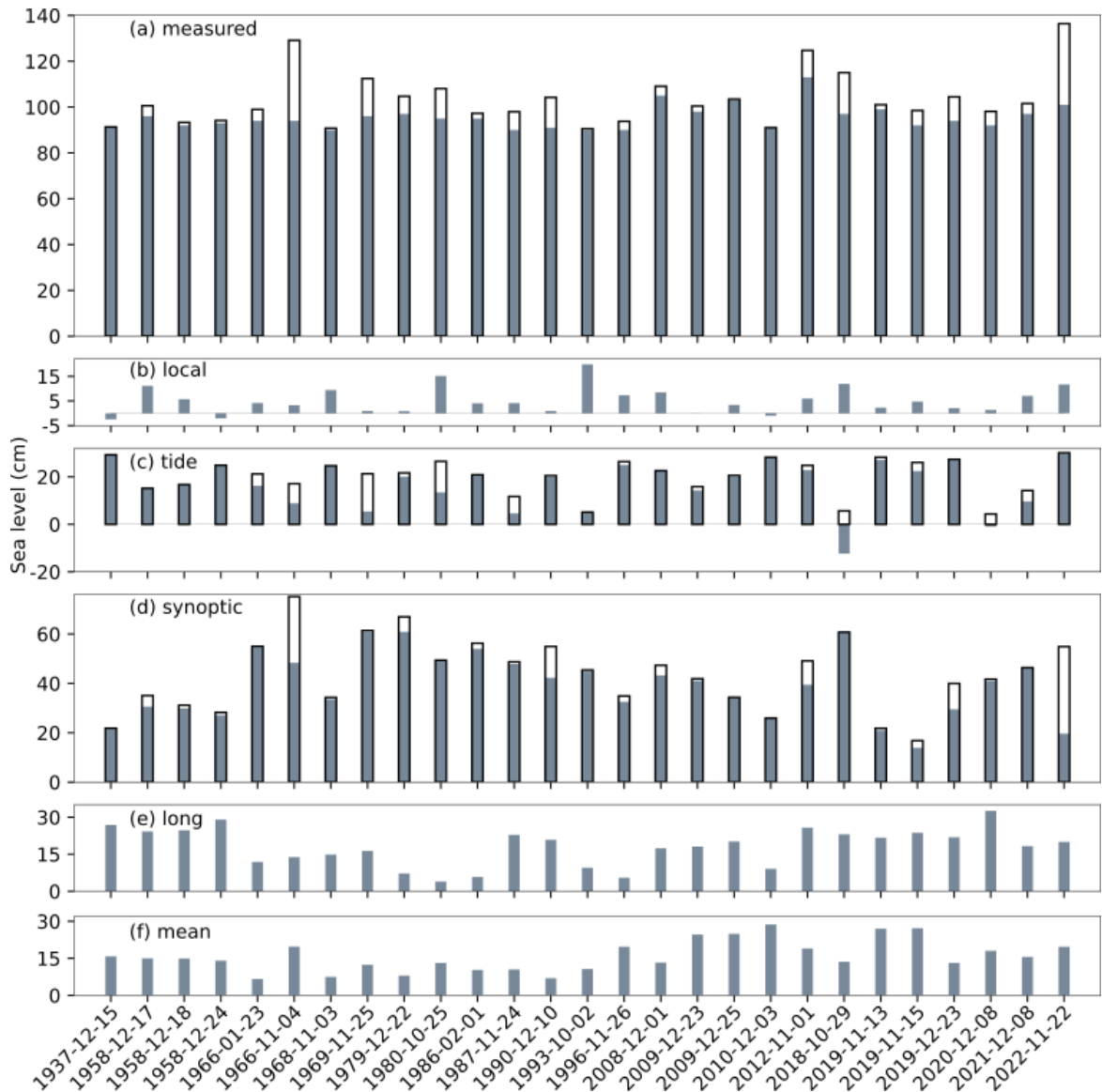
Figure 73: (a) Total SL maxima (grey bars) observed in Bakar during the 27 flooding episodes, along with hypothetical SL maxima

2135 (black) representing the superposition of the maximum tide (marked black in (c)), maximum synoptic component (marked black in (d)), and the contributions of the other three components. Contributions of SL components to observed maxima: (b) *local processes*, (c) *tide* and the maximum tide within a 24 h interval surrounding an episode, (d) *synoptic component* and maximum of *synoptic component* during a storm (black), (e) *long-period sea-level component*, and (f) *mean sea-level changes*.

Additionally, two cases stand out because the MSLP gradients over the Adriatic were not caused by Mediterranean cyclones
2140 crossing the Adriatic but instead resulted from much larger MSLP distributions. On 25 December 2009, a significant MSLP
gradient across Europe was driven by an anticyclone in eastern Europe and two cyclones in the west—one over the Bay of
Biscay and another over northern Italy (Fig. 28c). Similarly, on 17 and 18 December 1958, no cyclones crossed the Adriatic.
Instead, the MSLP gradient, and consequently Sirocco winds, were generated by an upper-level trough spanning almost all
of Europe and a ridge penetrating from northwest Africa to the eastern Mediterranean. At lower levels, this setup supported
2145 cyclonic activity over the Atlantic (Fig. 67ac) and an increase in MSLP in the east.

The cyclones were usually accompanied by precipitation, which was often more intense in the northern Adriatic than in the
middle and southern Adriatic and frequently exceeded 30 mm in 24 h.

A review of newspapers and online sources revealed that these episodes can impact the entire coastline, with the northern
and middle Adriatic being particularly affected. Common types of damage include: (i) flooded streets, city centers, homes,
2150 shops, restaurants, and business premises; (ii) damaged roads, beaches, and breakwaters; (iii) disruptions to road traffic,
ferry, and catamaran services; (iv) boats, ships, and sailing vessels being damaged or sunk; (v) damaged cars; (vi) landslides.
Strong winds often cause additional damage, such as tearing off roofs, toppling antennas and trees, and damaging parts of
buildings. These events are usually accompanied by heavy rain, leading to contamination of drinking water, sewage
overflows and landslides. In some cases, industrial production is also affected (e.g., shipyards and saltworks). To a lesser
2155 extent, these episodes can result in fires, the evacuation of residents, injuries, people stranded in flooded areas, or accidents
such as ship collisions.

Author contribution

IM planned and led this work, conducted the SL analysis, produced all figures (except Fig. 1), wrote most of the manuscript,
drafted and developed content for the web catalog, prepared the SL analysis for it, and reviewed the existing literature on
2160 floods. KJ analyzed the synoptic background of several floods, wrote the corresponding text, assessed the impact of floods
for the paper (and wrote the corresponding text), and did the final review and proofreading of the manuscript. She also
prepared image and text material for the web catalog. DD assessed the impact of flooding for the paper (and wrote the
corresponding text), contributed to the final review and proofreading of the manuscript, and prepared image and text material
for the web catalog. JK analyzed the synoptic background of the floods, wrote the corresponding text, prepared precipitation
2165 and wind data from Croatian coastal stations, revised the text and performed the final review and proofreading. JŠ
contributed to the writing of parts of the text, helped determine the final scope and structure of the paper, prepared Fig. 1,
revised the text, and performed the final review and proofreading of the manuscript. IV prepared materials on the impact of
flooding (National and University Library), prepared Table 1, and did the final review and proofreading of the manuscript.
GG prepared video material for the web catalog, contributed to the design of the final version of the article, and did the final

295

2170 review and proofreading of the manuscript.

Acknowledgments

This research has been supported by the Croatian Science Foundation projects IP-2019-04-5875 StVar-Adri and IP-2022-10-4144 CroClimExtremes, ERC-StG 853045 SHExtreme. The authors express their gratitude to Miroslava Pasarić for her valuable suggestions, advice, text corrections, and engaging discussions.

2175 **Data availability**

The hourly sea levels measured in Bakar are publicly available in the SEANOE database under the CC-BY-NC license (https://doi.org/10.17882/85171). The spatial fields of the ERA5 reanalysis are publicly available in the Copernicus Marine Service Repository (hourly data on single levels: https://doi.org/10.24381/cds.adbb2d47; hourly data on pressure levels: https://doi.org/10.24381/cds.bd0915c6). Meteorological measurements from the Croatian Meteorological and Hydrological

2180 Service (DHMZ) are available on request (https://meteo.hr/proizvodi_e.php?section=proizvodi_usluge¶m=services). The NOAA-CIRES-DOE 20th Century Reanalysis (V3) was provided by NOAA PSL, Boulder, Colorado, USA, on their website https://psl.noaa.gov. Support for the Twentieth Century Reanalysis Project version 3 dataset is provided by the U.S. Department of Energy, Office of Science Biological and Environmental Research (BER), by the National Oceanic and Atmospheric Administration Climate Program Office, and by the NOAA Earth System Research Laboratory Physical

2185 Sciences Laboratory. Serial publications (newspapers) are available at the Croatian National and University Library (https://nsk.hr/en/).

Appendix A

Mean sea-level changes, on a time scale of more than 100 d, include the seasonal cycle, interannual changes, (multi)decadal fluctuations and secular change. These variations are determined by atmospheric and ocean drivers in the broader region

2190 including the Atlantic Ocean. The Adriatic seasonal cycle is well described by the sum of the annual and semiannual cosine functions. At the Bakar site, this process reaches its maxima in spring and fall with amplitudes of the annual and semiannual components of 1.7 cm and 3.4 cm, respectively (Pasarić, 2000). The seasonal variability in the Mediterranean is determined by buoyancy changes (seasonal warming and cooling) and wind effects (Fukumori et al., 2007), but also by seasonal mass transport across the sea surface and through the Strait of Gibraltar (Pinardi et al., 2014). The annual and interannual SL

2195 variability in the Mediterranean is related to positive/negative NAO phases associated with westward/eastward winds over the Strait of Gibraltar causing water masses to flow out of/into the Mediterranean (Landerer and Volkov, 2013; Volkov et al., 2019). The decadal variability of SL is considerable and is observed at several tide-gage stations in the Mediterranean

(up to 15 cm). It is strongly correlated with the NAO and is associated with the effects of offshore winds and wave propagation along the eastern Atlantic (Calafat et al., 2012). Three minima associated with this oscillation were observed in the 1950s, 1970s and 1990s. Going to longer time scales (10 y < T), the amplitudes of the processes become much smaller. The bidecadal fluctuations of the Adriatic SL have an amplitude of ~2 cm and are assumed to be a response to global bidecadal changes (Orlić and Pasarić, 2000 and sources cited therein). There were two maxima associated with this oscillation: in the early 1960s and in the 1980s, which are likely related to the low atmospheric pressure and high air and sea-surface temperatures that occurred at that time concurrent with the low salinity in the eastern Mediterranean in the early 1980s. Then, the (multi)decadal changes in the Adriatic were assumed to be due to the thermal fluctuations observed in the atmosphere over the northern Atlantic, but also due to anthropogenic changes in the Mediterranean freshwater budget (construction of the Aswan Dam) (Orlić and Pasarić, 2000 and sources cited therein). As for the secular change (i.e. the linear trend), it is caused by various processes: direct atmospheric influences, thermohaline processes, mass changes and crustal movements. Its rate depends strongly on the time interval over which it is calculated. Šepić et al. (2022) reported a positive trend of mean SL at TGs from Venice to Dubrovnik in the period 1956–2020: the values ranged from 0.99 mm/y in Rovinj to 2.99 mm/y in Venice (the locations of the stations are shown in Fig. 1). Strong sea-level rise relative to land in Venice is due to local subsidence caused by the pumping of underground water sources (Pirazzoli, 1987; Tosi et al., 2013). The study also found that the positive trend did not significantly affect the positive/negative Adriatic sea-level extremes.
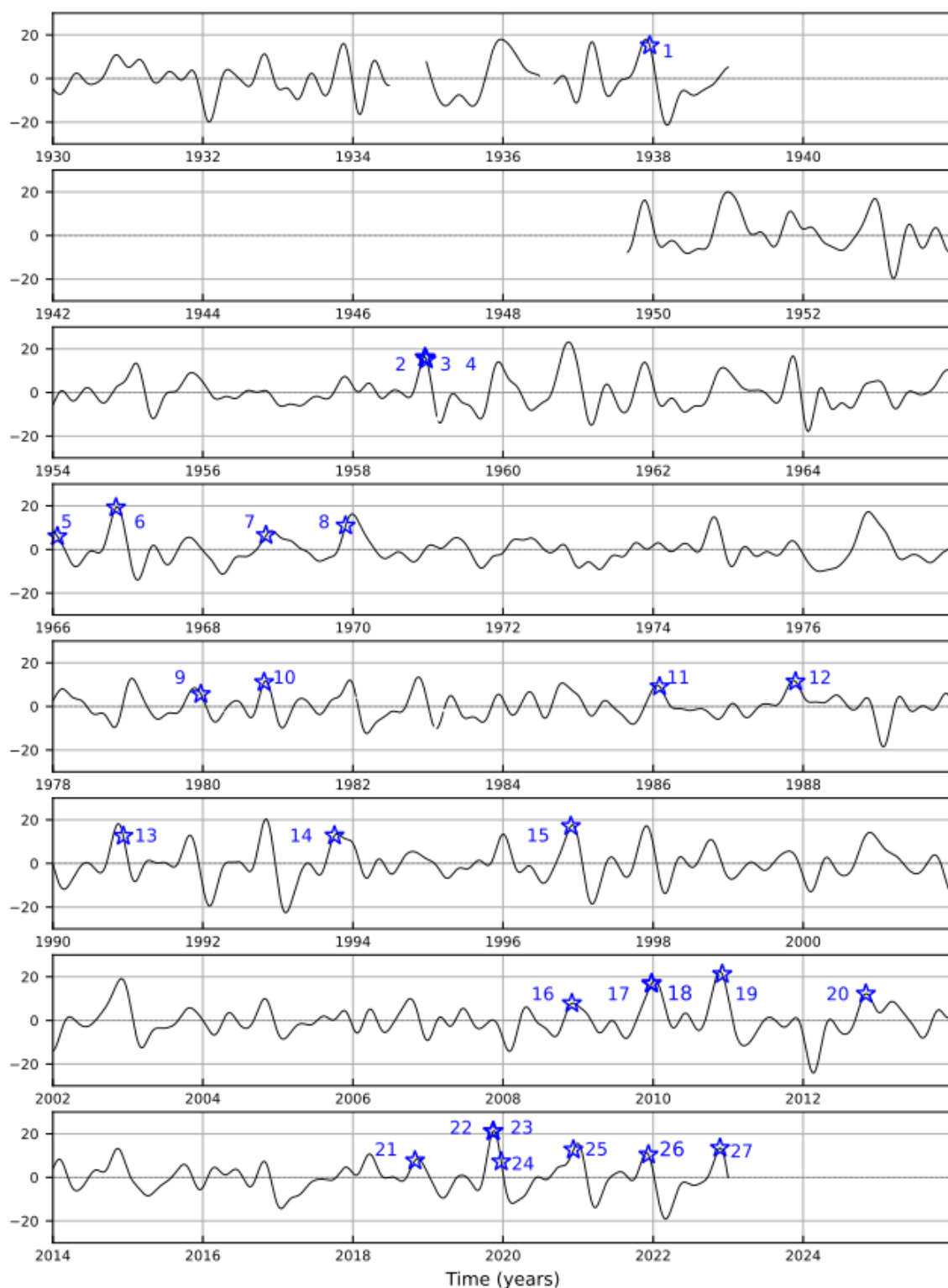
305

Figure A1: *Mean sea-level changes* (cm) over periods of 100 d < T. Blue stars indicate extracted flooding episodes, labeled by their IDs from Table 2.
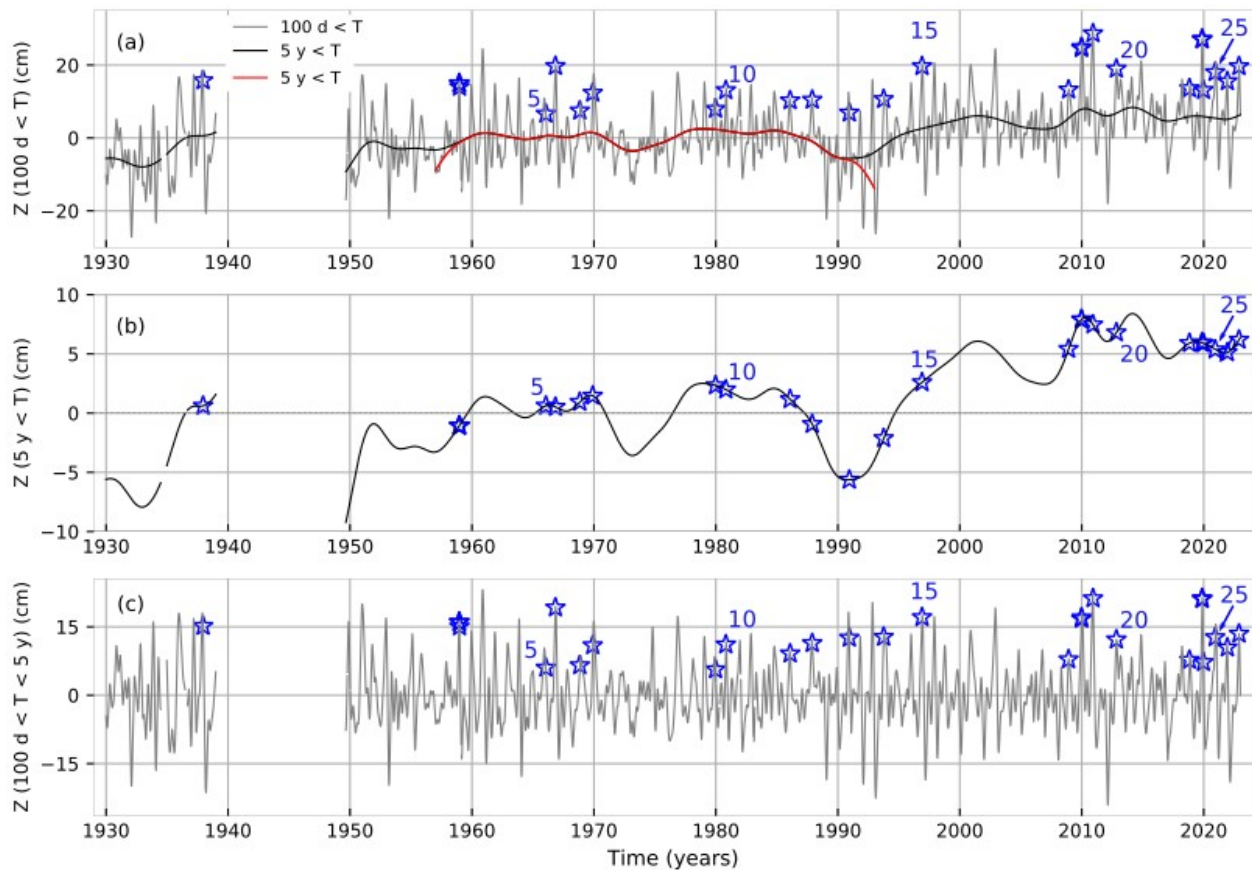
Figure A2: (a) *Mean sea-level changes* for periods longer than 100 d (grey line) and low-pass filtered SL (5 y < T), shown for the 1929–
2240   2022 interval (black) and the 1957–1992 interval (red). (b) Low-pass filtered SL (5 y < T), representing a combination of (multi)decadal and secular change. (c) *Mean sea-level changes* (100 d < T) after subtracting the low-pass filtered SL (5 y < T), representing the seasonal cycle and interannual changes. Blue stars indicate extracted flooding episodes, with every fifth episode labeled by its ID from Table 2.
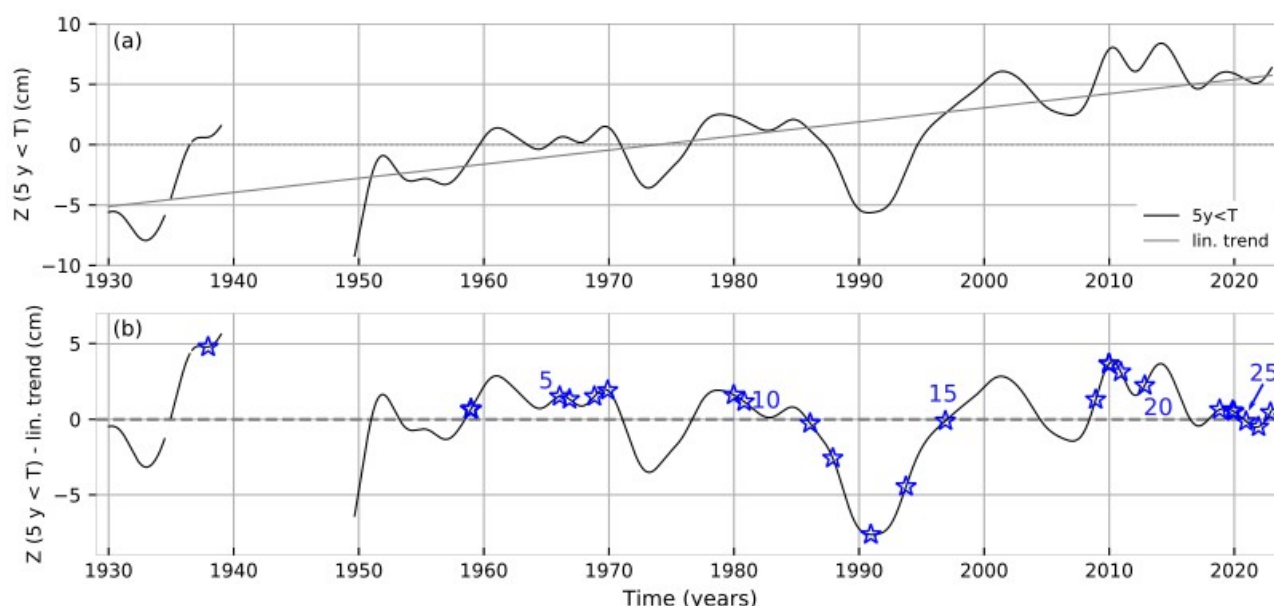
Figure A3: (a) Low-pass filtered SL (5 y < T) (black line) and linear trend (grey). (b) De-trended low-pass filtered SL (5 y < T), representing (multi)decadal changes. Blue stars indicate extracted flooding episodes, with every fifth episode labeled by its ID from Table 2.

Competing interests

The contact author has declared that none of the authors has any competing interests.

References

Accerboni, E. and Manca, B.: Storm surge forecasting in the Adriatic Sea by means of a 2d hydrodynamical numerical model, Boll Geofis Teor Appl, 15(57), 3–22, 1973.

Bajo, M., Međugorac, I., Umgiesser, G., and Orlić, M.: Storm surge and seiche modelling in the Adriatic Sea and the impact of data assimilation, Q. J. R. Meteorol. Soc., 145, 2070–2084, https://doi.org/10.1002/qj.3544, 2019.

Bajo, M., Ferrarin, C., Umgiesser, G., Bonometto, A., and Coraci, E.: Modelling the barotropic sea level in the Mediterranean Sea using data assimilation, Ocean Sci., 19, 559–579, https://doi.org/10.5194/os-19-559-2023, 2023.

Bertotti, L., Bidlot, J.-R., Buizza, R., Cavaleri, L., and Janousek, M.: Deterministic and ensemble-based prediction of Adriatic Sea sirocco storms leading to 'acqua alta' in Venice, Q. J. R. Meteorol. Soc., 137, 1446–1466, https://doi.org/10.1002/qj.861, 2011.

Biolchi, S., Denamiel, C., Devoto, S., Korbar, T., Macovaz, V., Scicchitano, G., Vilibić, I., and Furlani, S.: Impact of the October 2018 Storm Vaia on Coastal Boulders in the Northern Adriatic Sea, Water, 11, 2229,

310

https://doi.org/10.3390/w11112229, 2019.

Calafat, F. M., Chambers, D. P., and Tsimplis, M. N.: Mechanisms of decadal sea level variability in the eastern North Atlantic and the Mediterranean Sea, J. Geophys. Res. Oceans, 117, 2012JC008285, https://doi.org/10.1029/2012JC008285, 2012.

2265   Canestrelli, P., Mandich, M., Pirazzoli, P.A., Tomasin, A.: Wind, Depression and Seiches: Tidal Perturbations in Venice (1950 – 2000). https://www.comune.venezia.it/sites/comune.venezia.it/files/documenti/centro_maree/bibliografia/Venti_depressioni_e_sesse_ridotto.pdf, 2001.

Cavaleri, L., Bertotti, L., Buizza, R., Buzzi, A., Masato, V., Umgiesser, G., and Zampieri, M.: Predictability of extreme meteo-oceanographic events in the Adriatic Sea, Q. J. R. Meteorol. Soc., 136, 400–413, https://doi.org/10.1002/qj.567, 2010.

2270   Cavaleri, L., Bajo, M., Barbariol, F., Bastianini, M., Benetazzo, A., Bertotti, L., Chiggiato, J., Davolio, S., Ferrarin, C., Magnusson, L., Papa, A., Pezzutto, P., Pomaro, A., and Umgiesser, G.: The October 29, 2018 storm in Northern Italy – An exceptional event and its modeling, Prog. Oceanogr., 178, 102178, https://doi.org/10.1016/j.pocean.2019.102178, 2019.

Cavaleri, L., Bajo, M., Barbariol, F., Bastianini, M., Benetazzo, A., Bertotti, L., Chiggiato, J., Ferrarin, C., Trincardi, F., and Umgiesser, G.: The 2019 Flooding of Venice and Its Implications for Future Predictions, Oceanography, 33, 42–49,
2275   https://doi.org/10.5670/oceanog.2020.105, 2020.

Cerovečki, I., Orlić, M., and Hendershott, M. C.: Adriatic seiche decay and energy loss to the Mediterranean, Deep Sea Res. Part Oceanogr. Res. Pap., 44, 2007–2029, https://doi.org/10.1016/S0967-0637(97)00056-3, 1997.

Corsini,   S.,   Ferla,   M.:   Sea   level   observing   activity   in   Italy. https://gloss-sealevel.org/sites/gloss/files/publications/documents/italy_gexi2009.pdf, 2009.

2280   De Zolt, S., Lionello, P., Nuhu, A., and Tomasin, A.: The disastrous storm of 4 November 1966 on Italy, Nat. Hazards Earth Syst. Sci., 6, 861–879, https://doi.org/10.5194/nhess-6-861-2006, 2006.

DHMZ: https://meteo.hr/proizvodi_e.php?section=proizvodi_usluge¶m=services, last access: 10 December 2024.

DWD: https://www.wetter3.de/archiv_dwd_dt.html, last access: 1 October 2024.

Enzi, S. and Camuffo, D.: Documentary sources of the sea surges in Venice fromad 787 to 1867, Nat. Hazards, 12, 225–287,
2285   https://doi.org/10.1007/BF00596222, 1995.

Ferrarin, C., Valentini, A., Vodopivec, M., Klaric, D., Massaro, G., Bajo, M., De Pascalis, F., Fadini, A., Ghezzo, M., Menegon, S., Bressan, L., Unguendoli, S., Fettich, A., Jerman, J., Ličer, M., Fustar, L., Papa, A., and Carraro, E.: Integrated sea storm management strategy: the 29 October 2018 event in the Adriatic Sea, Nat. Hazards Earth Syst. Sci., 20, 73–93, https://doi.org/10.5194/nhess-20-73-2020, 2020.

2290   Ferrarin, C., Bajo, M., Benetazzo, A., Cavaleri, L., Chiggiato, J., Davison, S., Davolio, S., Lionello, P., Orlić, M., and Umgiesser, G.: Local and large-scale controls of the exceptional Venice floods of November 2019, Prog. Oceanogr., 197, 102628, https://doi.org/10.1016/j.pocean.2021.102628, 2021.

Ferrarin, C., Lionello, P., Orlić, M., Raicich, F., and Salvadori, G.: Venice as a paradigm of coastal flooding under multiple

compound drivers, Sci. Rep., 12, 5754, https://doi.org/10.1038/s41598-022-09652-5, 2022.

Ferrarin, C., Orlić, M., Bajo, M., Davolio, S., Umgiesser, G., and Lionello, P.: The contribution of a mesoscale cyclone and associated meteotsunami to the exceptional flood in Venice on November 12, 2019, Q. J. R. Meteorol. Soc., 149, 2929–2942, https://doi.org/10.1002/qj.4539, 2023.

Finizio, C., Palmieri, S., and Riccucci, A.: A numerical model of the Adriatic for the prediction of high tides at Venice, Q. J. R. Meteorol. Soc., 98, 86–104, https://doi.org/10.1002/qj.49709841508, 1972.

Fukumori, I., Menemenlis, D., and Lee, T.: A Near-Uniform Basin-Wide Sea Level Fluctuation of the Mediterranean Sea, J. Phys. Oceanogr., 37, 338–358, https://doi.org/10.1175/JPO3016.1, 2007.

Goldberg, J. and Kempni, K.: On the sea level oscillations in Bakar Bay and on the problem of bay seiches in general, Prirodosl. Istraživanja Kralj. Jugosl., 21, 9–235, 1938.

Grisogono, B. and Belušić, D.: A review of recent advances in understanding the mesoand microscale properties of the severe Bora wind, Tellus A, 61(1), 1-16, https://doi.org/10.1111/j.1600-0870.2008.00369.x, 2009.

Hersbach, H., Bell, B., Berrisford, P., Hirahara, S., Horányi, A., Muñoz-Sabater, J., Nicolas, J., Peubey, C., Radu, R., Schepers, D., Simmons, A., Soci, C., Abdalla, S., Abellan, X., Balsamo, G., Bechtold, P., Biavati, G., Bidlot, J., Bonavita, M., De Chiara, G., Dahlgren, P., Dee, D., Diamantakis, M., Dragani, R., Flemming, J., Forbes, R., Fuentes, M., Geer, A., Haimberger, L., Healy, S., Hogan, R. J., Hólm, E., Janisková, M., Keeley, S., Laloyaux, P., Lopez, P., Lupu, C., Radnoti, G., de Rosnay, P., Rozum, I., Vamborg, F., Villaume, S., and Thépaut, J.-N.: The ERA5 global reanalysis, Q. J. R. Meteorol. Soc., 146, 1999–2049, https://doi.org/10.1002/qj.3803, 2020.

Hersbach, H., Bell, B., Berrisford, P., Biavati, G., Horányi, A., Muñoz Sabater, J., Nicolas, J., Peubey, C., Radu, R., Rozum, I., Schepers, D., Simmons, A., Soci, C., Dee, D., Thépaut, J-N.: ERA5 hourly data on pressure levels from 1940 to present. Copernicus Climate Change Service (C3S) Climate Data Store (CDS), DOI: 10.24381/cds.bd0915c6 , last access: 20 September 2024. 2023a.

Hersbach, H., Bell, B., Berrisford, P., Biavati, G., Horányi, A., Muñoz Sabater, J., Nicolas, J., Peubey, C., Radu, R., Rozum, I., Schepers, D., Simmons, A., Soci, C., Dee, D., Thépaut, J-N.: ERA5 hourly data on single levels from 1940 to present. Copernicus Climate Change Service (C3S) Climate Data Store (CDS), DOI: 10.24381/cds.adbb2d47 , last access: 20 September 2024. 2023b.

HHI: https://www.weatherzone.com.au/news/recordbreaking-wave-in-adriatic-sea/530516, last access: 1 October 2024.

Janeković, I. and Kuzmić, M.: Numerical simulation of the Adriatic Sea principal tidal constituents, Ann. Geophys., 23, 3207–3218, https://doi.org/10.5194/angeo-23-3207-2005, 2005.

Korbar, T., Navratil, D., Denamiel, C., Kordić, B., Biolchi, S., Vilibić, I., and Furlani, S.: Coarse-Clast Storm Deposit and Solitary Boulders on the Island of Mana (NP Kornati, Central Adriatic, Croatia), Geosciences, 12, 355, https://doi.org/10.3390/geosciences12100355, 2022.

Landerer, F. W. and Volkov, D. L.: The anatomy of recent large sea level fluctuations in the Mediterranean Sea, Geophys.

Res. Lett., 40, 553–557, https://doi.org/10.1002/grl.50140, 2013.

Ličer, M., Estival, S., Reyes-Suarez, C., Deponte, D., and Fettich, A.: Lagrangian modelling of a person lost at sea during the Adriatic scirocco storm of 29 October 2018, Nat. Hazards Earth Syst. Sci., 20, 2335–2349, https://doi.org/10.5194/nhess-20-
2330   2335-2020, 2020.

Lionello, P., Mufato, R., and Tomasin, A.: Sensitivity of free and forced oscillations of the Adriatic Sea to sea level rise, Clim. Res., 29, 23–39, https://doi.org/10.3354/cr029023, 2005.

Lionello, P., Sanna, A., Elvini, E., and Mufato, R.: A data assimilation procedure for operational prediction of storm surge in the northern Adriatic Sea, Cont. Shelf Res., 26, 539–553, https://doi.org/10.1016/j.csr.2006.01.003, 2006.

2335   Lionello, P., Barriopedro, D., Ferrarin, C., Nicholls, R. J., Orlić, M., Raicich, F., Reale, M., Umgiesser, G., Vousdoukas, M., and Zanchettin, D.: Extreme floods of Venice: characteristics, dynamics, past and future evolution (review article), Nat. Hazards Earth Syst. Sci., 21, 2705–2731, https://doi.org/10.5194/nhess-21-2705-2021, 2021.

A catastrophic event: the Vaia Storm: https://www.guidedolomiti.com/en/miscellaneous/storm-vaia/, last access: 4 October 2024.

2340   Malguzzi, P., Grossi, G., Buzzi, A., Ranzi, R., and Buizza, R.: The 1966 "century" flood in Italy: A meteorological and hydrological revisitation, J. Geophys. Res. Atmospheres, 111, https://doi.org/10.1029/2006JD007111, 2006.

Marcos, M., Tsimplis, M. N., and Shaw, A. G. P.: Sea level extremes in southern Europe, J. Geophys. Res. Oceans, 114, C01007, https://doi.org/10.1029/2008JC004912, 2009.

Međugorac, I., Pasarić, M., and Orlić, M.: Severe flooding along the eastern Adriatic coast: the case of 1 December 2008,
2345   Ocean Dyn., 65, 817–830, https://doi.org/10.1007/s10236-015-0835-9, 2015.

Međugorac, I., Pasarić, M., Pasarić, Z., and Orlić, M.: Two recent storm-surge episodes in the Adriatic, Int. J. Saf. Secur. Eng., 6, 589–596, https://doi.org/10.2495/SAFE-V6-N3-589-596, 2016.

Međugorac, I., Orlić, M., Janeković, I., Pasarić, Z., and Pasarić, M.: Adriatic storm surges and related cross-basin sea-level slope, J. Mar. Syst., 181, 79–90, https://doi.org/10.1016/j.jmarsys.2018.02.005, 2018.

2350   Međugorac, I., Pasarić, M., and Güttler, I.: Will the wind associated with the Adriatic storm surges change in future climate?, Theor. Appl. Climatol., 143, 1–18, https://doi.org/10.1007/s00704-020-03379-x, 2021.

Međugorac, I., Pasarić, M., and Orlić, M.: Long-term measurements at Bakar tide-gauge station (east Adriatic), Geofizika, 39, 149–162, https://doi.org/10.15233/gfz.2022.39.8, 2022.

Međugorac, I., Pasarić, M., and Orlić, M.: Historical sea-level measurements at Bakar (east Adriatic),
2355   https://doi.org/10.17882/85171, 2024. [data set]

Međugorac, I., Jambrošić, K., Dolički, D., Kuzmić, J., Šepić, J., Vrkić Seidl, I., Gašparac, G.: Adriatic storm surge catalogue. https://projekti.pmfst.unist.hr/floods/storm-surges/, last access: 18 December 2024.

Međugorac, I. and Pasarić, M.: Exceptionally high sea levels in the northern Adriatic Sea, in: Marine Hazards, Coastal Vulnerability and Risk (mis)Perceptions. CIESM Workshop Monograph n° 52, edited by: Briand, F., CIESM Publisher,

320

2360 Paris, Monaco, https://ciesm.org/online/monographs/index.htm [in press].

Medvedev, I. P., Vilibić, I., and Rabinovich, A. B.: Tidal Resonance in the Adriatic Sea: Observational Evidence, J. Geophys. Res. Oceans, 125, e2020JC016168, https://doi.org/10.1029/2020JC016168, 2020.

Mel, R. A., Coraci, E., Morucci, S., Crosato, F., Cornello, M., Casaioli, M., Mariani, S., Carniello, L., Papa, A., Bonometto, A., and Ferla, M.: Insights on the Extreme Storm Surge Event of the 22 November 2022 in the Venice Lagoon, J. Mar. Sci.

2365 Eng., 11, 1750, https://doi.org/10.3390/jmse11091750, 2023.

METEOALARM: https://www.meteoalarm.org/en/live/, last access: 1 October 2024.

Morucci, S., Coraci, E., Crosato, F., and Ferla, M.: Extreme events in Venice and in the North Adriatic Sea: 28–29 October 2018, Rendiconti Lincei Sci. Fis. E Nat., 31, 113–122, https://doi.org/10.1007/s12210-020-00882-1, 2020.

Mosetti, F.: Problems on storm surges forecasting in the Northern Adriatic Sea, Boll Oceanol Teor Appl, 3(4), 263–297,

2370 1985.

Orlić, M. and Pasarić, M.: Sea-level changes and crustal movements recorded along the east Adriatic coast, Il Nuovo Cimento C, 23 C, 351–364, 2000.

Orlić, M. and Pasarić, M.: How to disentangle sea-level rise and a number of other processes influencing coastal floods?, Rendiconti Lincei Sci. Fis. E Nat., 35, 371–380, https://doi.org/10.1007/s12210-024-01242-z, 2024.

2375 Pasarić, M.: Variations of sea level in the Adriatic caused by slowly changing air pressure and wind, University of Zagreb, Zagreb, 113 pp., 2000.

Pasarić, M. and Orlić, M.: Long-term meteorological preconditioning of the North Adriatic coastal floods, Cont. Shelf Res., 21, 263–278, https://doi.org/10.1016/S0278-4343(00)00078-9, 2001.

Pasarić, M., Pasarić, Z., and Orlić, M.: Response of the Adriatic sea level to the air pressure and wind forcing at low

2380 frequencies (0.01–0.1 cpd), J. Geophys. Res. Oceans, 105, 11423–11439, https://doi.org/10.1029/2000JC900023, 2000.

Pawlowicz, R., Beardsley, B., and Lentz, S.: Classical tidal harmonic analysis including error estimates in MATLAB using T_TIDE, Comput. Geosci., 28, 929–937, https://doi.org/10.1016/S0098-3004(02)00013-4, 2002.

Pérez Gómez, B., Vilibić, I., Šepić, J., Međugorac, I., Ličer, M., Testut, L., Fraboul, C., Marcos, M., Abdellaoui, H., Álvarez Fanjul, E., Barbalić, D., Casas, B., Castaño-Tierno, A., Čupić, S., Drago, A., Fraile, M. A., Galliano, D. A., Gauci, A.,

2385 Gloginja, B., Martín Guijarro, V., Jeromel, M., Larrad Revuelto, M., Lazar, A., Keskin, I. H., Medvedev, I., Menassri, A., Meslem, M. A., Mihanović, H., Morucci, S., Niculescu, D., Quijano De Benito, J. M., Pascual, J., Palazov, A., Picone, M., Raicich, F., Said, M., Salat, J., Sezen, E., Simav, M., Sylaios, G., Tel, E., Tintoré, J., Zaimi, K., and Zodiatis, G.: Coastal sea level monitoring in the Mediterranean and Black seas, Ocean Sci., 18, 997–1053, https://doi.org/10.5194/os-18-997-2022, 2022.

2390 Pervan, M. and Šepić, J.: Analysis of the eastern Adriatic sea level extremes, St Open, 4, 1–19, https://doi.org/10.48188/so.4.10, 2023.

Pinardi, N., Bonaduce, A., Navarra, A., Dobricic, S., and Oddo, P.: The Mean Sea Level Equation and Its Application to the

Mediterranean Sea, J. Clim., 27, 442–447, https://doi.org/10.1175/JCLI-D-13-00139.1, 2014.

Pirazzoli, P. A.: Recent sea-level changes and related engineering problems in the Lagoon of Venice (Italy), Prog.
2395 Oceanogr., 18, 323–346, https://doi.org/10.1016/0079-6611(87)90038-3, 1987.

Pugh, D. T. and Thompson, K. R.: The subtidal behaviour of the Celtic Sea—I. Sea level and bottom pressures, Cont. Shelf
Res., 5, 293–319, https://doi.org/10.1016/0278-4343(86)90001-4, 1986.

Raicich, F.: Recent evolution of sea-level extremes at Trieste (Northern Adriatic), Cont. Shelf Res., 23, 225–235,
https://doi.org/10.1016/S0278-4343(02)00224-8, 2003.

2400 Raicich, F., Orlic, M., and Malacic, V.: A case study of the Adriatic seiches (December 1997), Nuovo Cimento Della Soc.
Ital. Fis. Sezione C, 22C, 1999.

Roland, A., Cucco, A., Ferrarin, C., Hsu, T.-W., Liau, J.-M., Ou, S.-H., Umgiesser, G., and Zanke, U.: On the development
and verification of a 2-D coupled wave-current model on unstructured meshes, J. Mar. Syst., 78, S244–S254,
https://doi.org/10.1016/j.jmarsys.2009.01.026, 2009.

2405 Rožić, N.: Hrvatski transformacijski model visina, 2009.

Ruić, K., Šepić, J., Mlinar, M., and Međugorac, I.: Contribution of high-frequency (T < 2 h) sea level oscillations to the
Adriatic sea level maxima, Nat. Hazards, 116, 3747–3777, https://doi.org/10.1007/s11069-023-05834-0, 2023.

Rus, M., Fettich, A., Kristan, M., and Ličer, M.: HIDRA2: deep-learning ensemble sea level and storm tide forecasting in the
presence of seiches – the case of the northern Adriatic, Geosci. Model Dev., 16, 271–288, https://doi.org/10.5194/gmd-16-
2410 271-2023, 2023.

Rus, M., Mihanović, H., Ličer, M., and Kristan, M.: HIDRA3: a robust deep-learning model for multi-point ensemble sea
level forecasting, EGUsphere, 1–21, https://doi.org/10.5194/egusphere-2024-2068, 2024.

Schwab, D. J. and Rao, D. B.: Barotropic oscillations of the Mediterranean and Adriatic Seas1, Tellus A, 35A, 417–427,
https://doi.org/10.1111/j.1600-0870.1983.tb00216.x, 1983.

2415 Šepić, J., Pasarić, M., Međugorac, I., Vilibić, I., Karlović, M., and Mlinar, M.: Climatology and process-oriented analysis of
the Adriatic sea level extremes, Prog. Oceanogr., 209, 102908, https://doi.org/10.1016/j.pocean.2022.102908, 2022.

Slivinski, L. C., Compo, G. P., Whitaker, J. S., Sardeshmukh, P. D., Giese, B. S., McColl, C., Allan, R., Yin, X., Vose, R.,
Titchner, H., Kennedy, J., Spencer, L. J., Ashcroft, L., Brönnimann, S., Brunet, M., Camuffo, D., Cornes, R., Cram, T. A.,
Crouthamel, R., Domínguez-Castro, F., Freeman, J. E., Gergis, J., Hawkins, E., Jones, P. D., Jourdain, S., Kaplan, A.,
2420 Kubota, H., Blancq, F. L., Lee, T.-C., Lorrey, A., Luterbacher, J., Maugeri, M., Mock, C. J., Moore, G. W. K., Przybylak, R.,
Pudmenzky, C., Reason, C., Slonosky, V. C., Smith, C. A., Tinz, B., Trewin, B., Valente, M. A., Wang, X. L., Wilkinson,
C., Wood, K., and Wyszyński, P.: Towards a more reliable historical reanalysis: Improvements for version 3 of the
Twentieth Century Reanalysis system, Q. J. R. Meteorol. Soc., 145, 2876–2908, https://doi.org/10.1002/qj.3598, 2019.

Storm Barra | Copernicus: https://www.copernicus.eu/hr/node/11329, last access: 28 July 2024.

2425 Stravisi, F. and Marussi, S.A.: Analysis of a storm surge in Adriatic Sea by means of a 2-dimensional linear-model, Atti

325

Accad Naz Lincei Cl Sci Fis Mat Nat, 54(2), 243–260, 1973.

Tide-gauge station Bakar: https://www.pmf.unizg.hr/geof/en/research/oceanography/tide-gauge_station_bakar, last access: 1 October 2024.

Toomey, T., Amores, A., Marcos, M., and Orfila, A.: Coastal sea levels and wind-waves in the Mediterranean Sea since 1950 from a high-resolution ocean reanalysis, Front. Mar. Sci., 9, https://doi.org/10.3389/fmars.2022.991504, 2022.

Tosi, L., Teatini, P., and Strozzi, T.: Natural versus anthropogenic subsidence of Venice, Sci. Rep., 3, 2710, https://doi.org/10.1038/srep02710, 2013.

Trigo, I. F. and Davies, T. D.: Meteorological conditions associated with sea surges in Venice: a 40 year climatology, Int. J. Climatol., 22, 787–803, https://doi.org/10.1002/joc.719, 2002.

Trincardi, F., Barbanti, A., Bastianini, M., Cavaleri, L., and Chiggiato, J.: The 1966 Flooding of Venice: What Time Taught Us for the Future, Oceanography, 29, 178–186, https://doi.org/10.5670/oceanog.2016.87, 2016.

Venice Municipality: https://www.comune.venezia.it/it/content/le-acque-alte-eccezionali, last access: 1 October 2024.

Volkov, D. L., Baringer, M., Smeed, D., Johns, W., and Landerer, F. W.: Teleconnection between the Atlantic Meridional Overturning Circulation and Sea Level in the Mediterranean Sea, J. Clim., 32, 935–955, https://doi.org/10.1175/JCLI-D-18-0474.1, 2019.

Zampato, L., Bajo, M., Canestrelli, P., and Umgiesser, G.: Storm surge modelling in Venice: two years of operational results, J. Oper. Oceanogr., 9, s46–s57, https://doi.org/10.1080/1755876X.2015.1118804, 2016.

Žust, L., Fettich, A., Kristan, M., and Ličer, M.: HIDRA 1.0: deep-learning-based ensemble sea level forecasting in the northern Adriatic, Geosci. Model Dev., 14, 2057–2074, https://doi.org/10.5194/gmd-14-2057-2021, 2021.

Other sources (daily newspapers and online references)

Civilna zaštita, 24 December 2019, https://civilna-zastita.gov.hr/vijesti/posljedice-olujnog-nevremena-2055/2055

Dalmacija Danas, 9 December 2021, https://www.dalmacijadanas.hr/nevrijeme-pogodilo-dalmaciju-olujno-jugo-do-112-km-h-napravilo-kaos-na-splitskim-plazama-dio-obale-ponovno-pod-morem/

Dubrovački vjesnik, 22 November 2022, https://dubrovacki.slobodnadalmacija.hr/dubrovnik/zupanija/dubrovnik/poplavljena-lapadska-obala-more-uslo-u-bazen-hotela-lapad-a-pogledajte-kako-tek-izgleda-slano-1242695

Glas Istre, 25 and 26 December 2009, https://glasistrenovine.hr/arhiva-portala/pregled-vijesti/jugo-zaprijetilo-poplavom-151266,
https://glasistrenovine.hr/arhiva-portala/pregled-vijesti/poplavljena-kantrida-151351

Hrvatska Danas, 9 December 2021, https://hrvatska-danas.com/2021/12/09/video-olujno-jugo-rusilo-stabla-po-splitu-vatrogasci-intervenirali-na-sve-strane-trajektne-linije-u-prekidu/

Hrvatska vatrogasna zajednica, 23 December 2019, https://hvz.gov.hr/vijesti/753

Index.hr, 22 November 2022, https://www.index.hr/vijesti/clanak/poplave-u-splitu-sibeniku-trogiru-objavljene-nove-prognoze/2414003.aspx

Istramet, 8 December 2020, https://www.istramet.hr

2460 Jutarnji list, 25 December 2009, https://www.jutarnji.hr/vijesti/hrvatska/obilne-kise-pretvorile-stadion-kantridu-u-ogromni-bazen-2882312

Jutarnji list, 2 December 2008

Jutarnji list, 29 October 2018

Jutarnji list, 31 October–1 November 2018

2465 Jutarnji list, 14 and 17 November 2019

Jutarnji list, 8 December 2020

Jutarnji list, 22 November 2022,

https://www.jutarnji.hr/vijesti/hrvatska/poplave-diljem-obale-niz-otoka-odsjeceno-od-kopna-vjetar-rusi-stabla-rive-pod-vodom-problemi-i-u-sloveniji-15278693

2470 MorskiHR, 9 December 2021, https://www.morski.hr/dubrovacke-zidine-lupaju-valovi-visine-dvokatnice/

Novi list, 24 January 1966

Novi list, 4–7 November 1966

Novi list, 25–27 November 1969

Novi list, 24–26 December 1979

2475 Novi list, 27 October 1980

Novi list, 3 February 1986

Novi list, 25 November 1987

Novi list, 11 December 1990

Novi list, 2 and 3 December 2008

2480 Novi list, 24 December 2009

Novi list, 2 November 2012

Novi list, 30 October 2018

Novi list, 31 October–1 November 2018

Novi List, 10 December 2021, https://projekti.pmfst.unist.hr/floods/storm-surges/episode-26-8-december-2021/

2485 Novi list, 22 November 2022,

https://www.novilist.hr/novosti/hrvatska/diljem-obale-poplave-i-odroni-olujni-vjetar-stvara-velike-probleme-u-prometu/

Obzor, 16 December 1937

Otvoreno.hr, 24 December 2019,

https://www.otvoreno.hr/vijesti/zbog-jakog-nevremena-ostecene-zadarske-morske-orgulje-valovi-izbacili-kamene-blokove/

330

2490 [238611](#)

Primorske novine, 17 December 1937

Portal Istra Terra Magica, 22 November 2022, https://www.istriaterramagica.eu/novosti/jako-nevrijeme-diljem-istarske-obale-u-puli-more-poraslo-za-cak-60-cm/

Radio Dalmacija, 9 December 2021, https://www.radiodalmacija.hr/split-olujno-jugo-rusilo-stabla-daska-sa-skele-pala-na-
2495 prolaznika/

Slobodna Dalmacija, 26 December 1958

Slobodna Dalmacija, 27 November 1969

Slobodna Dalmacija, 24 and 25 December 1979

Slobodna Dalmacija, 27 October 1980

2500 Slobodna Dalmacija, 3 February 1986

Slobodna Dalmacija, 26 November 1987

Slobodna Dalmacija, 11 December 1990

Slobodna Dalmacija, 2 December 2008

Slobodna Dalmacija, 4 December 2010

2505 Slobodna Dalmacija, 2 and 3 November 2012

Slobodna Dalmacija, 30 October–1 November 2018

Slobodna Dalmacija, 25 December 2019, https://projekti.pmfst.unist.hr/floods/storm-surges/episode-24-23-december-2019/

Slobodna Dalmacija, 4 December 2020

Šibenski., 24 December 2019,

2510 https://sibenski.slobodnadalmacija.hr/sibenik/vijesti/crna-kronika/nevrijeme-odnijelo-i-jedan-zivot-muskarac-66-htio-privezati-brod-pa-upao-u-more-kcer-ga-izvukla-ali-spasa-mu-nije-bilo-639916

Šibenski portal Moć komunikacije, 22 November 2022, https://mok.hr/vijesti/item/36413-neprepoznatljiva-brodarica-more-poplavilo-gotovo-sva-mula-i-rivice-jako-jugo-na-cestu-izbacilo-sljunak

Vatrogasni portal, 25 December 2009, https://www.vatrogasni-portal.com/news.php?readmore=4081

2515 Večernji list, 5–7 November 1966

Večernji list, 24 January 1966

Večernji list, 4 November 1968

Večernji list, 28–30 November 1969

Večernji list, 24 December 1979

2520 Večernji list, 27 October 1980

Večernji list, 11 December 1990

Večernji list, 2 December 2008

335

Večernji list, 31 October–1 November 2018

Vjesnik, 5 November 1966

2525 Vjesnik, 2 December 2008

Vjesnik, 4 and 5 December 2010

Zadarski.hr, 23 December 2019,

https://zadarski.slobodnadalmacija.hr/zadar/fotoreport/pijavica-za-svega-30-sekundi-ostavila-pravu-pustos-rusila-krovove-lomila-stabla-639948